

# The Monte Carlo event generator PHOJET

(Program version 1.12a from Sep. '98)

Ralph Engel<sup>1</sup>

*Forschungszentrum Karlsruhe, Postfach 3640,  
76021 Karlsruhe, Germany*

Johannes Ranft<sup>2</sup>

*FIGS and Physics Dept., University Siegen,  
D-57068 Siegen, Germany*

Stefan Roesler<sup>3</sup>

*CERN, CH-1211 Geneva 23, Switzerland*

---

<sup>1</sup>e-mail: [Ralph.Engel@ik.fzk.de](mailto:Ralph.Engel@ik.fzk.de)

<sup>2</sup>e-mail: [Johannes.Ranft@cern.ch](mailto:Johannes.Ranft@cern.ch)

<sup>3</sup>e-mail: [Stefan.Roesler@cern.ch](mailto:Stefan.Roesler@cern.ch)

# Contents

<b>1</b>	<b>Introduction</b>	<b>5</b>
<b>I</b>	<b>Physics overview</b>	<b>6</b>
<b>2</b>	<b>Amplitudes and cross sections</b>	<b>7</b>
2.1	General remarks . . . . .	7
2.2	Impact parameter representation . . . . .	8
2.3	Born-graph amplitudes and cross sections . . . . .	9
2.3.1	Hadron-hadron interactions . . . . .	10
2.3.2	Photon-hadron and photon-photon interactions . . . . .	11
2.4	Cross sections involving weakly virtual photons . . . . .	13
2.5	Unitarization . . . . .	14
2.5.1	General remarks . . . . .	14
2.5.2	Gribov's Reggeon field theory . . . . .	15
2.6	Determination of model parameters . . . . .	17
<b>3</b>	<b>Multiparticle production</b>	<b>19</b>
3.1	Cutting rules and cross sections . . . . .	19
3.2	Non-diffractive interactions . . . . .	23
3.2.1	Low- $p_{\perp}$ final states . . . . .	23
3.2.2	High- $p_{\perp}$ final states . . . . .	24
3.2.3	Parton showers . . . . .	26
3.3	Diffractive interactions . . . . .	26
3.3.1	Elastic and quasi-elastic scattering . . . . .	26
3.3.2	Single/double diffraction dissociation . . . . .	27
3.3.3	Central diffraction . . . . .	28
3.4	Fragmentation . . . . .	30
<b>4</b>	<b>Photon flux calculation</b>	<b>31</b>
4.1	Bremsstrahlung . . . . .	32
4.1.1	Kinematics . . . . .	32
4.1.2	Bremsstrahlung of fermions . . . . .	33
4.1.3	Bremsstrahlung of hadrons . . . . .	34
4.2	Beamstrahlung . . . . .	36
4.3	Laser-backscattering . . . . .	36

<b>II</b>	<b>Program manual</b>	<b>38</b>
<b>5</b>	<b>Program overview</b>	<b>39</b>
5.1	Intention of the program . . . . .	39
5.2	History of the program . . . . .	39
5.3	General structure of the program . . . . .	40
<b>6</b>	<b>Installation and quick start</b>	<b>41</b>
6.1	General program structure . . . . .	41
6.2	How to run the program . . . . .	41
6.2.1	Files and update/bugfix information . . . . .	41
6.2.2	Calling PHOJET as a subroutine . . . . .	42
6.2.3	Using pre-defined collision setups . . . . .	44
6.2.4	Event generation with input cards . . . . .	44
6.2.5	Photoproduction in lepton-hadron, lepton-lepton and hadron-hadron scattering	44
6.2.6	Histograming . . . . .	45
<b>7</b>	<b>Main subroutines and options</b>	<b>46</b>
7.1	Main subroutines . . . . .	46
7.2	Main options for event simulation . . . . .	48
7.2.1	COMMON /PROCES/ . . . . .	48
7.2.2	COMMON /MODELS/ . . . . .	49
7.2.3	Minimum bias event generation . . . . .	49
<b>8</b>	<b>Event record structure</b>	<b>51</b>
8.1	Standard particle record: COMMON /HEPEVS/ . . . . .	51
8.2	Particle codes and properties . . . . .	53
8.3	Comment entries . . . . .	54
8.3.1	Hard partonic interaction . . . . .	54
8.3.2	Diffractive dissociation . . . . .	55
8.3.3	Elastic/quasi-elastic scattering . . . . .	56
8.3.4	Central diffraction . . . . .	57
8.4	Additional generator dependent information . . . . .	57
8.4.1	COMMON /PROCES/ . . . . .	57
8.4.2	COMMON /DEBUG/ . . . . .	58
<b>9</b>	<b>Amplitude construction and unitarization</b>	<b>60</b>
9.1	Born graph amplitudes . . . . .	60
9.1.1	Parameters and options . . . . .	60
9.1.2	COMMON /REGGE/ . . . . .	60
9.1.3	COMMON /TWOCHA/ . . . . .	62
9.2	Unitarization, cross section . . . . .	62
9.2.1	COMMON /XSECT/ . . . . .	62
<b>10</b>	<b>Soft interactions</b>	<b>64</b>
10.0.2	Parameters and options . . . . .	64
10.0.3	COMMON /ABRSOF/ . . . . .	65

<b>11 Hard interactions</b>	<b>67</b>
11.1 Hard scattering subprocesses . . . . .	67
11.1.1 Scale calculations . . . . .	68
11.1.2 Parameters and options . . . . .	69
11.1.3 COMMON /HARSLT/ . . . . .	70
11.1.4 COMMON /HAXSEC/ . . . . .	71
11.1.5 COMMON /HAQQAP/ . . . . .	72
11.2 Initial and final state radiation . . . . .	72
11.3 Parton distribution functions . . . . .	73
11.3.1 COMMON /PARPDF/ . . . . .	73
<b>12 Diffractive interactions</b>	<b>76</b>
12.1 Elastic and quasi-elastic scattering . . . . .	76
12.2 Single- and double diffraction dissociation . . . . .	76
12.2.1 Parameters and options . . . . .	76
12.2.2 COMMON /QEVECM/ . . . . .	77
12.3 Central diffraction . . . . .	77
12.4 Pomeron-particle/pomeron scattering . . . . .	77
<b>13 Chain construction and fragmentation</b>	<b>79</b>
13.0.1 Options and parameters . . . . .	79
13.0.2 COMMON /POSTRG/ . . . . .	80
<b>14 Interactions involving weakly virtual photons</b>	<b>82</b>
<b>15 Photon flux generation</b>	<b>83</b>
15.0.3 Parameters and options . . . . .	83
15.0.4 COMMON /LEPCUT/ . . . . .	83
15.0.5 COMMON /PHOSRC/ . . . . .	84
<b>A Kinematics of hard scattering</b>	<b>86</b>
<b>B Resonances generated in low-mass diffraction</b>	<b>88</b>
<b>C Input data cards</b>	<b>89</b>
C.1 General structure of input cards . . . . .	89
C.2 List of input cards . . . . .	89
C.2.1 General cards . . . . .	89
C.2.2 Program execution . . . . .	89
C.2.3 Changing PHOJET parameters . . . . .	91
C.2.4 Changing JETSET parameters . . . . .	92
<b>D Table of particles</b>	<b>93</b>
<b>E Parton distribution functions</b>	<b>98</b>
<b>Bibliography</b>	<b>100</b>
<b>Index</b>	<b>104</b>

# Chapter 1

## Introduction

The model and the implementation as Monte Carlo (MC) event generator PHOJET described in this article are using the ideas of the Dual Parton Model (DPM, for a review see [1]) combined with perturbative QCD to give an almost complete picture of hadron-hadron, photon-hadron and photon-photon interactions at high energies.

The Dual Parton Model is a phenomenological realization of the large  $N_c, N_f$  expansion of QCD [2,3] in connection with general ideas of duality [4–6] and Gribov’s reggeon field theory [7,8]. Within this model, one can calculate both elastic processes (i.e. cross sections) and inelastic processes (i.e. multiparticle production). The model relates the free parameters necessary to describe the cross sections directly to multiparticle production. In its formulation with a soft and a hard component (two-component DPM) this model represents an attempt to give a consistent description of hadronic interactions at high energies. The two-component DPM [9–16] connects both soft and hard subprocesses by an unitarization scheme. At higher energies, the unified treatment of soft and hard processes is necessary because of the rapid increase of the minijet cross section.

The two-component DPM successfully describes most of the features of high energy hadronic processes. These features are for example violation of Feynman scaling, rising of central rapidity plateau, long range correlations, violation of Koba-Nielsen-Olesen scaling, and long range multiplicity correlations [9–16]. The model was also successfully applied to diffractive hadron production reactions [17] and even hard diffractive processes [18]. In [19] first studies of photon-hadron interactions were presented and in [20] the application of this model to photon-photon collisions was discussed. Recently, the two-component DPM was also used to obtain predictions on photoproduction off nuclei [21,22].

In the following, the implementation of the two-component DPM together with the extension to photons in the generator PHOJET is discussed [19,20]. Concerning hadron-hadron interactions, the realization of the model is similar to the MC generator DTUJET93 [12,23]. This generator is intended to simulate  $pp$  and  $p\bar{p}$  collisions up to very high energies.

According to the basic ideas of the model the discussion starts with amplitude calculations. Unitarizing the Born amplitudes, physical cross sections are calculated. The comparison of the model predictions with cross section data is used to determine the unknown parameters of the model. These model parameters are needed to generate multiparticle final states produced in inelastic reactions. For high- $p_\perp$  reactions, perturbative QCD together with the parton model is used. Low- $p_\perp$  interactions are modeled on the basis of Regge phenomenology. According to this the two-component structure of the model, soft and hard interactions as well as their connection due to unitarization are discussed.

## Part I

# Physics overview

## Chapter 2

# Amplitudes and cross sections

### 2.1 General remarks

In the following the scattering (incoming) particles are taken to be  $A$  and  $B$  with the four-momenta  $p_A$  and  $p_B$  respectively. The momenta of the scattered particles are denoted by  $p_{A'}$  and  $p_{B'}$ . To describe the kinematics of elastic scattering, Mandelstam variables

$$\begin{aligned} s &= (p_A + p_B)^2 \\ t &= (p_A - p_{A'})^2 \\ u &= (p_A - p_{B'})^2 \\ s + t + u &= m_A^2 + m_B^2 + m_{A'}^2 + m_{B'}^2 \end{aligned} \quad (2.1)$$

are used.

The (elastic) scattering amplitude is defined by the following relation to the differential elastic cross section

$$\frac{d\sigma_{\text{ela}}}{dt} = \frac{1}{16\pi s^2} |A(s, t)|^2 . \quad (2.2)$$

With the normalization (2.2), the amplitude  $A(s, t)$  becomes equal to the matrix element  $-\mathcal{M}(s, t)$  often used in perturbative calculations of Feynman graphs. The optical theorem reads

$$\sigma_{\text{tot}} = \frac{1}{4k\sqrt{s}} \text{disc}_s (A(s, t = 0)) \quad (2.3)$$

$$\approx \frac{1}{s} \Im m (A(s, t = 0)) . \quad (2.4)$$

Here,  $k$  denotes the center-of-mass system (CMS) momentum of the collision

$$k = \frac{1}{2\sqrt{s}} \lambda^{\frac{1}{2}}(s, m_A^2, m_B^2), \quad \lambda(x, y, z) = x^2 + y^2 + z^2 - 2xy - 2xz - 2yz . \quad (2.5)$$

The  $s$ -channel discontinuity of the amplitude  $A(s, t)$  is defined by

$$\text{disc}_s (A(s, t)) = \frac{1}{i} \lim_{\epsilon \rightarrow 0} (A(s + i\epsilon, t) - A(s - i\epsilon, t)) . \quad (2.6)$$

For functions being analytic in  $s$  this simplifies to

$$\text{disc}_s (A(s, t)) = 2\Im m (A(s, t)) \quad (2.7)$$

which has been used to obtain Eq. (2.4).

The data on high-energy elastic scattering of hadrons can be parametrized for  $|t| < 1(\text{GeV}/c)^2$  by

$$\frac{d\sigma_{\text{ela}}}{dt} = \left( \frac{d\sigma_{\text{ela}}}{dt} \right)_{t=0} \exp(b_{\text{ela}}(s)t) . \quad (2.8)$$

Here,  $b_{\text{ela}}(s)$  is elastic slope parameter.

Since the optical theorem connects the total and elastic cross sections, one can derive a few realtions implied by unitarity. For simplicity, the real part of the elastic amplitude is neglected and the parametrization (2.8) is used

$$\sigma_{\text{ela}} = \frac{\sigma_{\text{tot}}^2}{16\pi b_{\text{ela}}(s)} \quad \text{and} \quad \left. \frac{d\sigma_{\text{ela}}}{dt} \right|_{t=0} = \frac{\sigma_{\text{tot}}^2}{16\pi} . \quad (2.9)$$

## 2.2 Impact parameter representation

At high energies the scattering of particles can effectively described by applying geometrical models since the wavelength of the particles is smaller than the transverse size of the particles. Geometrical models allow for a very simple interpretation of many effects seen in high-energy scattering. In the following we will neglect effects depending on the spin of the scattering particles. The scattering particles are considered in CMS. The scattering angle  $\theta$  is given by

$$t = q^2 = -4k^2 \sin^2\left(\frac{\theta}{2}\right) \quad (2.10)$$

where  $q$  denotes the momentum transfer. Since the angular momentum is conserved during the scattering process, it is convenient to expand the scattering amplitude in partial waves

$$A(s, t) = 16\pi \sum_{l=0}^{\infty} (2l+1) a_l(s) P_l(\cos\theta) , \quad (2.11)$$

where  $a_l(s)$  is the amplitude of the  $l$ th partial wave. To turn to a classical (geometrical) description of the scattering, the  $l$ th term of (2.11) with angular momentum  $l$  is assumed to correspond to the scattering of two particles with the impact parameter  $\vec{B}$  satisfying

$$l = |\vec{B} \times \vec{k}| . \quad (2.12)$$

The impact parameter vector  $\vec{B}$  is by definition perpendicular to  $\vec{k}$  (two-dimensional impact parameter space). Using unitarity and the fact that the Legendre polynomials form a set of othogonal polynomials leads to the well known constraint on the partial wave amplitude,

$$0 \leq \Im m (a_l(s)) \leq 1 . \quad (2.13)$$

Together with the optical theorem (2.4) this leads to the restriction of the cross section of the  $l$ th partial wave to

$$\sigma_{\text{tot}}^l(s) \leq (2l+1) \frac{4\pi}{k^2} \quad (2.14)$$

Since the experimentally measured hadronic cross sections do not decrease with at energies, the number of partial waves contributing to the scattering increases with the energy. At high energies, this allows to convert the sum (2.11) into an integral

$$A(s, t) = 16\pi \int_{l=\frac{1}{2}}^{\infty} dl (2l+1) a_l(s) P_l(\cos\theta) \quad (2.15)$$

using for  $a_l(s)$  the analytic continuation in  $l$ . Eq. (2.15) can be written using (2.12),

$$P_l(\cos\theta) \rightarrow J_0((2l+1)\sin(\theta/2)) \quad \text{for} \quad l \rightarrow \infty \quad (2.16)$$

and

$$J_0(z) = \frac{1}{2\pi} \int_0^{2\pi} d\varphi \exp(iz \cos \varphi) \quad \text{with} \quad \vec{B} \cdot \vec{q} = \vec{B} \cdot \vec{q}_\perp = Bq_\perp \cos \varphi \quad (2.17)$$

in the form

$$A(s, t) = 4s \int d^2\vec{B} a(\vec{B}, s) e^{i\vec{q} \cdot \vec{B}}. \quad (2.18)$$

In the last step the impact parameter amplitude  $a(\vec{B}, s)$  was introduced with

$$a(\vec{B}, s) = a_l(s)|_{l=kB}. \quad (2.19)$$

Eq. (2.18) shows that the impact parameter amplitude is the Fourier transform of the elastic scattering amplitude. Inverting (2.18) one gets

$$a(\vec{B}, s) = \frac{-i}{4\pi s} \int \frac{d^2\vec{q}_\perp}{2\pi} A(s, t) e^{-i\vec{q}_\perp \cdot \vec{B}} \quad \vec{q}_\perp^2 = t \quad (2.20)$$

In analogy to geometrical optics, the function  $a(\vec{B}, s)$  can be interpreted as the density function for sources of scattered waves producing interference patterns.

Using the impact parameter representation, the total and the elastic cross sections can be written as

$$\begin{aligned} \sigma_{\text{tot}} &= 4 \int d^2\vec{B} \Im m(a(s, \vec{B})) \\ \sigma_{\text{ela}} &= 4 \int d^2\vec{B} |a(s, \vec{B})|^2. \end{aligned} \quad (2.21)$$

If the complex phase of  $a(\vec{B}, s)$  is independent of  $\vec{B}$ , the elastic slope  $b_{\text{ela}}(s)$  is given by [24]

$$b_{\text{ela}}(s) = \frac{\int d^2\vec{B} \vec{B}^2 a(s, \vec{B})}{2 \int d^2\vec{B} a(s, \vec{B})}. \quad (2.22)$$

Eq. (2.22) has a simple physical interpretation: the elastic slope  $b_{\text{ela}}(s)$  is a measure of the transverse size of the scattering objects.

## 2.3 Born-graph amplitudes and cross sections

The details concerning amplitudes and cross sections are given in Ref. [19]. Here, only the basic steps and results are discussed.

The total scattering cross sections are effectively parametrized by pomeron and reggeon amplitudes. Pomeron exchange involves mainly soft processes, but with increasing collision energy also hard processes become important. Hence, the Born-graph amplitudes are built up as a sum of soft and hard sub-amplitudes. This makes it possible to use the QCD-improved Parton Model for the calculation of hard interactions together with results obtained by general Regge arguments.

In the following we assume that hadronic interactions at high energies can be described by the exchange of a single effective pomeron. The pomeron exchange is taken to correspond to graphs with multiperipheral kinematics [25]. The total pomeron cross section can be calculated from the discontinuity of the elastic scattering amplitude. The optical theorem relates the discontinuity of the pomeron amplitude to diagrams with all possible final states (see Fig. 2.1). In order to get the cross section corresponding to such diagrams one has to sum and integrate over these states as intermediate particles with the momenta  $q_i$ . In general, the calculation of the cross section is not possible within perturbative QCD. However, the integration over the transverse momenta of the

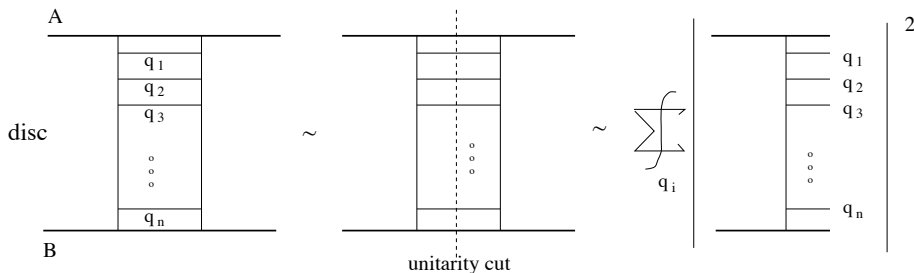


Figure 2.1: *Graphical presentation of the optical theorem: the discontinuity of the elastic scattering amplitude at vanishing momentum transfer can be considered as a unitarity cut through all intermediate particle propagators, restricting these particles to the mass shell. Besides trivial kinematical factors, the discontinuity corresponds to the total cross section.*

intermediate states can be split into two parts, the integration over momenta with  $p_{\perp} < p_{\perp}^{\text{cutoff}}$  and the integration over momenta with  $p_{\perp} \geq p_{\perp}^{\text{cutoff}}$ . The graphs are artificially subdivided into two classes, the first describes only *soft* processes and the second sums all the other graphs with at least one large momentum transfer (*hard* processes). For simplicity, all intermediate states are assumed to be partons. Soft and hard processes are distinguished by applying the transverse momentum cutoff  $p_{\perp}^{\text{cutoff}}$  to these partons.

For simplicity, in the model an exponential  $t$ -dependence is assumed for all amplitudes

$$A(s, t) = is\sigma_{\text{tot}}^{\text{Born}} \exp(b(s)t) \quad \text{with} \quad b(s) = \frac{1}{2}b_{\text{ela}}(s). \quad (2.23)$$

Furthermore, the real part of the amplitudes is neglected. In the program, there exist the possibility to use Regge signature factors together with finite energy sum rules to calculate also the real part of the amplitudes (see for example [26]). Within this approximation the amplitudes are determined by the total Born-graph cross sections together with the elastic slope parameters in forward direction. The amplitude (2.23) in impact parameter representation reads

$$a(s, \vec{B}) = \frac{\sigma_{\text{tot}}^{\text{Born}}}{16\pi b(s)} \exp\left(-\frac{\vec{B}^2}{4b(s)}\right). \quad (2.24)$$

In the following, the calculation of the total cross sections and the corresponding slope parameters is discussed.

### 2.3.1 Hadron-hadron interactions

Hadronic interactions involving transverse momenta being greater than the transverse momentum cutoff  $p_{\perp}^{\text{cutoff}}$  are considered as hard. Taking  $p_{\perp}^{\text{cutoff}} \gg \Lambda_{\text{QCD}}$  the cross section can be calculated within the Parton Model

$$\begin{aligned} \sigma^{\text{hard}}(s, p_{\perp}^{\text{cutoff}}) &= \int dx_1 dx_2 d\hat{t} \\ &\times \sum_{i,j,k,l} \frac{1}{1 + \delta_{k,l}} f_{A,i}(x_1, Q^2) f_{B,j}(x_2, Q^2) \frac{d\sigma_{i,j \rightarrow k,l}^{\text{QCD}}(\hat{s}, \hat{t})}{d\hat{t}} \Theta(p_{\perp} - p_{\perp}^{\text{cutoff}}), \end{aligned} \quad (2.25)$$

where  $f_{A,i}(x_1, Q^2)$  and  $f_{B,i}(x_2, Q^2)$  are the parton distribution functions of particle  $A$  and  $B$  for the parton  $i$ . The Mandelstam variables of the partonic scattering process are denoted by  $\hat{s}, \hat{t}$  and  $\hat{u}$ . For example, a hard interaction via gluon-quark scattering is shown in Fig. 2.2.

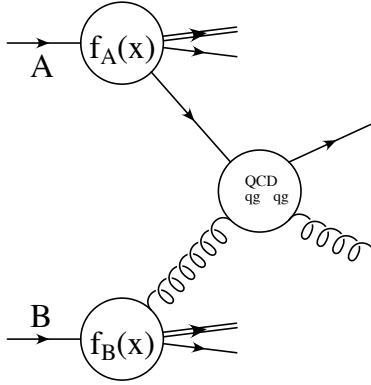


Figure 2.2: *Gluon-quark scattering as an example of a hard hadronic interaction.*

All the graphs of lowest order perturbative QCD form the *hard* part of the pomeron (hard pomeron). It is assumed that the remaining part can be described by a supercritical *soft* pomeron together with an effective reggeon. The resulting soft cross sections are parametrized by

$$\sigma_{A,B}^{\mathcal{P}}(s) = g_{A,\mathcal{P}}(0) g_{B,\mathcal{P}}(0) \left( \frac{s}{s_0} \right)^{\Delta_{\mathcal{P}}} \quad (2.26)$$

$$\sigma_{A,B}^{\mathcal{R}}(s) = g_{A,\mathcal{R}}(0) g_{B,\mathcal{R}}(0) \left( \frac{s}{s_0} \right)^{\Delta_{\mathcal{R}}} \quad (2.27)$$

with  $\Delta_{\mathcal{P}} = \alpha_{\mathcal{P}}(0) - 1$  and  $\Delta_{\mathcal{R}} = \alpha_{\mathcal{R}}(0) - 1$ . Here we denote with  $\alpha_{\mathcal{P}}(0)$  ( $\alpha_{\mathcal{R}}(0)$ ) the pomeron (reggeon) intercept, and with  $g_{A,\mathcal{P}}, g_{B,\mathcal{P}}$  ( $g_{A,\mathcal{R}}, g_{B,\mathcal{R}}$ ) the couplings of the pomeron (reggeon) to the particle  $A$  and  $B$ , respectively. It should be emphasized that the intercept  $\alpha_{\mathcal{P}}(0)$  is an effective parameter which depends on the transverse momentum cutoff  $p_{\perp}^{\text{cutoff}}$  and the parton distribution functions (PDFs) used in the calculation of the hard part.

The subdivision of hadronic interactions into soft and hard processes is totally artificial. Changing the transverse momentum cutoff, the cross sections of the hard and the soft part change. But within the model, the couplings and intercepts are adjusted in such a way, that the sum of soft and hard cross sections becomes almost independent on the cutoff. It should be mentioned that for values of  $p_{\perp}^{\text{cutoff}}$  below 2 GeV/c it is not possible to get a cutoff-independent total Born-graph cross section.

### 2.3.2 Photon-hadron and photon-photon interactions

To take into account the dual nature of the photon, the physical photon is subdivided into two states, the *bare* and the *hadronic* photon

$$|\gamma\rangle = \sqrt{Z_3} |\gamma_{\text{bare}}\rangle + |\gamma_{\text{had}}\rangle, \quad (2.28)$$

with  $Z_3$  being a normalization constant. According to the Vector Dominance Model (VDM, for a review see [27]), the hadronic part of the photon is built up by a superposition of hadronic states having the quantum numbers  $J^{PC} = 1^{--}$  as the photon. The mass (and hence the life-time) of these hadronic states ( $q\bar{q}$ -fluctuations) varies within a wide range. In the model, this is approximated by treating  $|\gamma_{\text{had}}\rangle$  as a superposition of low-mass vector mesons ( $\rho^0$ ,  $\omega$  and  $\phi$ , denoted by  $|q\bar{q}\rangle$ ) and an effective resonance state (denoted by  $|q\bar{q}^*\rangle$ )

$$|\gamma_{\text{had}}\rangle = \frac{e}{f_{q\bar{q}}} |q\bar{q}\rangle + \frac{e}{f_{q\bar{q}^*}} |q\bar{q}^*\rangle. \quad (2.29)$$

Here,  $e$  and  $e/f_{q\bar{q}}$ ,  $e/f_{q\bar{q}^*}$  denote the elementary charge and the VDM couplings to the  $|q\bar{q}\rangle$ ,  $|q\bar{q}^*\rangle$  states. With (2.29) the factor  $Z_3$  becomes

$$Z_3 = 1 - \frac{e^2}{f_{q\bar{q}}^2} - \frac{e^2}{f_{q\bar{q}^*}^2}. \quad (2.30)$$

In the following the Born-graph cross sections used to characterize photon-hadron scattering are discussed. The photon-photon cross sections are obtained from the photon-hadron cross sections by substituting the hadron by a photon.

In the model, direct and resolved photon interactions are distinguished.

(i) Direct photon interaction, i.e. the photon participates directly in the scattering process. For interactions involving sufficiently large momentum transfer, this contribution is estimated by

$$\sigma_{\text{dir}}(s, p_{\perp}^{\text{cutoff}}) = \int dx d\hat{t} \sum_{i,k,l} f_{B,i}(x, Q^2) \frac{d\sigma_{\gamma, i \rightarrow k, l}(\hat{s}, \hat{t})}{d\hat{t}} \Theta(p_{\perp} - p_{\perp}^{\text{cutoff}}), \quad (2.31)$$

where  $f_{B,i}(x, Q^2)$  denotes the PDF of particle  $B$  for the parton  $i$  and the sum runs over all possible parton configurations  $i, k, l$ .

Within the Parton Model at lowest order perturbative QCD only the two processes, photon-gluon fusion and gluon Compton scattering contribute (shown in Fig. 2.3).

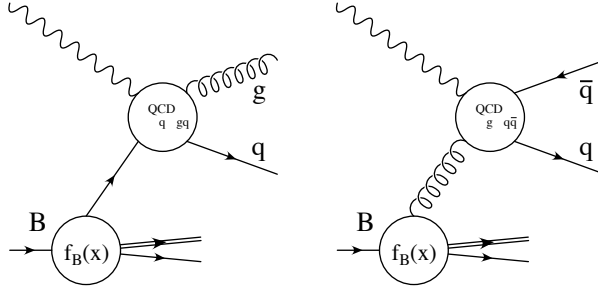


Figure 2.3: *Hard direct photon-hadron interaction: a) gluon Compton scattering and b) photon-gluon fusion.*

In photon-photon collisions, also (double-) direct interactions are considered. In the model, the graph shown in Fig. 2.4 is implemented.

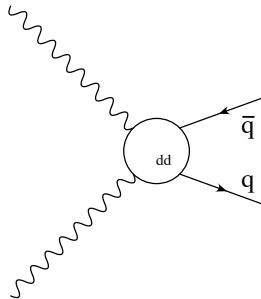


Figure 2.4: *Direct photon-photon interaction.*

(ii) Resolved photon interaction, i.e. the photon fluctuates into a  $q\bar{q}$  pair which interacts hadronically. Similar to the model for hadron-hadron collisions, this contribution is split into hard interactions and the remaining soft interactions. The cross section for hadronic subprocesses involving

transverse momenta being greater than the transverse momentum cutoff  $p_{\perp}^{\text{cutoff}}$  are given by

$$\sigma_{\text{res}}^{\text{hard}}(s, p_{\perp}^{\text{cutoff}}) = \int dx_1 dx_2 d\hat{t} \times \sum_{i,j,k,l} \frac{1}{1 + \delta_{k,l}} f_{\gamma,i}(x_1, Q^2) f_{B,j}(x_2, Q^2) \frac{d\sigma_{i,j \rightarrow k,l}^{\text{QCD}}(\hat{s}, \hat{t})}{d\hat{t}} \Theta(p_{\perp} - p_{\perp}^{\text{cutoff}}), \quad (2.32)$$

where  $f_{\gamma,i}(x_1, Q^2)$  and  $f_{B,i}(x_2, Q^2)$  are the PDFs of the photon and particle  $B$  for the parton  $i$  (for example, see Fig. 2.5). Since the full parton distribution function of the photon is used in (2.32)

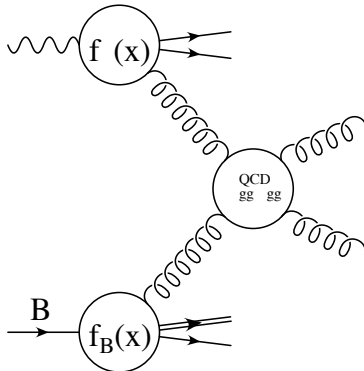


Figure 2.5: *Gluon-gluon scattering as an example of a hard resolved photon-hadron interaction.*

not only the VDM part but also the anomalous part of the photon structure function enters the resolved hard cross section.

The soft pomeron/reggeon cross sections are parametrized similar to (2.27) by

$$\sigma_{B,\mathbb{P}}^{\text{tot}}(s) = \frac{e^2}{f_{q\bar{q}}^2} g_{q\bar{q},\mathbb{P}}(0) g_{B,\mathbb{P}}(0) \left( \frac{s}{s_0} \right)^{\Delta_{\mathbb{P}}} \quad (2.33)$$

$$\sigma_{B,\mathbb{R}}^{\text{tot}}(s) = \frac{e^2}{f_{q\bar{q}}^2} g_{q\bar{q},\mathbb{R}}(0) g_{B,\mathbb{R}}(0) \left( \frac{s}{s_0} \right)^{\Delta_{\mathbb{R}}} \quad (2.34)$$

with  $g_{q\bar{q},\mathbb{P}}$  and  $g_{q\bar{q},\mathbb{R}}$  denoting the couplings of the pomeron and reggeon to the  $q\bar{q}$ -fluctuation of the photon.

## 2.4 Cross sections involving weakly virtual photons

The influence of a weak photon virtuality  $P^2$  on the total cross section is estimated using arguments of GVDM. For definiteness let's consider the photon-photon cross section at  $e^+e^-$  colliders. The total cross section can be divided into partial cross sections according to the photon polarizations ( $T$  ( $S$ ) for transverse (scalar) photons, see Ref. [28,29])

$$\begin{aligned} \sigma_{\gamma\gamma}^{\text{tot,exp}}(P_1^2, P_2^2, s) &= \sigma_{TT}^{\text{tot}}(P_1^2, P_2^2, s) + \epsilon_1 \sigma_{ST}^{\text{tot}}(P_1^2, P_2^2, s) \\ &+ \epsilon_2 \sigma_{TS}^{\text{tot}}(P_1^2, P_2^2, s) + \epsilon_1 \epsilon_2 \sigma_{SS}^{\text{tot}}(P_1^2, P_2^2, s). \end{aligned} \quad (2.35)$$

The polarization parameters  $\epsilon_i$  depend on the electron beams creating the photon flux. For unpolarized electron beams the value of  $\epsilon$  was found to be close to 1 (see for example [30]). In the following we use the approximation suggested in [29], setting  $\epsilon_1 = \epsilon_2 = 1$ . The experimental cross section is parametrized by [29]

$$\sigma_{\gamma\gamma}^{\text{tot,exp}}(P_1^2, P_2^2, s) = \sigma_{\gamma\gamma}^{\text{tot}}(0, 0, s) F(P_1^2) F(P_2^2) \quad (2.36)$$

with

$$F(P^2) = \sum_{V=\rho,\omega,\phi} r_V \frac{1 + P^2/(4m_V^2)}{(1 + P^2/m_V^2)^2} + r_{\text{eff}} \frac{1}{1 + P^2/m_{\text{eff}}^2}, \quad F(0) = 1. \quad (2.37)$$

The influence of high-mass vector mesons and continuum contributions is taken into account by the last term of the sum. The parameters occurring in Eq. (2.37) are given in [29].

The suppression of the parton content of the photon due to the photon virtuality  $P^2$  is approximated by the parametrizations [31–33]

$$f_{\gamma,q_i}(x, Q^2, P^2) = f_{\gamma,q_i}(x, Q^2) \frac{\ln Q^2/(P^2 + m_\rho^2)}{\ln Q^2/m_\rho^2} \quad (2.38)$$

$$f_{\gamma,g}(x, Q^2, P^2) = f_{\gamma,g}(x, Q^2) \frac{\ln^2 Q^2/(P^2 + m_\rho^2)}{\ln^2 Q^2/m_\rho^2}. \quad (2.39)$$

This effective treatment of the photon virtuality is a good approximation for small values of  $P^2$ . However, for virtualities  $P^2 \sim p_\perp^{\text{cutoff}}$  it cannot be justified and may be invalid.

## 2.5 Unitarization

### 2.5.1 General remarks

Both soft and hard Born-graph cross sections increase with energy like powers of  $s$  whereas the total cross section is proportional to  $(\ln s)^2$  so that the input cross sections exceed the Froissart bound [34] and hence the total cross section at high energies. Assuming that the Born-graph cross sections are correctly calculated, this is a clear sign that unitarity corrections become more and more important with increasing collision energies.

It is also clear that a simple pomeron-pole description of the total cross sections [35] violates unitarity at high energies. The partial wave decomposition of the scattering amplitude can be used to estimate the energy region where the single-pomeron exchange model becomes invalid. At high energies, the total cross section is approximated by (considering, for example, the scattering of two hadrons  $A$ )

$$\sigma_{\text{tot}} = g_{A,P}(0)g_{A,P}(0) \left(\frac{s}{s_0}\right)^{\Delta_P}. \quad (2.40)$$

Assuming an exponential  $t$ -dependence of the coupling

$$g_{A,P}(t) = g_0 \exp\left(\frac{1}{2}b_0 t\right), \quad (2.41)$$

the imaginary part of the elastic scattering amplitude reads

$$\Im m A^{\text{ela}}(s, t) = s_0 g_0^2 \left(\frac{s}{s_0}\right)^{\alpha_P(0)} \exp\left\{\left(b_0 + \alpha'_P(0) \ln\left(\frac{s}{s_0}\right)\right) t\right\} \quad (2.42)$$

with the impact parameter representation

$$a(s, \vec{B}) = \frac{g_0^2}{8\pi(b_0 + \alpha'_P(t) \ln(\frac{s}{s_0}))} \left(\frac{s}{s_0}\right)^{\Delta_P} \exp\left(-\frac{\vec{B}^2}{4(b_0 + \alpha'_P(t) \ln(\frac{s}{s_0}))}\right). \quad (2.43)$$

From Eq. (2.13) follows that unitarity is violated for

$$\frac{g_0^2}{16\pi(b_0 + \alpha'_P(t) \ln(\frac{s}{s_0}))} \left(\frac{s}{s_0}\right)^{\Delta_P} > 1. \quad (2.44)$$

## 2.5.2 Gribov's Reggeon field theory

Within the Reggeon field theory the dominant unitarity corrections (absorptive corrections) are given by graphs with multiple pomeron exchange as shown in Fig. 2.6. As a consequence, the average multiplicities of hard and soft interactions in an inelastic event increase with the energy. At high energy a sizable part of events has more than one soft or hard interaction.

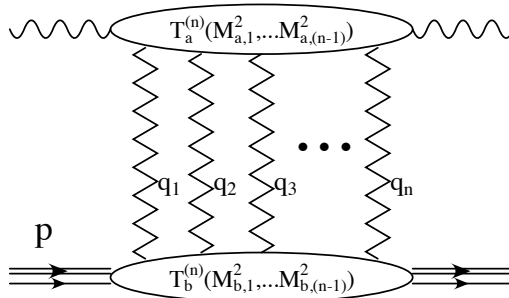


Figure 2.6: *Multiple pomeron exchange graph.*

The calculation of the absorptive corrections in the framework of Gribov's reggeon calculus [7,8] and the assumption that the multiple discontinuity (see Fig. 2.6)

$$N_a^{(n)}(\vec{q}_i) = \int \frac{dM_{a,1}^2}{\pi} \dots \frac{dM_{a,(n-1)}^2}{\pi} \text{disc}_{M_{a,1}^2 \dots M_{a,(n-1)}^2} T_a^{(n)}(\vec{q}_i, M_{a,1}^2, \dots, M_{a,(n-1)}^2) \quad (2.45)$$

can be approximated by the product of pole contributions (i.e. coupling constants)

$$N_a^{(n)}(\vec{q}_i) \approx \prod_{k=1}^n g_{P,a}(\vec{q}_k) \quad (2.46)$$

lead to the standard eikonal approximation (see for example [36] and references therein).

Usually, absorptive corrections involving elastically scattered hadrons as intermediate states are considered only. In this case, intermediate hadronic states with masses higher than the incoming particles are neglected. It is known from hadron-hadron collider experiments that the total diffractive cross section at high energies becomes comparable to the elastic cross section. In  $\gamma p$  collisions at HERA, the cross section of photon diffraction even exceeds the cross section of quasi-elastic  $\rho^0$  production. Therefore, inelastic absorptive corrections due to diffractive intermediate states are important. The main contribution to these corrections results from diffractive states with low masses. For definiteness, let's consider the diffractive contribution given by the two Pomeron exchange graph shown in Fig. 2.7. In Fig. 2.7 (a), the dashed line indicates that the unitarity cut along this line is considered. According to the optical theorem this cut can be expressed as the sum/integral of the squared graphs shown in Fig. 2.7 (b) and (c). In the model, the unitarity sum running over all possible intermediate states is split into elastic, low-mass and high-mass states. In the following diffractively produced particle systems with a squared mass lower than  $\Sigma_L = 5\text{GeV}^2$  are called low mass excitations. In the case of the photon as incoming particle the quasi-elastically produced vector mesons  $\rho^0$ ,  $\omega$  and  $\phi$  are considered as elastic states. Assuming multiperipheral kinematics one can use Regge theory to estimate the amplitudes for the elastic and high-mass intermediate states. The low-mass states can be treated by summing all possible resonances up to a certain mass scale. In order to get an efficient approximation, it is reasonable to introduce for hadron  $A$  and  $B$  generic low-mass resonances  $A^*$  and  $B^*$  as done in Ref. [37]. For photons, the corresponding low-mass resonance is identified with the  $|qq^*\rangle$  state. The contributions of higher diffractive masses  $M_D^2 > \Sigma_L$  to the diffractive cut are calculated using the triple- and loop-pomeron graphs (see Fig. 2.8) [38,37]. For example, the differential triple-pomeron cross section reads

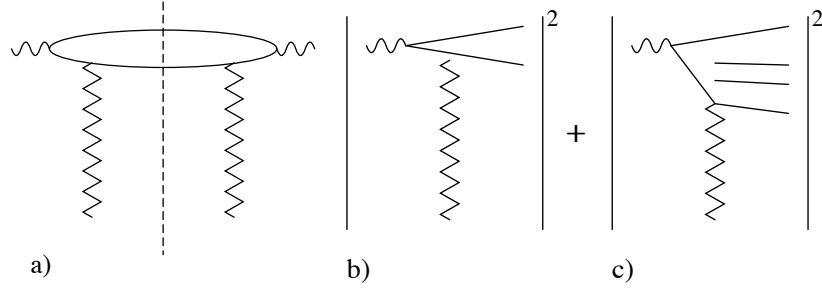


Figure 2.7: Approximation of the diffractive contribution resulting from the two pomeron graph: a) Two pomeron graph with diffractive cut, b) low-mass and elastic states, and c) multiperipheral high-mass states.

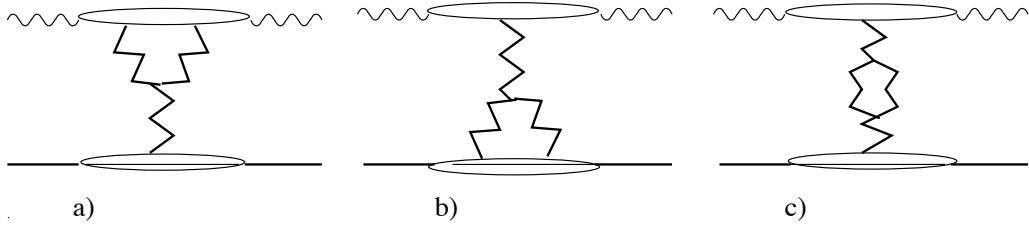


Figure 2.8: Examples of the enhanced graphs: a) triple-pomeron graph (high-mass state on photon side), b) triple-pomeron graph (high-mass state on hadron side), c) loop pomeron graph (high-mass intermediate states on both sides)

$$\frac{d\sigma_T}{dt dM_D^2} = -\frac{1}{16\pi s^2} g_{P,q\bar{q}}(0) g_{PPP}(t) g_{P,p}^2(t) \left(\frac{M_D^2}{s_0}\right)^{\alpha_P(0)} \left(\frac{s}{M_D^2}\right)^{2\alpha_P(t)}. \quad (2.47)$$

The couplings of the effective resonance states to the pomeron/reggeon are connected by finite mass sum rules to the couplings of the elastic hadronic states and the triple-pomeron coupling [19].

At higher energies (above  $\sqrt{s} \approx 500$  GeV) it is necessary to include further graphs in the unitarization [39]. The dominant higher-order graphs are shown in Fig. 2.9.

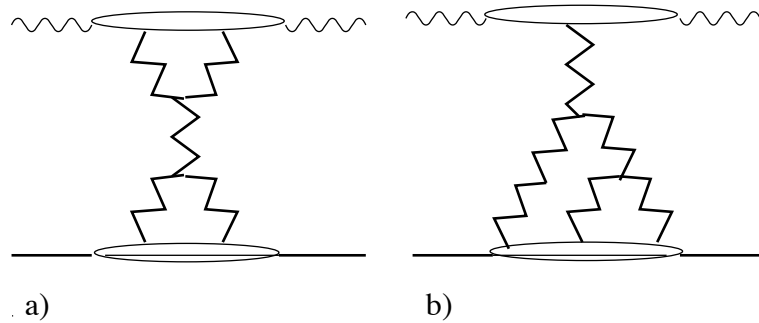


Figure 2.9: Examples of enhanced graphs reducing the total size of diffraction at high energies: a) X-iterated triple-pomeron graph, and b) YY-iterated triple pomeron graph.

Note that the introduction of intermediate hadronic states which differ from the initial hadronic particles increases the total amount of multiple interactions and absorption considerably.

The absorptive corrections to the direct photon interactions are suppressed by the factor  $e^2/f^2$  and can be neglected. Therefore, only the resolved Born amplitude is unitarized by eikonalization. Note that the hadronic states of the photon are used for unitarization instead of the photon itself. Therefore it is necessary to calculate the  $q\bar{q}$ -hadron and  $q\bar{q}$ - $q\bar{q}$  cross sections. This is done by

factorizing out the VDM couplings. The parton distribution function of the  $|q\bar{q}\rangle$ -states is taken to be

$$f_{q\bar{q}}(x, Q^2) = f_{q\bar{q}^*}(x, Q^2) = f_\gamma(x, Q^2) \left( \frac{e^2}{f_{q\bar{q}}^2} + \frac{e^2}{f_{q\bar{q}^*}^2} \right)^{-1} \quad (2.48)$$

In impact parameter representation, the eikonized scattering amplitude for resolved photon interactions is given by

$$a_{\text{res}}(s, \vec{B}) = \frac{i}{2}(1 - e^{-\chi(s, \vec{B})}) \quad (2.49)$$

with the eikonal function

$$\chi(s, \vec{B}) = \chi_S(s, \vec{B}) + \chi_H(s, \vec{B}) + \chi_D(s, \vec{B}) + \chi_C(s, \vec{B}). \quad (2.50)$$

Here,  $\chi_i(s, \vec{B})$  denotes the contributions from the different Born graph amplitudes  $a_i(s, \vec{B})$ : (S) soft (pomeron and reggeon), (H) hard, (T) triple- and loop-pomeron amplitudes, and (C) higher order corrections (shown in Fig. 2.9). All the partial eikonal functions  $\chi_i(s, \vec{B})$  are approximated by

$$\chi_i(s, \vec{B}) = 2a_i(s, \vec{B}) = \frac{\sigma_i(s)}{8\pi b_i(s)} \exp \left\{ -\frac{\vec{B}^2}{4 b_i(s)} \right\} \quad (2.51)$$

with

$$\sigma_i(s) = 2 \int d^2 \vec{B} \chi_i(s, \vec{B}). \quad (2.52)$$

Here,  $b_i(s)$  is the energy dependent slope parameter of the amplitude  $i$ .

Once the total amplitude and its decomposition is known cross sections can be calculated. For example, with the normalization (2.2) the cross sections for photon-hadron scattering are given by:

$$\sigma_{\text{tot}} = 4 \int d^2 \vec{B} \Im m \left( Z_3 a_{\text{dir}}(s, \vec{B}) + \langle \gamma_{\text{had}}, p | a_{\text{res}}(s, \vec{B}) | \gamma_{\text{had}}, p \rangle \right) \quad (2.53)$$

$$\sigma_{\text{ela}} = 4 \int d^2 \vec{B} \left| Z_3 a_{\text{dir}}(s, \vec{B}) + \langle \gamma_{\text{had}}, p | a_{\text{res}}(s, \vec{B}) | \gamma_{\text{had}}, p \rangle \right|^2 \quad (2.54)$$

$$\begin{aligned} \frac{d\sigma_{\text{ela}}}{dt} &= 4\pi \left| \int_0^\infty B dB J_0(B\sqrt{-t}) \right. \\ &\quad \left. \times \left( Z_3 a_{\text{dir}}(s, \vec{B}) + \langle \gamma_{\text{had}}, p | a_{\text{res}}(s, \vec{B}) | \gamma_{\text{had}}, p \rangle \right) \right|^2 \end{aligned} \quad (2.55)$$

$$\sigma_{\text{qel}} = 4 \int d^2 \vec{B} \left| \langle q\bar{q}, p | a_{\text{res}}(s, \vec{B}) | \gamma, p \rangle \right|^2 \quad (2.56)$$

where the impact parameter amplitude  $a_{\text{dir}}(s, \vec{B})$  parametrizes the direct photon interaction.

## 2.6 Determination of model parameters

As a result of the unitarization one gets an effective scattering amplitude describing total, elastic and diffractive cross sections in hadron-hadron, hadron-photon and photon-photon scattering involving a number of free parameters (couplings, intercepts and slope parameters).

Assuming universality of the soft hadronic interaction, Regge factorization can be applied. For example, the couplings  $g_{B, \mathbb{P}}$ ,  $g_{B, \mathbb{R}}$  and the pomeron (reggeon) intercept  $\alpha_{\mathbb{P}}(0)$  ( $\alpha_{\mathbb{R}}(0)$ ) in Eq. (2.34) are the same as in (2.27). This strongly reduces the free parameter of the model. For example,  $p\bar{p}$  cross sections are used to determine the proton-pomeron coupling  $g_{p, \mathbb{P}}$ , the triple pomeron coupling  $g_{\mathbb{P}\mathbb{P}\mathbb{P}}(0)$ , and the effective intercept  $\alpha_{\mathbb{P}}(0)$  of the soft pomeron. Once these parameters are fixed, one can fit photoproduction cross sections to get an estimate for the  $g_{q\bar{q}, \mathbb{P}}$  coupling. The details of the fits are given in [19]. It should be mentioned that due to the strong correlation of the couplings

$e^2/f_i^2$  and  $g_{i,P}$  ( $i = q\bar{q}, q\bar{q}^*$ ) it is not possible to fix all the parameters for  $\gamma p$  scattering by a global fit to photoproduction data alone.

Note, that using different PDFs for hadrons and photons in the cross section calculations, the universality assumption is restricted to the low- $p_\perp$  contributions of hadronic interactions. For the high- $p_\perp$  part of the interactions, the well tested QCD improved Parton Model is applied.

Especially the asymmetric  $\gamma p$  reaction channel can be used to test the model. For example, since the proton-pomeron coupling  $g_{p,P}$  is larger than the coupling of the  $q\bar{q}$ -pomeron coupling  $g_{P,q\bar{q}}$ , the model predicts a ratio between the photon and proton diffraction dissociation cross sections in the range 1.6 to 2.0 (see Eq. (2.47)). This has also important consequences for the inelastic final states.

Within the model, all the parameters necessary to describe  $\gamma\gamma$  collisions can be determined by fitting  $pp$ ,  $p\bar{p}$  and  $\gamma p$  cross sections and slopes. This means that the model results on  $\gamma\gamma$  scattering are obtained without introducing new parameters and can be used to test the predictive power of the approach.

Finally it should be emphasized that the model parameters and also the model predictions depend strongly on the parton distribution functions used for the cross section fits.

## Chapter 3

# Multiparticle production

### 3.1 Cutting rules and cross sections

Besides trivial kinematical factors, the discontinuity of the scattering amplitude taken at vanishing momentum transfer corresponds to the total cross section (see (2.4)). The discontinuity of a graph can be considered as a unitarity cut through intermediate particle propagators, moving these particles on mass shell (see Fig. 2.1). In general, there are many possibilities to cut such diagrams. If one considers graphs involving multiple pomerons, the number of cuts increases further. In the high-energy limit, the contribution of the leading cut configurations to the total discontinuity can be calculated using the Abramovskii-Gribov-Kancheli (AGK) cutting rules [40].

Let us recall the basic results of AGK needed for the following discussion.

- The dominant contributions are given by cut configurations where the cut involves all intermediate particle states of a pomeron (a contribution due to a partially cut pomeron is subleading).
- For a graph with  $n$ -pomeron exchange, the contribution to the discontinuity with  $\nu$  cut pomeron propagators is  $B_\nu^n \text{Im} (A^{(n)})$ . Here,  $A^{(n)}$  denotes the  $n$ -pomeron amplitude and  $\nu$  is restricted to  $(0 \leq \nu \leq n)$ . The combinatorial weight factors  $B_\nu^n$  are

$$B_\nu^n = \begin{cases} (-1)^{n-\nu-1} \frac{n!}{\nu!(n-\nu)!} 2^{n-1} & : \nu \geq 1 \\ (-1)^{n-1} (2^{n-1} - 1) & : \nu = 0 \end{cases} \quad (3.1)$$

- The coefficients  $B_\nu^n$  satisfy

$$\sum_{\nu=0}^n B_\nu^n = 1 \quad (3.2)$$

which means that all leading contributions to the total discontinuity are included.

The factors  $B_\nu^n$  are called AGK weights since they give the relative size of the  $\nu$ -pomeron cut in reference to the total discontinuity of the  $n$ -pomeron graph.

For example, the total discontinuity of the two-pomeron exchange graph shown in Fig. 3.1 can be subdivided into the diffractive cut with the weight -1 (Fig. 3.1 (a)), the one-pomeron cut with the weight 4 (Fig. 3.1 (b)), and the two-pomeron cut with the weight -2 (Fig. 3.1 (c)).

In eikonal approximation, the two-pomeron amplitude is given in impact parameter representation by

$$a^{(2)}(s, \vec{B}) = -\frac{i}{2} \frac{(\chi_P(s, \vec{B}))^2}{2!}. \quad (3.3)$$

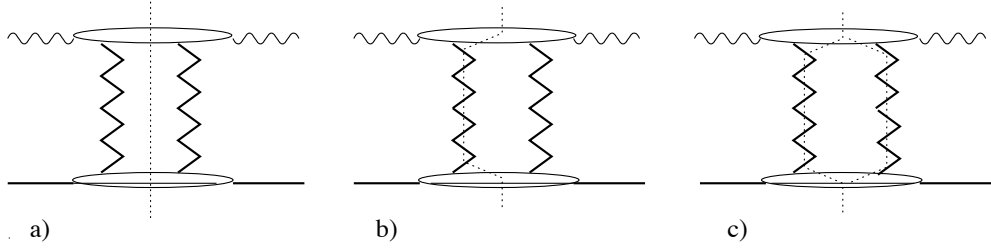


Figure 3.1: *The total discontinuity of the two-pomeron exchange graph of the eikonal sum: a) the diffractive cut describing low-mass diffraction, b) the one-pomeron cut, and c) the two-pomeron cut.*

The imaginary part of this amplitude has negative sign (absorptive correction). However, applying the AGK cutting rules one gets a positive elastic/diffractive contribution of this graph to the total cross section since the corresponding AGK factor is  $(-1)$ . In contrast, the one-pomeron cut of this graph gives a negative contribution to the total cross section and manifests the absorptive character of the two-pomeron exchange. However, since the structure of the one-pomeron cut is independent on the total numbers of pomerons involved in the graph, one has to sum the one-pomeron cuts of all graphs to get the total cross section of this final state configuration. Taking this into account, the partial cross sections for  $n$ -pomeron cuts become positive even if some graphs are contributing with negative sign.

The cutting rules can be extended for different pomerons or particles. For simplicity, in the following formulae we neglect again the effective resonance states  $p^*$  and  $q\bar{q}^*$ . The complete expressions will be given in [41]. Then the amplitude  $a_{\text{res}}(s, B)$  Eq. (2.49) can be written in the following form

$$a_{\text{res}}(s, \vec{B}) = -\frac{i}{2} \sum_{k+l+m+n=1}^{\infty} \frac{(-1)^{k+l+m+n}}{k! l! m! n!} \chi_S(s, \vec{B})^k \chi_H(s, \vec{B})^l \chi_D(s, \vec{B})^m \chi_C(s, \vec{B})^n \quad (3.4)$$

where each term with the variables  $(k, l, m, n)$  corresponds directly to the eikonal amplitude built up of  $k$  soft pomerons or reggeons,  $l$  hard pomerons,  $m$  triple- and loop-pomeron graphs, and  $n$  double-pomeron graphs.

Using (3.1), the discontinuity of (3.4) can be re-summed according to the number of cut Born graphs [42,43]. Within this scheme one gets the following impact parameter expression for the exclusive cross section for  $k_c$  cut soft pomerons,  $l_c$  cut hard pomerons,  $m_c$  cut triple- and loop-pomeron graphs and  $n_c$  cut double-pomeron graphs [12]

$$\sigma(k_c, l_c, m_c, n_c, s, \vec{B}) = \frac{(2\chi_S)^{k_c}}{k_c!} \frac{(2\chi_H)^{l_c}}{l_c!} \frac{(2\chi_D)^{m_c}}{m_c!} \frac{(2\chi_C)^{n_c}}{n_c!} \exp[-2\chi(s, \vec{B})] \quad (3.5)$$

with

$$\int d^2\vec{B} \sum_{k_c+l_c+m_c+n_c \geq 1}^{\infty} \sigma(k_c, l_c, m_c, n_c, s, \vec{B}) = \sigma_{\text{tot}} - \sigma_{\text{qel}}. \quad (3.6)$$

Using Eq. (3.5), the cross sections (probabilities) of the different cut configurations are calculated for event simulation. These cross sections depend only on the free parameters of the Born amplitudes determined by fits to cross section data.

In the scattering of virtual photons, events with  $k_c$  soft pomeron cuts ( $k_c \geq 2$ , multiple interaction) are suppressed with a factor

$$P_{\text{sup}} = \left( \frac{m_{\text{sup}}^2}{(P_1^2 + m_{\text{sup}}^2)} \frac{m_{\text{sup}}^2}{(P_2^2 + m_{\text{sup}}^2)} \right)^{k_c-1}, \quad (3.7)$$

where the effective mass  $m_{\text{sup}}$  is assumed to be the  $\rho$  mass.

It should be mentioned that after re-summation one cut triple- or loop-pomeron graph gives still a negative cross sections in the sum (3.5). The reason is simply the missing subdivision of these graphs into elementary pomeron cuts. Similar to the subdivision of the discontinuity of the two-pomeron graph, the cut of more complex graphs like the triple- or loop-pomeron graphs has to be resolved into elementary pomeron cuts. For example, in Fig. 3.2 the contributions to the discontinuity of a triple-pomeron graph is shown. Again, according to the number of cut pomerons

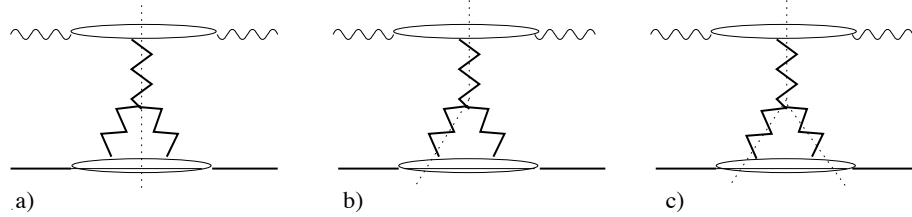


Figure 3.2: *The total discontinuity of the triple-pomeron graph can be approximated by the sum of three cuts: a) the diffractive cut describing high-mass diffraction (weight -1), b) the one-pomeron cut (weight 4), and c) the two-pomeron cut (weight -2).*

a re-summation is done to get finally positive cross sections for all cut configurations.

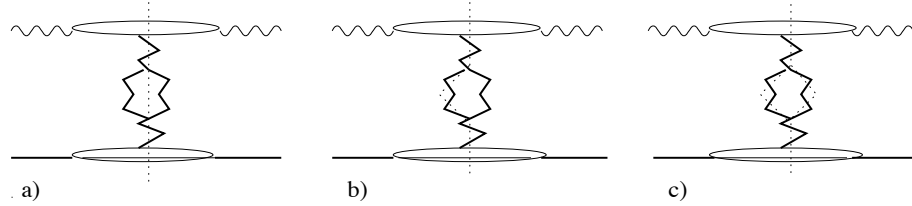


Figure 3.3: *The three different cuts contributing to the discontinuity of the loop-pomeron graph: a) the diffractive cut describing high-mass double diffraction (weight -1), b) the one-pomeron cut (weight 4), and c) the two-pomeron cut (weight -2).*

At HERA energies, the average number of cut pomerons per event is about 1.7.

To relate the cross sections (3.5) to parton configurations, the correspondence of the reggeon and pomeron exchange amplitudes to certain color flow topologies is used [44]. In Fig. 3.4 and Fig. 3.5 the color flows of a reggeon and pomeron exchange process (a) are shown together with the corresponding cut (b). Whereas a cut reggeon yields one color-field chain (string), a cut pomeron

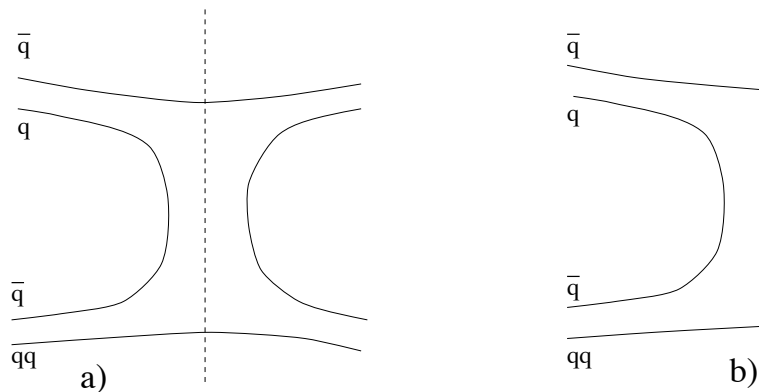


Figure 3.4: *Color flow picture of (a) a single reggeon exchange graph and (b) the corresponding unitarity cut*

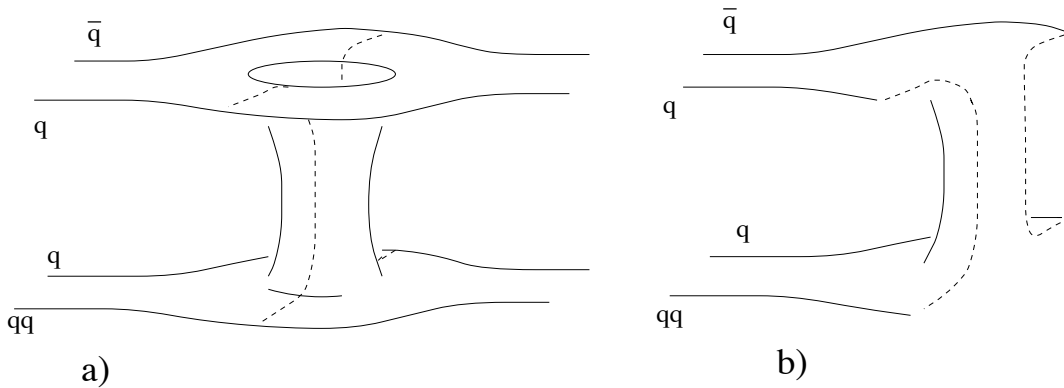


Figure 3.5: Color flow picture of (a) a one-pomeron exchange graph and (b) the corresponding unitarity cut

results in two chains assumed to fragment almost independently into hadrons. In the large  $N_c$  limit of QCD the color flow picture of the pomeron is found in hard interactions of partons (even with initial and final state radiation). This allows to identify the hard Parton Model cross sections (2.32) with the hard part of the single pomeron exchange cross section. Practically, the pomeron amplitude is split into a *soft* and *hard* part which enter the unitarization separately (see (3.4),(3.5)). Then the total discontinuity of a pomeron is given by the sum of the soft and the hard pomeron discontinuities as illustrated in Fig. 3.6. At high energies, the gluon-gluon scattering (shown in

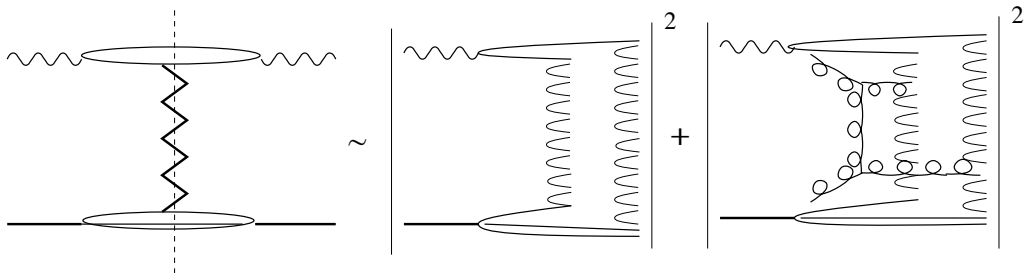


Figure 3.6: Unitarity cut of a one-pomeron exchange graph

Fig. 3.6) gives the dominant contribution to the hard cross section. The corresponding chain system is similar to the chains resulting from a soft pomeron cut, but with high- $p_\perp$  "kinks". In general, the hard scattered partons are connected to soft (low- $p_\perp$ ) partons by color strings.

Besides the single pomeron and reggeon cuts discussed so far, unitarity predicts also cuts involving not only one pomeron. For example, in Fig. 3.7 a diffractive cut of the two pomeron exchange amplitude is shown. The resulting chain system leads to a large rapidity gap between the final state hadrons. This chain system involves also the elastically scattered particles itself and is the basic configuration to describe low-mass diffraction. In Fig. 3.8 the diffractive triple pomeron cut and the chain system for photon high-mass diffractive dissociation is shown. As an example for another unitarity cut, a two pomeron cut (three different cuts are possible) is shown in Fig. 3.9. The chain system shown in this figure corresponds to a high multiplicity final state and is often called a multiple interaction event. It should be mentioned that each of the pomeron cut can involve hard parton configurations according to Fig. 3.6, but the dominant process is multiple soft interaction.

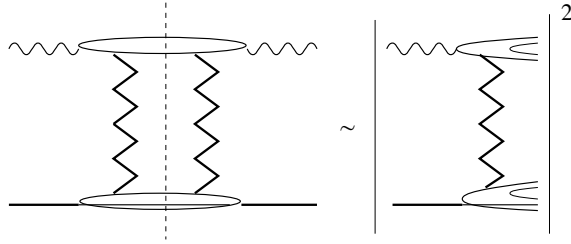


Figure 3.7: *Low mass diffractive dissociation*

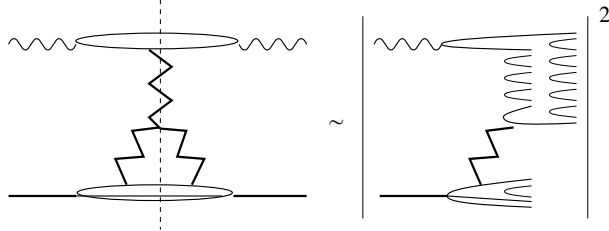


Figure 3.8: *High-mass photon diffractive dissociation*

## 3.2 Non-diffractive interactions

### 3.2.1 Low- $p_{\perp}$ final states

Within the Dual Parton Model the longitudinal momentum fractions of the partons connected to the chain ends in soft processes are given by Regge asymptotics [45–48]. One obtains for the valence quark ( $x$ ) and diquark ( $1 - x$ ) distribution inside proton

$$\rho(x) \sim \frac{1}{\sqrt{x}}(1 - x)^{1.5} \quad (3.8)$$

and for the quark antiquark distribution inside the photon

$$\rho(x) \sim \frac{1}{\sqrt{x(1 - x)}}. \quad (3.9)$$

For multiple interaction events, sea quark momenta are sampled from a

$$\rho(x) \sim \frac{1}{x^a} \quad (3.10)$$

distribution with  $a = 1$  for the photon and  $a = 0.7$  for the proton. The different parameters  $a$  result from the asymmetric triple pomeron cross section [41].

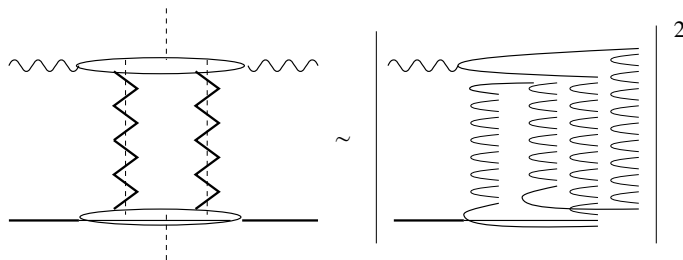


Figure 3.9: *Example for a chain system resulting from a two-pomeron cut*

The selection of flavours at the ends of low- $p_{\perp}$  chains is done according to the statistical bootstrap model. The probability to generate the parton flavour  $f$  at a chain end reads [49]

$$P_f(m_{ch}) = \frac{1}{\sum_i P_i(m_{ch})} \int_{m_f}^{m_{ch}} E \exp(-\beta_f E) dE, \quad (3.11)$$

whereas the sum includes all possible flavours. Here,  $m_{ch}$  and  $m_f$  denote the invariant chain mass and the constituent mass of parton  $f$ . With the parameter  $\beta_f = 8 \text{ GeV}^{-1}$  one gets for not too small chain masses the probabilities

$$\begin{aligned} P_d = P_u &\approx 0.43 \\ P_s &\approx 0.14 \\ P_c &\approx 0.0001. \end{aligned} \quad (3.12)$$

The method to select flavours at the "soft" chain ends described above can be changed optionally to a schema with energy and chain mass independent probabilities. These mass-independent probabilities are also used if a sea flavour is sampled without chain mass information available.

The transverse momentum distribution of partons belonging to soft chains is not predicted by the Dual Parton Model. In PHOJET, assumptions similar to Ref. [10] are used. The transverse momentum of the partons is sampled from an exponential distribution

$$\frac{dN_{\text{soft}}}{d^2p_{\perp}} \sim \exp(-\beta m_{\perp}), \quad (3.13)$$

with  $m_{\perp} = \sqrt{m_0^2 + p_{\perp}^2}$ ,  $m_0$  being the pion mass. The slope parameter  $\beta$  follows from the requirement to have a smooth transition [10] between the soft constituents  $N_{\text{soft}}$  and the hard scattered partons  $N_{\text{hard}}$  which are given by the QCD improved parton model.

$$\left. \frac{dN_{\text{soft}}}{dp_{\perp}} \right|_{p_{\perp}=p_{\perp}^{\text{cutoff}}} = \left. \frac{dN_{\text{hard}}}{dp_{\perp}} \right|_{p_{\perp}=p_{\perp}^{\text{cutoff}}} \quad (3.14)$$

Note that the parameter  $\beta$  depends on the energy and the parton distribution functions of the scattering particles. Especially it differs for photons and hadrons. In general, the transverse momentum distribution of the soft partons is harder in  $p_{\perp}$  for photons than for hadrons.

### 3.2.2 High- $p_{\perp}$ final states

The parton configurations of the hard processes are calculated using parton distribution functions together with lowest order QCD matrix elements. The kinematics of parton-parton scattering is given in appendix A.

In the following, a list of hard scattering subprocesses and the corresponding matrix elements [50,51] treated in the program is given. The processes are sorted according to the primary particles (hadrons and real photon, pomeron) where the partons are belonging to (see Tab. 11.1). The matrix elements  $\mathcal{A}$  are calculated summing over spin and color of the final state partons and averaging over the spin of the initial state partons. The normalization is defined by

$$\frac{d\hat{\sigma}}{d\hat{t}} = \frac{\pi}{\hat{s}^2} \mathcal{A}(s, t). \quad (3.15)$$

- $qq' \rightarrow qq'$

$$\alpha_s^2 \left[ \frac{4 \hat{s}^2 + \hat{u}^2}{9 \hat{t}^2} \right] \quad (3.16)$$

- $qq \rightarrow qq$

$$\alpha_s^2 \left[ \frac{4}{9} \left( \frac{\hat{s}^2 + \hat{u}^2}{\hat{t}^2} + \frac{\hat{s}^2 + \hat{t}^2}{\hat{u}^2} \right) - \frac{8}{27} \frac{\hat{s}^2}{\hat{u}\hat{t}} \right] \quad (3.17)$$

- $q\bar{q} \rightarrow q'\bar{q}'$

$$\alpha_s^2 \left[ \frac{4}{9} \frac{\hat{t}^2 + \hat{u}^2}{\hat{s}^2} \right] \quad (3.18)$$

- $q\bar{q} \rightarrow q\bar{q}$

$$\alpha_s^2 \left[ \frac{4}{9} \left( \frac{\hat{s}^2 + \hat{u}^2}{\hat{t}^2} + \frac{\hat{t}^2 + \hat{u}^2}{\hat{s}^2} \right) - \frac{8}{27} \frac{\hat{u}^2}{\hat{s}\hat{t}} \right] \quad (3.19)$$

- $q\bar{q} \rightarrow gg$

$$\alpha_s^2 \left[ \frac{32}{27} \frac{\hat{t}^2 + \hat{u}^2}{\hat{t}\hat{u}} - \frac{8}{3} \frac{\hat{t}^2 + \hat{u}^2}{\hat{s}^2} \right] \quad (3.20)$$

- $gg \rightarrow q\bar{q}$

$$\alpha_s^2 \left[ \frac{1}{6} \frac{\hat{t}^2 + \hat{u}^2}{\hat{t}\hat{u}} - \frac{3}{8} \frac{\hat{t}^2 + \hat{u}^2}{\hat{s}^2} \right] \quad (3.21)$$

- $gq \rightarrow gq$

$$\alpha_s^2 \left[ -\frac{4}{9} \frac{\hat{s}^2 + \hat{u}^2}{\hat{s}\hat{u}} + \frac{\hat{u}^2 + \hat{s}^2}{\hat{t}^2} \right] \quad (3.22)$$

- $gg \rightarrow gg$

$$\alpha_s^2 \left[ \frac{9}{2} \left( 3 - \frac{\hat{t}\hat{u}}{\hat{s}^2} - \frac{\hat{s}\hat{u}}{\hat{t}^2} - \frac{\hat{s}\hat{t}}{\hat{u}^2} \right) \right] \quad (3.23)$$

- $q\gamma \rightarrow qq$

$$\alpha_s \alpha_{\text{em}} e_q^2 \left[ -\frac{8}{3} \frac{\hat{u}^2 + \hat{s}^2}{\hat{s}\hat{u}} \right] \quad (3.24)$$

- $g\gamma \rightarrow q\bar{q}$

$$\alpha_s \alpha_{\text{em}} e_q^2 \left[ \frac{\hat{u}^2 + \hat{t}^2}{\hat{t}\hat{u}} \right] \quad (3.25)$$

- $\gamma\gamma \rightarrow q\bar{q}$

$$\alpha_{\text{em}}^2 e_q^4 \left[ 6 \frac{\hat{u}^2 + \hat{t}^2}{\hat{u}\hat{t}} \right] \quad (3.26)$$

In order to approximate pointlike pomeron interactions (non-factorizing contributions) direct pomeron-quark interactions can be simulated. In direct pomeron-quark interactions the pomeron is treated similar to virtual photons. By default, no direct pomeron processes are generated since the pomeron-quark coupling is set to 0.

The partonic color flow in the hard scattering is calculated according to the cross sections for the color combinations the matrix element corresponds to [52].

### 3.2.3 Parton showers

The program offers the possibility to generate initial state radiation for hard scatterings according to the DGLAP evolution equations. The implemented backward-evolution algorithm is similar to the algorithms discussed in [53,54] and involves angular ordering for the parton emissions. To avoid double-counting, the evolution is limited to emissions of partons with  $p_{\perp} > p_{\perp}^{\text{cutoff}}$  since the soft background is generated separately. This reduces the amount of emissions significantly since almost all partons are radiated with very low  $p_{\perp}$ . For interacting photons, the direct splitting  $\gamma \rightarrow q\bar{q}$  is approximately taken into account. During the parton shower generation, the probability to have a direct photon splitting is calculated comparing the anomalous contribution [55]

$$q(x, Q^2) = \frac{3\alpha_{\text{em}}}{2\pi} e_q^2 \left( (x^2 + (1-x)^2) \ln \frac{1-x}{x} \frac{Q^2}{m_q^2} + 8x(1-x) - 1 \right) \quad (3.27)$$

to the full photon PDF. The quark mass  $m_q$  in Eq. (3.27) depends on the parametrization of the photon PDF and is set fitting the PDF at large  $x$  and  $Q^2$ . As a consequence, for example, the number of partons radiated off the photon and the proton differ considerably in photon-proton collisions at HERA energies [56].

Final state radiation is generated using the Lund program JETSET [57].

## 3.3 Diffractive interactions

### 3.3.1 Elastic and quasi-elastic scattering

In photon-hadron collisions, quasi-elastic vector meson production is sampled according to the cross sections discussed in [19].

The squared momentum transfer  $t$  is sampled from an exponential distribution

$$\frac{d\sigma_{\text{qel},V}}{dt} \sim \exp(b_V t). \quad (3.28)$$

The slope  $b_V$  of the exponential can be supplied by the user or calculated using the model parametrizations. In general, the energy dependence of the slope can be parametrized by

$$b_V = b_{V,0} + 2\alpha'_P(0) \ln\left(\frac{s}{s_0}\right) \quad (3.29)$$

with a constant  $b_{V,0}$  which depends on the scattered particles only. For example, the default slope parameters used for HERA energies are for quasi-elastic  $\rho$ ,  $\omega$ , and  $\phi$  production  $b_{\rho} = 11 \text{ GeV}^{-2}$ ,  $b_{\omega} = 10 \text{ GeV}^{-2}$ , and  $b_{\phi} = 6 \text{ GeV}^{-2}$ .

The mass distributions of the vector mesons are calculated from the relativistic Breit-Wigner resonance formulae

$$\frac{d\sigma_{\text{qel},V}}{dm^2} \sim \frac{\Gamma_V}{(m^2 - m_V^2)^2 + m_V^2 \Gamma_V^2} \quad (3.30)$$

where  $m_V$  and  $\Gamma_V$  are the mass and the decay width of the vector meson  $V$ .

In case of  $\rho^0$  photoproduction, the mass is sampled from the Ross-Stodolsky parametrization [58]

$$\frac{d\sigma_{\text{qel},\rho}}{dm^2} \sim \frac{\Gamma(m^2)}{(m^2 - m_V^2)^2 + m_V^2 \Gamma^2(m^2)} \left(\frac{m_{\rho}}{m}\right)^n \quad (3.31)$$

with

$$\Gamma(m^2) = \Gamma_{\rho} \left( \frac{m^2 - 4m_{\pi}^2}{m_{\rho}^2 - 4m_{\pi}^2} \right)^{3/2}. \quad (3.32)$$

Here,  $m_{\pi}$  and  $\Gamma_{\rho}$  denote the pion mass and  $\rho^0$  decay width. For the exponent  $n$  of the Ross-Stodolsky factor  $(m_{\rho}/m)^n$ , the value  $n = 4.2$  is used [59].

### 3.3.2 Single/double diffraction dissociation

In single diffractive dissociation, the mass  $M_D$  of the diffractively produced particle system is calculated according to the triple-pomeron kinematics (for example, diffractive dissociation of particle  $A$ , particle  $B$  quasi-elastically deflected)

$$\begin{aligned} \frac{d^2\sigma_{\text{hm}}}{dt dM_D^2} &= \frac{1}{16\pi} g_{\mathbb{P},A}(0) g_{\mathbb{P}\mathbb{P}\mathbb{P}}(0) g_{\mathbb{P},B}^2(0) \left(\frac{s}{s_0}\right)^{2\Delta_{\mathbb{P}}} \left(\frac{s_0}{M_D^2}\right)^{\alpha_{\mathbb{P}}(0)} \\ &\times \exp\left\{2b_{\mathbb{P}}(M_A^2, M_B^2, M_D^2, M_B^2) t\right\}. \end{aligned} \quad (3.33)$$

The pomeron slope  $b_{\mathbb{P}}$  is given below. It should be emphasized that Eq. (3.33) is derived from Regge Theory assuming  $s \gg M_D^2 \gg s_0$  and  $M_D^2 \gg t$ .

The limits for the diffractively produced mass in a collision with the CMS energy  $\sqrt{s}$  are given by the mass  $m_A$  of the diffractively dissociating particle itself

$$M_{D,\text{min}}^2 = (m_A + m_{\Delta})^2 \quad (3.34)$$

and the coherence constraint ( $m_B$  being the mass of the elastically deflected particle)

$$M_{D,\text{max}}^2 = (m_{\pi}/m_B)s. \quad (3.35)$$

The momentum transfer is sampled from an single exponential distribution with mass dependent slope [19]

$$\begin{aligned} b &= 2b_{\mathbb{P}}(m_A^2, m_B^2, m_{A'}^2, m_{B'}^2) \\ &= b_A e^{-c(m_A - m_{A'})^2} + b_B e^{-c(m_B - m_{B'})^2} \\ &\quad + 2\alpha'(0) \ln\left(2 + \frac{ss_0}{(m_A^2 + m_{A'}^2)(M_B^2 + M_{B'}^2)}\right) \end{aligned} \quad (3.36)$$

where  $m_A$ ,  $m_B$  and  $m_{A'}$ ,  $m_{B'}$  are the masses of the incoming and outgoing particles or diffractive excitations respectively. This slope parametrization gives a steady transition from elastic scattering to single and double diffractive dissociation. For quasi-real photons, the  $\rho^0$  mass is used instead of the photon virtuality since it acts as hadronic scale of the photon. The parameters  $b_A$ ,  $b_B$  and  $c$  are determined by cross section and slope fits and are given in [19].

The low-mass resonance structure is approximately taken into account by multiplying the mass distribution

$$\frac{d\sigma}{dM_D^2} \sim \frac{1}{(M_D^2 - m_A^2)^{\alpha_{\mathbb{P}}(0)}} \quad (3.37)$$

with the factor  $f(M_D^2)$

$$f(M_D^2) = \begin{cases} \frac{(M_{D,\text{min}}^2 + M_{\Delta}^2)(M_D^2 - M_{D,\text{min}}^2)}{M_{\Delta}^2 M_D^2} & : M_D^2 \leq M_{D,\text{min}}^2 + M_{\Delta}^2 \\ 1 & : M_D^2 > M_{D,\text{min}}^2 + M_{\Delta}^2 \end{cases} \quad (3.38)$$

with

$$M_{\Delta}^2 = 1.1\text{GeV}^2. \quad (3.39)$$

The suppression of low masses is compensated by adding resonances to this distribution according to finite mass sum rules. In photon diffraction, for example, the resonances  $\omega(1420)$ ,  $\rho(1450)$ ,  $\omega(1600)$ ,  $\phi(1680)$ , and  $\rho(1700)$  are generated separately. The resonance masses are selected according to Breit-Wigner distributions. The relative probability to generate different resonances follows the  $1/M_{\text{res}}^2$  law multiplied by SU(3) weight factors. Despite the special treatment of resonances, the

multiparticle final state in diffraction is generated by simulating a pomeron-hadron or pomeron-photon scattering with the same implementation of the Dual Parton Model used in nondiffractive hadron-hadron or hadron-photon scatterings. As a first approximation, the pomeron is treated like a virtual meson. The soft and hard scatterings are generated according to the cross sections given by Regge parametrisations and the QCD Parton Model. For example, the cross sections for reggeon and pomeron exchange in pomeron- $A$  scattering read

$$\sigma^R = g_{RPP}(0) g_{A,R}(0) \left( \frac{M_D}{s_0} \right)^{\alpha_R(0)-1} \quad (3.40)$$

and

$$\sigma^P = g_{PPP}(0) g_{P,A}(0) \left( \frac{M_D}{s_0} \right)^{\alpha_P(0)-1} \quad (3.41)$$

with  $g_{RPP}(0) = 3.6 g_{PPP}(0)$ . Assigning the pomeron a parton distribution function, the cross sections for hard pomeron- $A$  scattering is calculated within the QCD Parton Model [18].

$$\begin{aligned} \sigma^{\text{hard}}(s, p_{\perp}^{\text{cutoff}}) &= \int dx_1 dx_2 d\hat{t} \\ &\times \sum_{i,j,k,l} \frac{1}{1 + \delta_{k,l}} f_{A,i}(x_1, Q^2) f_{P,j}(x_2, Q^2) \frac{d\sigma_{i,j \rightarrow k,l}^{\text{QCD}}(\hat{s}, \hat{t})}{d\hat{t}} \Theta(p_{\perp} - p_{\perp}^{\text{cutoff}}). \end{aligned} \quad (3.42)$$

For diffractively dissociating photons, direct hard scatterings are also simulated according to the cross section

$$\sigma_{\text{dir}}^{\text{hard}}(s, p_{\perp}^{\text{cutoff}}) = \int dx d\hat{t} \sum_{i,k,l} f_{P,i}(x, Q^2) \frac{d\sigma_{\gamma, i \rightarrow k,l}^{\text{QCD}}(\hat{s}, \hat{t})}{d\hat{t}} \Theta(p_{\perp} - p_{\perp}^{\text{cutoff}}). \quad (3.43)$$

Furthermore, direct pomeron interactions can be simulated by setting the pomeron-quark coupling  $g_{q,P}$  to a non-vanishing value (default:  $g_{q,P} = 0$ ). In case of photon-pomeron scattering with  $g_{q,P} \neq 0$ , direct interactions ("box" diagram) are also generated.

To take into account the transverse polarization of the incoming photon, the decay of the quasi-elastically produced vector mesons and resonances into two or three particles is done in helicity frame according to the angular distributions given in [60,61].

### 3.3.3 Central diffraction

A direct consequence of the interpretation of diffraction by pomeron-particle scattering is the prediction of the existence of pomeron-pomeron scattering (double-pomeron scattering) [62,63].

Assuming multiperipheral pomeron kinematics, the mass  $M_{\text{CD}}$  of the centrally produced diffractive system is given by

$$M_{\text{CD}}^2 = \frac{s_1 s_2}{s}. \quad (3.44)$$

The rapidity gaps between the central system and the elastically scattered particles can be approximated by

$$\eta_{\text{gap1}} \approx \ln\left(\frac{s}{s_2}\right) \quad \eta_{\text{gap2}} \approx \ln\left(\frac{s}{s_1}\right) \quad (3.45)$$

Denoting the Feynman  $x_F$  of the elastically scattered particles  $A$  and  $B$  by  $x_A$  and  $x_B$  one gets [64]

$$x_A = 1 - \frac{s_2}{s} \quad x_B = -\left(1 - \frac{s_1}{s}\right) \quad (3.46)$$

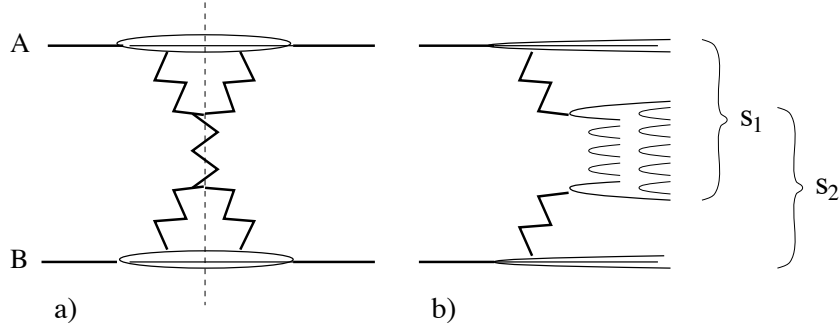


Figure 3.10: *Diffractive cut of the double-pomeron graph a) and the corresponding chain system b).*

and

$$\begin{aligned}
M_{\text{CD}}^2 &\approx (1 - |x_A|)(1 - |x_B|)s \\
\eta_{\text{gap1}} &\approx \ln\left(\frac{1}{1 - |x_A|}\right) & \eta_{\text{gap2}} &\approx \ln\left(\frac{1}{1 - |x_B|}\right)
\end{aligned} \tag{3.47}$$

Using the Feynman rules of Gribov's Reggeon calculus, the differential double-pomeron cross section follows from ( $q_1$  and  $q_2$  denote the loop momentum of the upper and lower pomeron-particle loop in Fig. 3.10,  $q_1^2 = t_1$ ,  $q_2^2 = t_2$ )

$$\begin{aligned}
\frac{d\sigma_{\text{DP}}}{dt_1 ds_1 dt_2 ds_2} &= \frac{1}{s} \Im m \left( \frac{dA(s, t=0)}{dt_1 ds_1 dt_2 ds_2} \right) \\
&= \frac{1}{256\pi^2} \frac{1}{s_0} \left(\frac{s}{s_0}\right)^{\Delta_P} \left(\frac{s}{s_1}\right)^{\Delta_P} \left(\frac{s}{s_2}\right)^{\Delta_P} \\
&\times (g_{AP}(0))^2 g_{PPP}(0) \frac{1}{s_1} \exp \left\{ (b_{AP} + b_{PPP} + 2\alpha'_P(0) \ln\left(\frac{s}{s_2}\right)) t_1 \right\} \\
&\times (g_{BP}(0))^2 g_{PPP}(0) \frac{1}{s_2} \exp \left\{ (b_{BP} + b_{PPP} + 2\alpha'_P(0) \ln\left(\frac{s}{s_1}\right)) t_2 \right\}
\end{aligned} \tag{3.48}$$

$$\tag{3.49}$$

After integration over  $t_1$  and  $t_2$  one gets

$$\begin{aligned}
\frac{d\sigma_{\text{CD}}}{ds_1 dM_{\text{CD}}^2} &= \frac{1}{256\pi^2} \sigma_{PP}(M_{\text{CD}}^2) \left(\frac{s}{M_{\text{CD}}^2}\right)^{2\Delta_P} \frac{1}{M_{\text{CD}}^2} \frac{1}{s_1} \\
&\times \frac{(g_{AP}(0) g_{BP}(0))^2}{\left(b_{AP} + b_{PPP} + 2\alpha'_P(0) \ln\left(\frac{s_1}{M_{\text{CD}}^2}\right)\right) \left(b_{BP} + b_{PPP} + 2\alpha'_P(0) \ln\left(\frac{s}{s_1}\right)\right)}
\end{aligned} \tag{3.50}$$

with

$$\sigma_{PP}(M_{\text{CD}}^2) = (g_{PPP}(0))^2 \left(\frac{M_{\text{CD}}^2}{s_0}\right)^{\Delta_P}. \tag{3.51}$$

Assuming the experimentally motivated cuts [64]

$$\begin{aligned}
x_A &\geq c, & x_B &\geq c, \\
M_{\text{CD},\text{min}}^2 &\leq M_{\text{CD}}^2 \leq (1 - c)^2 s
\end{aligned} \tag{3.52}$$

the integration over  $s_1$  can be performed

$$\frac{M_{\text{CD}}^2}{1 - c} \leq s_1 \leq (1 - c)s \tag{3.53}$$

$$\begin{aligned}
M_{\text{CD}}^2 \frac{d\sigma}{dM_{\text{CD}}^2} &= \frac{1}{256\pi^2} \sigma_{\text{PIP}}(M_{\text{CD}}^2) (g_{\text{AP}}(0) g_{\text{BP}}(0))^2 \left( \frac{s}{M_{\text{CD}}^2} \right)^{2\Delta_{\text{P}}} \\
&\times \frac{\ln \left( \frac{b_{\text{AP}} + b_{\text{PPP}} + 2\alpha'_{\text{P}}(0) \ln((1-c)s/M_{\text{CD}}^2)}{b_{\text{BP}} + b_{\text{PPP}} + 2\alpha'_{\text{P}}(0) \ln(1/(1-c))} \right)}{\alpha'_{\text{P}}(0) (b_{\text{AP}} + b_{\text{BP}} + 2b_{\text{PPP}} + 2\alpha'_{\text{P}}(0) \ln(s/M_{\text{CD}}^2))}
\end{aligned} \tag{3.54}$$

### 3.4 Fragmentation

It should be mentioned that due to this scheme and the mixing of soft and hard interactions a large number of different parton configurations (and event topologies) are generated and the conventional terms "hard" and "soft" cannot directly be used to characterize the events.

For the fragmentation of the chains (strings) JETSET [57] is used.

## Chapter 4

# Photon flux calculation

It is convenient to define the luminosity function for the photon flux in hadron-hadron, lepton-hadron, and lepton-lepton scattering by

$$\frac{dL}{dy_1 dP_1^2 dy_2 dP_2^2} = f_{1,2}(y_1, p_1^2; y_2, p_2^2) \Theta(s_{1,2} - s_{\min}). \quad (4.1)$$

Here,  $p_1$  and  $p_2$  are the four momenta of the incoming particles forming the photon-photon or photon-hadron subsystem.  $p_1^2 = -P_1^2$  and  $p_2^2 = -P_2^2$  are the squared particle masses (in case of photons the virtualities). The variables  $y_1$  and  $y_2$  denote approximately the energy fractions taken from the photon off the initial particle (lepton, hadron) as explained below. The Heavyside function in (4.1) restricts the invariant mass of the system formed by momenta  $p_1$  and  $p_2$  to allow the application of the model.

In the following we consider the case that the photon flux function  $f_{1,2}(y_1, p_1^2; y_2, p_2^2)$  can be factorized into two independent functions

$$\frac{dL}{dy_1 dP_1^2 dy_2 dP_2^2} = f_1(y_1, p_1^2) f_2(y_2, p_2^2) \Theta(s_{1,2} - s_{\min}). \quad (4.2)$$

As will be shown below, this factorization holds in the limit of high collision energies and low photon virtualities. Eq. (4.2) can be used for interactions involving one or two photons. For example, in the case of photoproduction in  $ep$  collisions, the second flux function  $f_2(y_2, p_2^2)$  corresponds to the proton and simplifies to

$$f_2(y_2, p_2^2) = \delta(y_2 - 1) \delta(p_2^2 - m_p^2). \quad (4.3)$$

Often the luminosity function is given in dependence of the invariant mass  $m$  and rapidity  $y_r$  of the subsystem

$$\frac{dL}{dy_1 dy_2} = \frac{s}{2m} \frac{dL}{dy_r dm} = s \frac{dL}{dy_r dm^2} \quad (4.4)$$

The lab. rapidity of the photon-hadron or photon-photon system can be written as

$$y_r = \frac{1}{2} \ln \frac{E_1}{E_2}. \quad (4.5)$$

To obtain the cross sections for the processes mentioned above, the luminosity function is folded with the  $\gamma\gamma$  or  $\gamma h$  cross section (for example, written for  $e^+e^-$  interactions)

$$\frac{d\sigma(e^+e^- \rightarrow Xe^+e^-)}{dy_1 dP_1^2 dy_2 dP_2^2} = \frac{dL}{dy_1 dP_1^2 dy_2 dP_2^2} \sigma_{\gamma\gamma}(s_{\gamma\gamma}, P_1^2, P_2^2). \quad (4.6)$$

## 4.1 Bremsstrahlung

### 4.1.1 Kinematics

As first step, the kinematics of  $ep$  scattering, shown in Fig. 4.1, is discussed. The results can easily be extended to all the other reaction channels considered in this section.

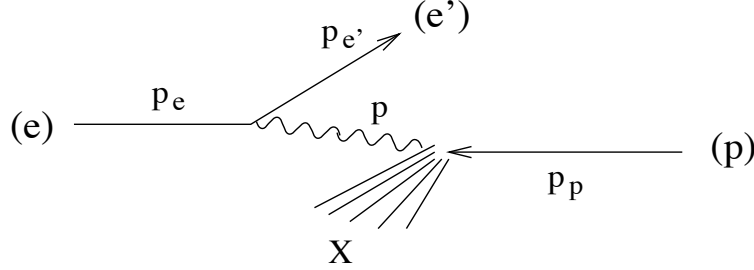


Figure 4.1: *Diagram of  $ep$  scattering via one-photon exchange.*

To characterize deep-inelastic scattering, it is common to use the variables  $x$  and  $y$

$$x = \frac{P^2}{2(p_p \cdot p)} \quad y = \frac{(p \cdot p_p)}{(p_e \cdot p_p)} \quad (4.7)$$

where  $x$  denotes Bjorken's scaling variable.

The differential cross section for  $ep$  scattering can be written in terms of a leptonic and hadronic tensor (e.g. [65])

$$\frac{d\sigma_{ep}}{dydP^2} = \frac{\pi\alpha_{em}^2}{(p_e \cdot p_p)} \frac{1}{P^4} L_{\mu\nu} W_{(ep)}^{\mu\nu} . \quad (4.8)$$

In lowest order in  $\alpha_{em}$  the leptonic tensor reads

$$L^{\mu\nu} = 2(p_e^\mu p_{e'}^\nu + p_{e'}^\mu p_e^\nu) - P^2 g^{\mu\nu} . \quad (4.9)$$

The hadronic tensor can be parametrized according to the Lorentz structure, charge and parity conservation constraints as

$$\begin{aligned} W_{(ep)}^{\mu\nu} &= \left( \frac{p^\mu p^\nu}{p^2} - g^{\mu\nu} \right) F_1(x, P^2) \\ &+ \frac{1}{(p_p \cdot p)} \left( p_p^\mu - \frac{(p_p \cdot p)}{p^2} p^\mu \right) \left( p_p^\nu - \frac{(p_p \cdot p)}{p^2} p^\nu \right) F_2(x, P^2) \end{aligned} \quad (4.10)$$

where  $F_1(x, P^2)$  and  $F_2(x, P^2)$  are the structure functions of the proton. Inserting the exact expressions for  $x$  and  $y$  one gets

$$\begin{aligned} \frac{d\sigma_{ep}}{dydP^2} &= \frac{4\pi\alpha_{em}^2}{P^4} \left( xy \left( 1 - \frac{2m_e^2}{P^2} \right) F_1(x, P^2) \right. \\ &\left. + \frac{1}{y} \left( 1 - y - \frac{m_p^2 P^2}{((p_e \cdot p_p)^2 - m_e^2 - m_p^2)^2} \right) F_2(x, P^2) \right) . \end{aligned} \quad (4.11)$$

In the limit of high collision energies, terms proportional to  $m_p^2/(p_e \cdot p_p)^2$  and  $m_e^2/(p_e \cdot p_p)^2$  can be neglected.

Using the optical theorem, the structure functions can be related to the total  $\gamma p$  cross sections for virtual photons with transverse polarisation (helicity  $\pm 1$ )  $\sigma_T^{\gamma p}$  and longitudinal polarisation (helicity 0)  $\sigma_S^{\gamma p}$  [66,28]

$$F_1(x, P^2) = \frac{(p_p \cdot p)(1-x)}{8\pi^2 \alpha_{\text{em}}} \sigma_T^{\gamma p} \quad (4.12)$$

$$F_2(x, P^2) = 2 \frac{P^2(1-x)}{8\pi^2 \alpha_{\text{em}}(1 - m_p^2 P^2 / (p_p \cdot p))} (\sigma_T^{\gamma p} + \sigma_S^{\gamma p}) . \quad (4.13)$$

It should be emphasized that the quantities  $\sigma_T^{\gamma p}$  and  $\sigma_S^{\gamma p}$  are not precisely defined for virtual photons. Some convention is needed to define the flux factor for virtual photons. Here, the commonly used convention of Ref. [66] is applied.

We obtain for small  $P^2$

$$\frac{d\sigma_{ep}}{dy dP^2} = \frac{\alpha_{\text{em}}}{2\pi P^2} \left( \frac{1 + (1-y)^2}{y} - 2m_e^2 y \frac{1}{P^2} \right) \sigma_T^{\gamma p} . \quad (4.14)$$

It should be emphasized that in the high energy limit the flux of weakly virtual photons can be factorized out and is independent of the second scattering particle (in this case the proton). The proton specific properties enter the  $\gamma p$  cross section only. This allows to introduce the generic photon flux function for bremsstrahlung

$$f_{\gamma,e}(y, P^2) = \frac{\alpha_{\text{em}}}{2\pi P^2} \left( \frac{1 + (1-y)^2}{y} - 2m_e^2 y \frac{1}{P^2} \right) . \quad (4.15)$$

Finally, the kinematics of the photon emission vertex in the limit  $m_e/E_e \rightarrow 0$ , (see Fig. 4.1) can be written as

$$\begin{aligned} p_e &= (E_e, 0, 0, E_e) \\ p_{e'} &= \left( (1-y)E_e + \frac{P^2}{4E_e}, \sqrt{(1-y)P^2} \cos \varphi, \sqrt{(1-y)P^2} \sin \varphi, \right. \\ &\quad \left. (1-y)E_e - \frac{P^2}{4E_e} \right) \\ p &= \left( yE_e - \frac{P^2}{4E_e}, -\sqrt{(1-y)P^2} \cos \varphi, -\sqrt{(1-y)P^2} \sin \varphi, yE_e + \frac{P^2}{4E_e} \right) . \end{aligned} \quad (4.16)$$

The polar scattering angle  $\theta$  follows from

$$\cos \theta = \frac{yE_e - \frac{P^2}{4E_e}}{yE_e + \frac{P^2}{4E_e}} . \quad (4.17)$$

#### 4.1.2 Bremsstrahlung of fermions

Using (4.2,4.15) the  $ep \rightarrow eX$  photoproduction cross section is approximated by

$$\frac{d\sigma_{ep}}{dy dP^2} = f_{\gamma,e}(y, P^2) \sigma_{\gamma p}(s, P^2) . \quad (4.18)$$

Neglecting the dependence of the  $\gamma p$  cross section on  $P^2$  in Eq. (4.18), the well known equivalent photon approximation [28] is obtained

$$f_{\gamma,e}(y) = \frac{\alpha_{\text{em}}}{2\pi} \left( \frac{1 + (1-y)^2}{y} \ln \frac{P_{\text{max}}^2}{P_{\text{min}}^2} - 2m_e^2 y \left( \frac{1}{P_{\text{min}}^2} - \frac{1}{P_{\text{max}}^2} \right) \right) . \quad (4.19)$$

For example, taking the kinematic limit  $P_{\min, \text{kin}}^2$  as lowest photon virtuality allowed

$$P_{\min, \text{kin}}^2 = \frac{m_e^2 y^2}{1-y} \quad (4.20)$$

this simplifies to

$$f_{\gamma, e}(y) = \frac{\alpha_{\text{em}}}{2\pi} \left( \frac{1 + (1-y)^2}{y} \ln \frac{(1-y)}{m_e^2 y^2} P_{\max}^2 - \frac{2(1-y)}{y} \right). \quad (4.21)$$

In the Weizsäcker-Williams approximation [67,68], the second term of (4.19) is neglected

$$f_{\gamma, e}^{\text{WW}}(y) = \frac{\alpha_{\text{em}}}{2\pi} \frac{1 + (1-y)^2}{y} \ln \frac{P_{\max}^2}{P_{\min}^2}. \quad (4.22)$$

Using this approximation integrated up to the kinematical limit (4.20) leads to about 20% overestimation of the photon flux.

An expression similar to (4.18) is used for  $ee \rightarrow ee + X$  scattering involving photons with small virtualities

$$\frac{d^2 \sigma_{ee}}{dy_1 dP_1^2 dy_2 dP_2^2} = f_{\gamma, e}(y_1, P_1^2) f_{\gamma, e}(y_2, P_2^2) \sigma_{\gamma\gamma}(s_{\gamma\gamma}, P_1^2, P_2^2). \quad (4.23)$$

### 4.1.3 Bremsstrahlung of hadrons

Due to the complex structure of the charge distribution  $\rho(\vec{x})$  in hadrons, several approximations and assumptions are necessary to calculate the flux of weakly virtual photons. The approaches in literature can be divided into two types: (i) methods using charge form factors for the hadrons (for example [69,70]) and (ii) methods using the geometrical interpretations on the basis of the impact parameter representations (for example [71–73]).

In the form factor approach, the formulae developed for electron-positron scattering can be used directly. The effects due to the finite charge space-distribution can be included by substituting

$$\alpha_{\text{em}} \longrightarrow Z^2 \alpha_{\text{em}} |F(p^2)|^2 \quad (4.24)$$

for each colliding hadron where  $Z$  denotes the electric charge number. Only the electric form factor  $F(p_i^2)$  is used – in the limit  $P^2/(4m^2) \rightarrow 0$ , the form factor of the magnetic moment can be neglected. The weak point on this approach are the almost unknown form factors  $F(p^2)$  for heavy ions. For pions and protons, the form factors are known [74],

$$F_{\pi}(p^2) \approx \left( 1 - \frac{p^2}{0.47 \text{GeV}^2} \right)^{-1} \quad F_p(p^2) \approx \left( 1 - \frac{p^2}{0.71 \text{GeV}^2} \right)^{-2}. \quad (4.25)$$

The simplest assumption for the heavy ion elastic form factor is motivated by the geometrical interpretation: In the classical picture one should only consider photons having an impact parameter  $\vec{B}$  relative to the hadron greater than the transverse hadron size  $R$ . With  $P^2 \sim 1/\vec{B}^2$  follows

$$F(p^2) = \int d^3x \rho(\vec{x}) e^{i\vec{p}\cdot\vec{x}} = \begin{cases} 1, & -p^2 < 1/R^2 \\ 0, & -p^2 \geq 1/R^2 \end{cases} \quad (4.26)$$

The hadron radius for heavy ions with the mass number  $A$  can be estimated with

$$R \approx 1.2 \text{fm} A^{1/3}. \quad (4.27)$$

More realistic parametrizations of the elastic form factor can be found in literature. For example, the form factor of  $^{206}\text{Pb}$  can be parametrized by a gaussian distribution [75]  $F(p^2) = \exp(p^2/Q_0^2)$  with  $Q_0 \approx 55 - 60$  MeV as used in Ref. [70].

The basis of the semi-classical (geometrical) methods is the fact that a fast-moving charged particle develops a magnetic field almost of the same size as the electric field. This can be described by photons moving parallel to the particle at an impact parameter  $\vec{B}$  (see Fig 4.2). The number of

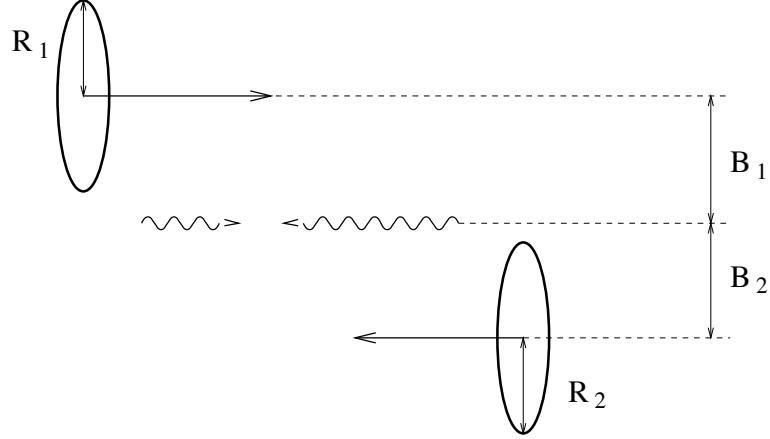


Figure 4.2: Geometrical model of the photon-photon scattering in hadron-hadron interactions.

equivalent photons is given by [76]

$$f(y, \vec{B}) = \frac{Z^2 \alpha_{\text{em}}}{\pi^2} (my)^2 \frac{1}{y} \left[ K_1^2(m|\vec{B}|y) + \frac{m^2}{E^2} K_0^2(m|\vec{B}|y) \right], \quad (4.28)$$

where  $K_0$  and  $K_1$  denote the modified Bessel functions,  $E$  and  $m$  are the energy and the mass of the hadron (heavy ion), respectively. Since the virtuality of the photons is neglected, the photon energy is given directly by  $\omega = yE$ . For hadronic photon interactions keeping the hadrons intact, the impact parameter of the equivalent photons is restricted to  $|\vec{B}| > R$ . The total photon flux follows from

$$f(y) = 2\pi \int_R^\infty f(y, \vec{B}) B dB = \frac{2}{y} \frac{Z^2 \alpha_{\text{em}}}{\pi} \left[ \xi K_0(\xi) K_1(\xi) - \frac{\xi^2}{2} (K_1^2(\xi) - K_0^2(\xi)) \right] \quad (4.29)$$

with  $\xi = mRy$ . The photon spectrum (4.29) is often called the classical photon flux model. For  $E \gg m$  and not too small  $y$ , Eq. (4.29) can be approximated by

$$f(y) = \frac{1}{y} \frac{Z^2 \alpha_{\text{em}}}{\pi} \ln \left[ \left( \frac{\delta}{mRy} \right)^2 + 1 \right] \quad \text{with} \quad \delta \approx 0.681. \quad (4.30)$$

The transverse distance between the particles should be larger than the transverse sizes of the particles to make sure that the particles do not interact hadronically [71]. Taking this into account, the luminosity function reads

$$\begin{aligned} \frac{dL}{dy_1 dy_2} &= \int_{|\vec{B}_1| > R_1} \int_{|\vec{B}_2| > R_2} f_1(y_1, \vec{B}_1) f_2(y_2, \vec{B}_2) \\ &\quad \times \Theta(s_{1,2} - s_{\text{min}}) \Theta(|\vec{B}_1 - \vec{B}_2| - (R_1 + R_2)) d^2 B_1 d^2 B_2. \end{aligned} \quad (4.31)$$

The high-energy part of the photon spectra is connected with collisions at small impact parameters. To approximate the high-energy spectrum correctly, it is necessary to improve (4.31) by an integration over the transverse charge distributions of the scattering particles [73].

Since the colliding hadrons are composite objects, they have rich spectra of excitations. Calculations taking excitation effects into account can be found in [77] and references therein. The excitation probability depends on the mass number and the impact parameter of the collision. For example, the excitation probability for Pb is about 40% in collisions with  $|\vec{B}_1 - \vec{B}_2| = 2R$  [77].

## 4.2 Beamstrahlung

The photon spectrum of beamstrahlung depends strongly on the shape of the particle bunches. Analytic calculations are very difficult to perform. In case of Gaussian beams, the effective beamstrahlung spectrum has been estimated by Chen et al. [78] fitting results of numerical calculations. The dependence of this photon spectrum on the particle-bunch parameters can be expressed by the beamstrahlung parameter  $\Upsilon$ :

$$\Upsilon = \frac{5r_e^2 EN}{6\alpha_{\text{em}}\sigma_z(\sigma_x + \sigma_y)m_e}. \quad (4.32)$$

Here,  $N$  is the number of electrons or positrons in a bunch,  $\sigma_x$  and  $\sigma_y$  are the transverse bunch dimensions,  $\sigma_z$  is the longitudinal bunch size, and  $r_e = 2.818 \cdot 10^{-12}$  mm is the classical electron radius. Following the approximations of [78,79], the beamstrahlung spectrum is given by

$$\begin{aligned} f_{\gamma,e}^{\text{beam}}(y) &= \frac{\kappa^{1/3}}{\Gamma(1/3)} y^{-2/3} (1-y)^{-1/3} e^{-\kappa y/(1-y)} \\ &\times \left\{ \frac{1-w}{\tilde{g}(y)} \left[ 1 - \frac{1}{\tilde{g}(y)n_\gamma} (1 - e^{-n_\gamma \tilde{g}(y)}) \right] \right. \\ &\left. + w \left[ 1 - \frac{1}{n_\gamma} (1 - e^{-n_\gamma}) \right] \right\}, \end{aligned} \quad (4.33)$$

with

$$\tilde{g}(y) = 1 - \frac{1}{2} (1-y)^{2/3} \left[ 1 - y + (1+y) \sqrt{1 + \Upsilon^{2/3}} \right] \quad (4.34)$$

and  $\kappa = 2/(3\Upsilon)$ ,  $w = 1/(6\sqrt{\kappa})$ . The average number of photons per electron  $n_\gamma$  is given by

$$n_\gamma = \frac{5\alpha_{\text{em}}^2 \sigma_z m_e}{2r_e E} \frac{\Upsilon}{\sqrt{1 + \Upsilon^{2/3}}}. \quad (4.35)$$

The approximations used to obtain Eq. (4.33) are expected to be valid for colliders with a beamstrahlung parameter satisfying  $\Upsilon < 5$  (for details see [78]).

## 4.3 Laser-backscattering

In 1981, Ginzburg, Kotkin, Serbo, and Telnov proposed to convert designed future linear  $e^+e^-$  colliders to  $\gamma e$  or  $\gamma\gamma$  colliders by Compton scattering of laser light [80,81]. The basic principle used for the conversion is the scattering of low-energy photons on high-energy electrons. Due to the kinematics, the backwards scattered photons carry a considerable fraction of the initial energy of the electrons. Depending on the polarization of the laser light, various photon spectra can be produced [82,83]. In the following, only the case of unpolarized electrons and unpolarized laser radiation is considered.

It is convenient to write the Compton scattering cross section using the variables

$$\begin{aligned} x_c &= \frac{4E_e E_0}{m_e^2} \cos^2 \frac{\alpha_0}{2} \\ y &= \frac{E_1}{E_e} \quad \text{with} \quad y \leq y_{c,\text{max}} = \frac{x_c}{x_c + 1}. \end{aligned} \quad (4.36)$$

The kinematics is shown in Fig. 4.3. The spectrum of backscattered photons is given by [81–83]

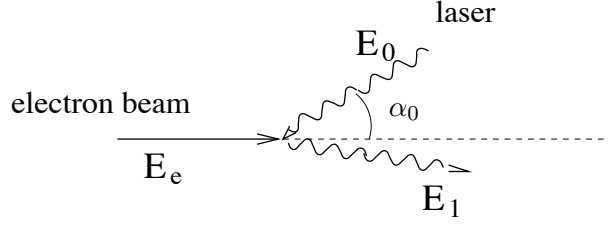


Figure 4.3: *Kinematics of Compton scattering. The initial photon energy  $E_0$  has to be lower than the  $e^+e^-$  pair creation threshold.*

$$f_{\gamma,e}^{\text{laser}}(y) = \frac{2\sigma_0}{x_c\sigma_c} \left( 1 - y + \frac{1}{1-y} - \frac{4y}{x_c(1-y)} + \frac{4y^2}{x_c^2(1-y)^2} \right) \quad (4.37)$$

with the total Compton cross section  $\sigma_c$

$$\sigma_c = \frac{2\sigma_0}{x_c} \left[ \left( 1 - \frac{4}{x_c} - \frac{8}{x_c^2} \right) \ln(1+x_c) + \frac{1}{2} + \frac{8}{x_c} - \frac{1}{2(1+x_c)^2} \right] \quad (4.38)$$

and

$$\sigma_0 = \pi \frac{e^4}{m_e^2} . \quad (4.39)$$

If the laser frequency is chosen according to the optimal value  $x_c = 2 + \sqrt{8}$  given in [83], the spectrum of the photon flux simplifies to

$$f_{\gamma,e}^{\text{laser}}(y) = \frac{-0.544 y^3 + 2.17 y^2 - 2.63 y + 1.09}{(1-y)^2} \Theta(0.828 - y). \quad (4.40)$$

**Part II**

**Program manual**

# Chapter 5

## Program overview

### 5.1 Intention of the program

The program is mainly developed to investigate the soft and semihard particle production at high energies. It is not designed to study jets at very large momentum transfer since the events are always completely generated including all soft background. Matrix elements in lowest order perturbative QCD together with leading-log parton showers are used to describe hard interactions. The model is limited to production mechanisms of strong interactions. In diffractive scattering, effects due to photon polarisation are taken into account.

The recent program version is suited to describe hadron-hadron, real/quasi-real photon-hadron, and real/quasi-real photon-photon interactions. The energy range treated reasonable within this first version of PHOJET depends on the scattering particles and is approximately given by  $2 \text{ GeV} \leq \sqrt{s} \leq 1000 \text{ GeV}$ . The extension of the model to higher energies is planned for near future.

### 5.2 History of the program

The ideas and methods used in the program PHOJET are based mainly on the DPM. Concerning many aspects of the program, the realization of the DPM is similar to the MC event generator DTUJET-93 [23,12] simulating multiparticle production in  $pp$  and  $p\bar{p}$  collisions up to very high energies. These are for example

- the model formulation by two components (a soft and a hard component)
- the two channel approximation of low mass diffraction dissociation
- and the transverse momentum distribution of soft partons.

Main differences to the ideas used within DTUJET are

- extension to different particles, especially to photon-photon, photon-hadron and meson-meson, meson-baryon reactions
- construction of impact parameter amplitudes (correlation between mass and slope, dependence on particle type)
- description of high mass diffraction by using the triple-, loop-, and double-pomeron graph with supercritical pomeron intercept
- scheme to connect partons to chains for fragmentation
- treatment of enhanced graphs (involving triple pomeron interactions)

- resummation of weights to get the probability distribution for different numbers of cuts
- complete treatment of all lowest order hard parton scattering processes including direct photon interactions
- extension to hard pomeron interactions (including resolved and direct interactions, including the possibility to have a direct pomeron-quark coupling)
- initial state radiation for hard interactions (taking into account the inhomogeneous part of the photon evolution equations)
- extension of the model to lower energies (reggeon-exchange)

Information on the latest program version is distributed via WWW

<http://www.physik.uni-leipzig.de/~eng/phojet.html>

The program code can be obtained by request from the author.

### 5.3 General structure of the program

There are two main types of applications:

(i) cross section calculations and (ii) generation of hadronic final states by MC.

(i) Cross section calculations:

PHOJET provides the user various tools to work with cross section data. Within the program, tables related to the amplitudes and cross sections before and after unitarization can be easily produced. This enables the user to investigate the influence of model parameters and to calculate high energy extrapolations. Furthermore, it is possible to read data files containing cross sections and to fit the free parameters of the model according to the data and different model options.

(ii) Generation of hadronic final states:

The main part of the program is used to generate multiparticle final states for different hadronic interactions. It is possible to simulate elastic, single and double diffractive, and nondiffractive inelastic events. This includes also quasi-elastic vector meson production in high energy photon-photon and photon-hadron reactions. Using program switches, different models can be selected and the influence of the model assumptions on the hadronic final state can be investigated. The full information concerning the different steps of event generation are accessible from outside by the standard particle numbering and history scheme [84,85].

# Chapter 6

## Installation and quick start

### 6.1 General program structure

There are two main types of applications:

(i) cross section calculations and (ii) generation of hadronic final states by MC.

(i) Cross section calculations:

PHOJET provides the user various tools to work with cross section data. Within the program, tables related to the amplitudes and cross sections before and after unitarization can be easily produced. This enables the user to investigate the influence of model parameters and to calculate high energy extrapolations. Furthermore, it is possible to read data files containing cross sections and to fit the free parameters of the model according to the data and different model options.

(ii) Generation of hadronic final states:

The main part of the program is used to generate multiparticle final states for different hadronic interactions. It is possible to simulate elastic, single and double diffractive, and nondiffractive inelastic events. This includes also quasi-elastic vector meson production in high energy photon-photon and photon-hadron reactions. Using program switches, different models can be selected and the influence of the model assumptions on the hadronic final state can be investigated. The full information concerning the different steps of event generation are accessible from outside by the standard particle numbering and history scheme [84,85].

### 6.2 How to run the program

#### 6.2.1 Files and update/bugfix information

Information on the latest program version is distributed via URL

<http://www-ik.fzk.de/~engel/phojet.html>

The program code can be downloaded from this location directly or can be requested from one of the authors.

To run the program the Lund string fragmentation model is needed. One of the following two codes has to be linked with PHOJET

- JETSET version 7.3 or higher or
- PYTHIA version 6.1 or higher.

Note that the naming conventions for the subroutines as well as the common blocks have changed from JETSET 7.X to PYTHIA 6.X. Correspondingly, the PHOJET Monte Carlo is provided in two versions, one with the interface to JETSET 7.X and another one with the interface to PYTHIA 6.X. To distinguish both versions check the comment header at the beginning of the file.

The Lund Monte Carlo programs can be downloaded from URL

<http://www.thep.lu.se/tf2/staff/torbjorn/Pythia.html>

For simulations of very high energy collisions the usage of PYTHIA 6.1 is strongly recommended (i.e. for LHC or cosmic ray interactions). The single precision interface to JETSET might cause severe energy-momentum conservation problems for highly boosted configurations.

## 6.2.2 Calling PHOJET as a subroutine

A flexible method of event generation is achieved if the PHOJET subroutines are called directly in the main program. In the following a short main program demonstrating the generation of events with PHOJET is shown.

```
PROGRAM DEMO
C*****
      IMPLICIT DOUBLE PRECISION (A-H,O-Z)
      SAVE

      DIMENSION P1(4),P2(4)
C
C  general initialization
      CALL PHO_INIT(-1,IREJ)

C  electron data
      EELEC = 26.7
C  proton data
      PROM = 0.938
      EPROT = 820.
C  proton momentum
      P1(1) = 0.DO
      P1(2) = 0.DO
      P1(3) = SQRT((EPROT-PROM)*(EPROT+PROM))
      P1(4) = EPROT
C  photon momentum
      EGAM = 0.45*EELEC
      P2(1) = 0.DO
      P2(2) = 0.DO
      P2(3) = -EGAM
      P2(4) = EGAM
C
C  set particles to scatter
      CALL PHO_SETPAR(1,2212,0,0.DO)
      CALL PHO_SETPAR(2,22,0,0.DO)
C
C  initialization
      CALL PHO_EVENT(-1,P1,P2,SIGMAX,IREJ)
C
C  main event generation loop
      DO 100 I=1,10000
C
C  generate one event
      CALL PHO_EVENT(1,P1,P2,SIGCUR,IREJ)
```

```

C
C print first 5 events
      CALL PHO_PREVNT(0)
C
C histograming etc...
C
100 CONTINUE
C
C output of PHOJET statistics (optional)
      CALL PHO_EVENT(-2,P1,P2,SIGMAX,IREJ)
C
      END
C
C dummy routines
C
      SUBROUTINE PHO_PHIST(I,X)
      IMPLICIT DOUBLE PRECISION(A-H,O-Z)
      END

      SUBROUTINE PHO_LHIST(I,X)
      IMPLICIT DOUBLE PRECISION(A-H,O-Z)
      END

```

To generate events, at first, a call to PHO\_INIT is necessary. This subroutine initializes the random number generator, prepares internal tables, sets the default parton distribution functions, and (optionally) reads data cards from a file which is connected to the unit number given as first argument. If the first argument is **-1** no data cards are read.

Sample call:

```
CALL PHO_INIT(LINP,IREJ)
```

LINP input unit,

-1 to work without input file at all

with:

IREJ 0 all cards can be interpreted

1 error during processing of input cards

After the call to PHOINP and before the first call to EVENT, model parameters can be changed by direct manipulation of the relevant variables.

The first call to the event generation subroutine EVENT with the option **-1** is used for initialization of the program. The center of mass system (CMS) energy given by the four-momenta P1 and P2 should be the highest energy expected for the following calculations<sup>1</sup>. Choosing the CMS energy much higher than the energy used for event generation increases the execution time of the program and reduces the precision of the results.

Each further call to EVENT generates one complete event (for details, see description of the subroutine). After each call the COMMON /HEPEVS/ contains the multiparticle final state. The rejection flag IREJ is set to **0** for an accepted event, otherwise to **1**.

The last call to EVENT with the option **-2** gives a short output of statistics characterizing the event generation. This call to EVENT is optional but many help to detect problems.

---

<sup>1</sup>During initialization, only the CMS energy and the particle virtualities are needed, the directions of the particle momenta are ignored.

### 6.2.3 Using pre-defined collision setups

### 6.2.4 Event generation with input cards

In order to run PHOJET using input data cards only, the following main program can be used.

```
PROGRAM DEMO
CALL PHOINP(5, IREJ)
END
```

An example using this method is given in the file **phoex1.f**. The subroutine PHOINP reads data cards from an input file to set program parameters and to control the program execution. The input cards are explained in Sec. C.

Since the program uses the Lund fragmentation program JETSET, the histograming of the events can be done using either the standard common block /HEPEVT/ as implemented in JETSET or the equivalent common block /HEPEVS/ of PHOJET. In addition to the final state particles, the common block /HEPEVS/ contains the complete history of the event and some additional comment entries. Therefore it is recommended to use the common block /HEPEVS/ instead of the common block /HEPEVT/.

To provide a simple interface, the two subroutines

POLUHI and POHIST

are called after each accepted event for histograming. Here the user should insert the event analysis and histograming code. The intention to use two routines for histograming is as follows. In POHIST, all the histograms using the PHOJET data structures are contained whereas POLUHI consists of histograms using only JETSET data common blocks. This splitting is necessary since the variables of the common blocks /HEPEVT/ and /HEPEVS/ have the same names. An short example is given in the file **phoex1.f**.

### 6.2.5 Photoproduction in lepton-hadron, lepton-lepton and hadron-hadron scattering

The basic processes generated in PHOJET are hardon-hadron, photon-hadron, photon-photon, pomeron-hadron, pomeron-photon, and pomeron-pomeron interactions with variable collision energies. However, for example, instead of photons leptons are scattered on other particles in many experimental setups. Therefore, the program package includes some interface routines to calculate the corresponding photon flux, kinematics and cross sections. Currently, the following routines are provided

- **GPHERA** photoproduction due to bremsstrahlung in lepton-proton scattering similar to HERA setup. The proton is the projectile, the lepton the target. Proton and lepton energies are given by the user.
- **GGEPEM** photoproduction due to bremsstrahlung in lepton-lepton scattering similar to LEP setup. The lepton energies can be different.
- **GGHIOF** photoproduction due to bremsstrahlung in electromagnetic hadron-hadron (heavy ion) interactions (collider setup). The form factor approach is used to calculate the photon flux.
- **GGHIOG** photoproduction due to bremsstrahlung in electromagnetic hadron-hadron (heavy ion) interactions (collider setup). The quasi-classical approximation (geometrical model) is used to calculate the photon flux.
- **GGBLSR** photoproduction due to back scattering of laser light off a lepton beam, lepton-lepton collider setup.

- **GGBEAM** photoproduction due to beamstrahlung by two identical colliding lepton beams, lepton-lepton collider setup.

In order to select the kinematic range of photoproduction, some cuts have to be applied to the lepton/hadron-photon vertex. These cuts have to be specified by the user before calling one of the routines listed above. In general, the cuts on the lepton/hadron-photon vertex are stored in the common `/LEPCUT/` and can be set using the input cards `E-TAG1` and `E-TAG2` or modifying the corresponding variables directly. Furthermore, the invariant mass range of the photon-hadron or photon-photon system may be restricted with the input card `ECMS-CUT` or the corresponding variables `ECMIN`, `ECMAX` in `/LEPCUT/`. For further details, see description of the interface routines and the common `/LEPCUT/`.

### 6.2.6 Histograming

Due to the structure of the program, cross sections are calculated for the basic minimum bias processes such as hadron-hadron, photon-hadron, and photon-photon scattering. The corresponding cross sections are stored after each event generation step in `SIGGEN(1-4)` in the common `/XSECTP/`. For variable energy simulations and especially photoproduction simulations, the cross sections are calculated in the interface routines listed in the previous section. To provide a convenient scheme for histograming, the two routines `POLUHI` and `POHIST` are called for initialization, event generation and final output with the following convention:

```
CALL POHIST(IMODE,WEIGHT)
IMODE  type of the call:
        -1 initialization call (first call)
        1 call after each generated and accepted event to collect statistics
        -2 final call to write out histograms
WEIGHT histogram weight:
        IMODE=-1: maximum cross section as stored in SIGGEN(4)
        IMODE=1: weight of last generated event, currently always 1
        IMODE=-2: cross section of generated events in mb (including lepton/hadron-photon vertex, the cross section in SIGGEN(1) corresponds to the generated cross section without lepton/hadron-photon vertex)
```

Note that if the main event generation routine `EVENT` is called directly by the user program, only the the cross section calculation for the hadron-hadron, photon-hadron, or photon-photon scattering process is done. In order to perform an external cross section calculation in variable energy calculations, the program has to be initialized with the highest energy expected for the following simulations. During initialization, the maximum of the cross section  $\sigma_{\max}$  according to the activated processes is determined and returned as 4th argument of `EVENT`. In each following call to `EVENT`, the rejection flag `IREJ` is set with the probability  $\sigma(s)/\sigma_{\max}$ . The cross section  $\sigma_{\max}$  is also stored in `SIGGEN(4)` in `/XSECTP/`.

# Chapter 7

## Main subroutines and options

### 7.1 Main subroutines

In this section, the basic subroutines needed to run PHOJET are described. The standard procedure to perform event generation is the following. At first, the subroutine PHOINP is called to initialize the general data structures and the random number generator of the event generator. During this initialization one can specify the scattering particles, energies by input cards. However, the specification of the particles etc. is also possible by calling for example the subroutine SETPAR. The initialization of the particle and energy dependent program parts is done by calling EVENT with the option **-1**. For the generation of each event one has to call EVENT with the option **1**. Finally, some information about cross sections and related quantities is printed after calling EVENT with the option **-2**.

If the input cards GG-EPEM, GP-HERA, BEAMST, BLASER, GG-HION-F, GG-HION-G, EVENT-CMS, or EVENT-LAB are used to generate events, the subroutines POLUHI and POHIST are called after each accepted event. These subroutines have to be supplied by the user (see description of the subroutines POLUHI and POHIST below and examples **phoex1.f** and **phoex2.f**).

SUBROUTINE PHOINP(LINP, IREJ)

- purpose:** initialization of global variables, tables and random number generation, evaluation of input cards
- input:** LINP  
>0: number of input unit to read the input cards  
-1: no input cards are read
- output:** IREJ rejection flag:  
0: initialization successfully performed  
else: some error occurred during interpretation of input cards

SUBROUTINE EVENT(NEV, P1, P2, FAC, IREJ)

- purpose:** main subroutine to generate events.
- input:** NEV  
-1: initialization of event generation  
1: generation of one event (variable energy possible). In order to allow for the integration with an external flux factor, the rejection flag IREJ is set with the probability  $\sigma(s)/\sigma_{\max}(s)$  for each event. This option is used in the interface routines provided in PHOJET.  
2: generation of one event (variable energy possible). Independent of the cross

section which may vary considerably with the energy, in each call an event is generated. The cross section for the selected processes at the given energy is stored in `SIGGEN(3) (/XSECTP/)`.

3: generation of one event (variable energy possible), independent of the cross section which may vary considerably with the energy, in each call an event is generated. The cross section for the selected processes at the given energy is stored in `SIGGEN(3) (/XSECTP/)`. The number of multiple interactions and especially the probability of hard interactions is calculated according to the initialization energy. This option may be used for the simulation of photon/hadron-nucleus and nucleus-nucleus interactions (i.e. Glauber approximation).

-2: output of event generation statistics (optional)

P1(4) four-momentum of particle 1 ( $E_1 = P1(4)$ )

P2(4) four-momentum of particle 2 ( $E_2 = P2(4)$ )

FAC weight factor

for `NEV = -2` the effective weight for the internal calculation of partial cross sections (for example, the total  $\gamma p$  cross section times the effective weight due to the photon flux)

**output:** FAC cross sections (mb):

for `NEV = -1`: maximum value of the total cross section for the activated processes (cross section at given initialization energy)

for `NEV = 1`: value of the total cross section for the activated processes at the energy currently given by P1 and P2 processes

IREJ rejection flag:

0: event accepted

else: event rejected

SUBROUTINE SETPAR(ISIDE, IDPDG, IDBAM, PVIR)

**purpose:** definition of scattering particles

**input:** ISIDE side for particle to be specified in this call: side 1 corresponds to the four-momentum P1 in the call to `EVENT`, side 2 corresponds to the four-momentum P2 in the call to `EVENT`

IDPDG number of particle according to Particle Data Group numbering scheme

IDBAM number of particle according to compressed particle code, this number is optional and can be set to `0`

PVIR particle virtuality  $P^2 \geq 0$  ( $\text{GeV}^2/c^2$ , only for photons)

SUBROUTINE POLUHI(IMODE, WEIGHT)

**purpose:** interface subroutine for user histograms, if the program is run with input cards only, this subroutine is provided to fill histograms via the standard common block `/HEPEVT/`. For more details, see the example given in the file `phoex1.f`.

**input:** IMODE flag to determine type of the call

-1: first call to perform histogram initialization

1: call to fill histograms after accepted event

-2: final call for output of histograms or related quantities

WEIGHT weight for histograms (mb):

for `IMODE = -1`: maximum of the total cross section of the selected processes (without photon flux factors)  
 for `IMODE = 1`: current weight of event, in `PHOJET` always `1`  
 for `IMODE = -2`: total weight for histograms including photon flux factors

`SUBROUTINE POHIST(IMODE,WEIGHT)`

**purpose:** interface subroutine for user histograms, if the program is run with input cards only, this subroutine is provided to fill histograms via the standard common block `/HEPEVS/` as implemented in `PHOJET`. For more details, see the example given in the file `phoex1.f`.

**input:** `IMODE` flag to determine type of the call  
 -1: first call to perform histogram initialization, the weight is set to the maximum of the total cross section of the selected processes  
 1: call to fill histograms after accepted event  
 -2: final call for the output of histograms or related quantities  
**WEIGHT** weight for histograms (mb):  
 for `IMODE = -1`: maximum of the total cross section of the selected processes (without photon flux factors)  
 for `IMODE = 1`: current weight of event, in `PHOJET` always `1`  
 for `IMODE = -2`: total weight for histograms including photon flux factors

## 7.2 Main options for event simulation

In the following, an overview of the important common blocks is given. The different variables stored in these common blocks are explained in detail in the part of the manual dealing with the corresponding physics.

### 7.2.1 COMMON /PROCES/

Structure:

```
C general process information
  INTEGER IPROCE, IDNODF, IDIFR1, IDIFR2, IDDPOM, IPRON
  COMMON /POPRCS/ IPROCE, IDNODF, IDIFR1, IDIFR2, IDDPOM, IPRON(15,4)
```

In the program, eight basic scattering processes are distinguished.

1. non-diffractive inelastic scattering
2. purely elastic scattering
3. quasi-elastic scattering, .e. quasi-elastic vector meson production
4. central diffraction (double-pomeron scattering)
5. single diffractive dissociation of particle 1
6. single diffractive dissociation of particle 2
7. double diffractive dissociation

8. hard direct interactions (in the case of  $\gamma\gamma$  scattering single resolved and direct hard interactions)

By setting the different IPRON elements of this common block, the basic interaction types can be switched on (1) or off (0). The cross section calculations, histogramming weights etc. refer always to the total cross section for the activated interaction types. The variables IPRON can be set by the input card PROCESS (see Sec. C.2.3).

IPRON(1)	non-diffractive (resolved) inelastic interaction
IPRON(2)	elastic scattering
IPRON(3)	quasi-elastic vector meson production
IPRON(4)	double-pomeron scattering
IPRON(5)	single diffractive dissociation of particle 1
IPRON(6)	single diffractive dissociation of particle 2
IPRON(7)	double diffractive dissociation
IPRON(8)	direct photon-hadron interaction
IPRON(9)	hard interactions in single diffractive dissociation of particle 1 (0 suppressed, 1 allowed)
IPRON(10)	hard interactions in single diffractive dissociation of particle 2 (0 suppressed, 1 allowed)
IPRON(11)	hard interactions in double-pomeron scattering (0 suppressed, 1 allowed)

By default, hard diffractive scattering is always switched on.

### 7.2.2 COMMON /MODELS/

Structure:

```

C model switches and parameters
  CHARACTER*8 MDLNA
  INTEGER ISWMDL,IPAMD
  DOUBLE PRECISION PARMDL
  COMMON /POMDLS/ MDLNA(50),ISWMDL(50),PARMDL(400),IPAMD(400)

```

This common block stores almost all parameters of the model PARMDL. The variables ISWMDL and IPAMD are used as flags to activate different program options. These variables can be set using the input cards SETPARAM and SETMODEL (see sec. C.2.3).

### 7.2.3 Minimum bias event generation

ISWMDL(2)	minimum bias event generation (D=1): 0: generation of single hard scattering processes only 1: generation of minimum bias events
ISWMDL(15)	multiple interaction used for inelastic events (D=3): -1: simple simulation of multiperipheral kinematics, only one soft pomeron or reggeon cut is sampled, all hard scattering processes are switched off 0: only one hard or soft interaction (reggeon/pomeron) used for event generation 1: multiple soft but only up to one hard interaction used for event generation

- 2: multiple hard but only up to one soft interaction used for event generation
  - 3: multiple hard and soft interactions according to unitarization
- ISWMDL(16) multiple interaction used for diffractive dissociation (particle-pomeron scattering,  $D=4$ ):
- 0: only one soft interaction (one or two chains with small transverse momenta)
  - 1: only one hard or soft interaction (reggeon/pomeron) used for event generation
  - 2: multiple soft but only up to one hard interaction used for event generation
  - 3: multiple hard but only up to one soft interaction used for event generation
  - 4: multiple hard and soft interactions according to unitarization
- ISWMDL(25) multiple interaction used for central diffraction (pomeron-pomeron scattering,  $D=4$ ):
- 0: only one soft interaction (one or two chains with small transverse momenta)
  - 1: only one hard or soft interaction (reggeon/pomeron) used for event generation
  - 2: multiple soft but only up to one hard interaction used for event generation
  - 3: multiple hard but only up to one soft interaction used for event generation
  - 4: multiple hard and soft interactions according to unitarization

## Chapter 8

# Event record structure

The complete event generated by PHOJET is recorded in 3 common blocks. The `COMMON /HEPEVS/` confirms the standard proposed by the Particle Data Group (PDG) [84,85]. To store additional information (parton colors for example) the `COMMON /HEPEVE/` is used. The position index of the particles within the two common blocks is always the same. Data specific to the fragmentation are collected in the `COMMON /STRING/`.

Since the PDG numbering of particles does not allow a compact storage of the particle properties, a compressed particle code (CPC) is used. This CPC is taken from the fragmentation program BAMJET [86–88]. The conversion table is given in the appendix, Tab. D.1.

In order to provide an almost program version independent interface to event analysis subroutines comment entries are added to the general event information in `COMMON /HEPEVS/` and `COMMON /HEPEVE/`.

### 8.1 Standard particle record: `COMMON /HEPEVS/`

Structure:

```
C standard particle data interface
  INTEGER NMXHEP

  PARAMETER (NMXHEP=2000)

  INTEGER NEVHEP, NHEP, ISTHEP, IDHEP, JMOHEP, JDAHEP
  DOUBLE PRECISION PHEP, VHEP
  COMMON /POEVT1/ NEVHEP, NHEP, ISTHEP (NMXHEP), IDHEP (NMXHEP),
&                JMOHEP (2, NMXHEP), JDAHEP (2, NMXHEP), PHEP (5, NMXHEP),
&                VHEP (4, NMXHEP)
C extension to standard particle data interface (PHOJET specific)
  INTEGER IMPART, IPHIST, ICOLOR
  COMMON /POEVT2/ IMPART (NMXHEP), IPHIST (2, NMXHEP), ICOLOR (2, NMXHEP)
```

**purpose:** Monte-Carlo-independent format of an event record

**NMXHEP:** maximum number of entries (partons/particles) that can be stored in the `COMMON` block.

default value: 2000; In the subroutine REGPAR called to write particles in that COMMON, it is checked that this value is not exceeded.

NEVHEP: event number, sequentially increased by 1 for each call to EVENT, starting with 1 for the first generated event;  
after fragmentation: index of first existing entry (see ISTHEP)

NHEP: actual number of entries stored in the current event. They are found in the the first NHEP positions of the respective arrays below. Index I,  $1 \leq I \leq NHEP$ , denotes the given entry

ISTEP(I) status code for entry I:  
0: null entry  
1: existing entry for particles (exceptions, see (-1)) which has not decayed or fragmented  
2: entry which has decayed, fragmented or copied to another place and is therefore not appearing in the final state, but is retained for event history information  
-1: partons, chains, clusters  
11-200: comment entries with special meaning of the variables (see below)

IDHEP(I): particle identity, according to the PDG standard (see section Particle numbering)

JMOHEP(1, I): pointer to the position of the first mother ; The value is 0 for initial entries  
JMOHEP(2, I): pointer to the position of the last mother;  
To allow more than two mothers (for example  $3 \rightarrow 2$  scattering), the pointer to the last mother is assigned to JMOHEP(2, I) with negative sign. Then all the particles between the entries JMOHEP(1, I) and JMOHEP(2, I) are additionally considered as mother particles. If only two mothers exist, the JMOHEP(2, I) points to the second mother (positive value). Then it is not necessary to store them sequentially.  
If only on mother exists, the pointer to the second mother is set to 0.

JDAHEP(1, I): pointer to the position of the first daughter;  
0: no decay occurred

JDAHEP(2, I): pointer to the position of the last daughter;  
0: no decay occurred  
Daughters are assumed to be stored sequentially, so that the whole range JDAHEP(1, I)-JDAHEP(2, I) contains daughters. This variable should be set also when only one daughter exists.

PHEP(1, I): momentum in the x direction, in GeV/c  
PHEP(2, I): momentum in the y direction, in GeV/c  
PHEP(3, I): momentum in the z direction, in GeV/c  
PHEP(4, I): energy, in GeV  
PHEP(5, I): mass, in GeV/c<sup>2</sup>. For space-like partons a negative mass according to  $PHEP(5, I) = -\sqrt{-m^2}$  is used

VHEP(1, I): production vertex x position, in mm (not used)  
VHEP(2, I): production vertex y position, in mm (not used)  
VHEP(3, I): production vertex z position, in mm (not used)  
VHEP(4, I): production time, in mm/c ( $\sim 3.33 \times 10^{-12}$ s) (not used)

IPHIST(1,I):

- partons:** number of pomeron the parton is belonging; soft pomerons are labeled sequentially starting with 1, hard pomerons are labeled sequentially starting with 100;  
negative values: partons created by hard scattering subprocesses
- chains, clusters:** chain number in COMMON /STRING/ (one pomeron leads to two chains)
- stable particles:** position index of the particle in the JETSET COMMON /HEPEVT/ (JETSET fragmentation only)

IPHIST(2,I):

- partons:** position index of the parton written to the JETSET COMMON /HEPEVT/ for fragmentation (JETSET fragmentation only)
- chains, clusters:** number of the pomeron the chain belongs to
- stable particles:** not used

ICOLOR(1,I):

- partons:** first color label
- chains, clusters:** three times the charge of the chain or cluster
- stable particles:** three times the charge of the particle

ICOLOR(2,I):

- gluons:** second color label
- di-/quarks:** 0 for sea quarks, 1 for valence quarks
- chains, clusters:** three times the baryon quantum number of the chain or cluster
- stable particles:** three times the baryon quantum number of the particle

## 8.2 Particle codes and properties

INTEGER FUNCTION MCIHAD(MCIND)

**purpose:** calculation of compressed particle code from PDG ID number

**input:** MCIND PDG particle number

INTEGER FUNCTION MPDGHA(MCIND)

**purpose:** calculation of the particle index according to the PDG convention

**input:** MCIND compressed particle code

CHARACTER\*8 FUNCTION PANAME(I)

**purpose:** output of particle name

**input:** particle index (location) in COMMON /HEPEVS/

DOUBLE PRECISION FUNCTION POPAMA(IDX,MODE)

**purpose:** average particle mass

**input:** MODE:

0 IDX is treated as compressed particle code

1 IDX is treated as PDG particle number

2 IDX is particle index (location) in COMMON /HEPEVS/

-1 initialization of internal tables (IDX ignored)

INTEGER FUNCTION IPOBA3(IDX,MODE)

**purpose:** three times the baryon charge

**input:** MODE:

0 IDX is treated as compressed particle code

1 IDX is treated as PDG particle number

2 IDX is particle index (location) in COMMON /HEPEVS/

INTEGER FUNCTION IPOCH3(IDX,MODE)

**purpose:** electric charge

**input:** MODE:

0 IDX is treated as compressed particle code

1 IDX is treated as PDG particle number

2 IDX is particle index (location) in COMMON /HEPEVS/

## 8.3 Comment entries

### 8.3.1 Hard partonic interaction

Hard partonic interactions are generated within the program for diffractive and nondiffractive events. Furthermore multiple hard scatterings within one event are allowed. Due to the complicated event structures possible it is necessary to assign each hard scattering process at least three comment entries. The first comment entry is labeled with  $ISTHEP(I) = 25$  and gives general data of the hard scattering generated. The following two entries with  $ISTHEP(I) = 20$  contain parton specific information.

Note that the  $IPHIST(1,I)$  and  $IPHIST(2,I)$  variables in the comment entry  $ISTHEP(I) = 25$  are not suited for determination of initial parton flavours. Instead of these entries the following two comment entries with  $ISTHEP(I) = 20$  should be used to get the initial parton flavours engaged in hard scattering.

- General hard scattering comment:

ISTHEP(I) 25

IDHEP(I) number to identify the mother particles where the hard scattering partons belong to:

1: particle 1 and particle 2

2: pomeron/reggeon and particle 1

3: pomeron/reggeon and particle 2

4: pomeron/reggeon and pomeron/reggeon

JMOHEP(1,I) PDG number of mother particle 1  
 JMOHEP(2,I) PDG number of mother particle 2  
 PHEP(1,I) momentum fraction  $x_1$  taken by parton 1 from mother particle 1 (value as sampled before generation of initial state radiation)  
 PHEP(2,I) momentum fraction  $x_2$  taken by parton 2 from mother particle 2 (value as sampled before generation of initial state radiation)  
 PHEP(3,I) squared transverse momentum of outgoing partons  $\hat{p}_\perp^2$  ( $\text{GeV}^2/c^2$ )  
 PHEP(4,I) momentum transfer scaled by subprocess energy  $v = \hat{t}/\hat{s}$   
  
 IMPART(I) hard scattering subprocess number (see Tab. 11.1)  
 IPHIST(1,I) flavour of initial parton 1 (internal numbering, valence quarks and sea quarks are distinguished)  
 IPHIST(2,I) flavour of initial parton 2 (internal numbering, valence quarks and sea quarks are distinguished)  
 ICOLOR(1,I) flavour of final parton 1 (PDG convention)  
 ICOLOR(2,I) flavour of final parton 2 (PDG convention)

• Parton hard scattering comment:

ISTHEP(I) 20  
 IDHEP(I) flavour of incoming parton (PDG convention)  
 JMOHEP(1,I) index of mother particle 1 in /HEPEVS/  
 JMOHEP(2,I) index of mother particle 2 in /HEPEVS/  
 PHEP(1,I) momentum of scattered parton in the x direction, ( $\text{GeV}/c$ )  
 PHEP(2,I) momentum of scattered parton in the y direction, ( $\text{GeV}/c$ )  
 PHEP(3,I) momentum of scattered parton in the z direction, ( $\text{GeV}/c$ )  
 PHEP(4,I)  $Q^2$  scale used for the evaluation of the parton densities ( $\text{GeV}^2$ )  
  
 IMPART(I) PDF code ( $1000 \cdot \text{IGRP} + \text{ISET}$ ), 0 for direct coupling  
 IPHIST(1,I) hard pomeron number times 100  
 IPHIST(2,I) PDG number of mother particle for parton  
 ICOLOR(1,I) color label 1 of parton  
 ICOLOR(2,I) color label 2 of parton

### 8.3.2 Diffractive dissociation

Each diffractive inelastic subprocess is preceded by a comment entry. Several diffractive interactions are possible within one event by sampling enhanced graphs (for example two diffractively cut triple pomerons). In double diffractive processes, for each diffraction vertex a separate comment entry is created. After the comment entry the diffractive dissociating particles and the corresponding pomerons are stored. For hard diffractive scatterings the comment entries for hard processes are also given.

ISTHEP(I) 30  
 IDHEP(I) process number according to IPROCE flag in COMMON /PROCES/

JMOHEP(1,I) index of diffractively scattered/decaying particle 1 in /HEPEVS/  
 JMOHEP(2,I) index of diffractively scattered/decaying particle 2 in /HEPEVS/  
 PHEP(1,I) mass of diffractive blob belonging to particle 1 (GeV/c<sup>2</sup>)  
 PHEP(2,I) mass of diffractive blob belonging to particle 2 (GeV/c<sup>2</sup>)  
 PHEP(3,I) momentum transfer (squared)  $t$  (GeV<sup>2</sup>/c<sup>2</sup>)  
 PHEP(4,I) total CMS energy of diffractively scattering system (GeV)

IMPART(I) IMODE flag of call to PODIFF:  
 0: diffractive cut  
 1: non-diffractive triple pomeron cut (not supported)  
 2: double-pomeron interaction

IPHIST(1,I) ID number of diffraction according to IDIFR1 in /PROCES  
 IPHIST(2,I) ID number of diffraction according to IDIFR2 in /PROCES  
 ICOLOR(K,I) elastic scattering of particle side K: index of elastically scattered particle (in case of an incoming photon index of the first particle which belongs to the quasi-elastically scattered vector meson or the decay products of it)  
 low-mass diffraction dissociation of particle side K: index of the first particle which belongs to the resonance decay products  
 high-mass diffraction dissociation of particle side K: index of the particle which scatters off the pomeron, the pomeron entry is always ICOLOR(K,I)+1.

### 8.3.3 Elastic/quasi-elastic scattering

In the program, elastic and quasi-elastic scattering is treated equally. The comment entries for elastic/quasi-elastic scatterings are similar to the comment structure used for diffraction dissociation.

ISTHEP(I) 35  
 IDHEP(I) process number according to IPROCE flag in COMMON /PROCES/  
 JMOHEP(1,I) index of diffractively scattered/decaying particle 1 in /HEPEVS/  
 JMOHEP(2,I) index of diffractively scattered/decaying particle 2 in /HEPEVS/  
 PHEP(1,I) mass of final particle/resonance 1 (GeV/c<sup>2</sup>)  
 PHEP(2,I) mass of final particle/resonance 2 (GeV/c<sup>2</sup>)  
 PHEP(3,I) momentum transfer (squared)  $t$  (GeV<sup>2</sup>/c<sup>2</sup>)  
 PHEP(4,I) total CMS energy of diffractively scattering system (GeV)

IMPART(I) not used  
 IPHIST(1,I) PDG number of final particle/resonance 1 (6666, if a pair of pions is directly produced, for example  $\gamma p \rightarrow \pi^+ \pi^- p$ )  
 IPHIST(2,I) PDG number of final particle/resonance 2 (6666, if a pair of pions is directly produced, for example  $\gamma \gamma \rightarrow \rho^0 \pi^+ \pi^-$ )  
 ICOLOR(1,I) index of the (quasi-)elastically scattered particle 1, in case of  $\pi^+ \pi^-$  background in photoproduction, index of the first produced particle (pion)  
 ICOLOR(2,I) index of the (quasi-)elastically scattered particle 2, in case of  $\pi^+ \pi^-$  background in photoproduction, index of the first produced particle (pion)

### 8.3.4 Central diffraction

Central diffraction is generated by simulation two diffractive scatterings. As a result two pomeron entries are filled in /HEPEVS/. Afterwards the pomeron-pomeron scattering is calculated. For each of the diffractive scatterings the comment entry for diffraction dissociation is also stored in /HEPEVS/. In addition, a comment entry for the pomeron-pomeron scattering is written. Note that the the order of the pomeron emissions is sampled randomly. This means that the first pomeron entry do not always belong to mother particle 1. To get the index of the particle the pomeron belongs to one has to take the JMOHEP(1,I) entry of the pomeron itself.

```
ISTHEP(I) 40
  IDHEP(I) process number according to IPROCE flag in COMMON /PROCES/
JMOHEP(1,I) index of (quasi-)elastically scattered particle 1 in /HEPEVS/
JMOHEP(2,I) index of (quasi-)elastically scattered particle 2 in /HEPEVS/
PHEP(1-4,I) four momentum of central diffractive blob (GeV/c)
  PHEP(5,I) invariant mass of central diffractive system (GeV/c2)
  IMPART(I) process index according to IDDPOM in /PROCES/

IPHIST(1,I) index of first pomeron in /HEPEVS/
IPHIST(2,I) index of second pomeron in /HEPEVS/
ICOLOR(1,I) PDG number of mother particle 1
ICOLOR(2,I) PDG number of mother particle 2
```

## 8.4 Additional generator dependent information

During each step of the event generation, the common blocks /PROCES/ and /DEBUG/ are filled with some basic, currently available information on the processes sampled. Since a single event can consist of several processes, the flags stored in the common blocks are not sufficient to get a detailed description of the event. This problem is solved by introducing comment cards specific to all possible processes which can be generated. The comment cards are stored in the common blocks /HEPEVS/ and /HEPEVE/. This schema reduces the dependence of event analysis subroutines on the internal common block structure. Following the general guidelines of the structure of the event history common block /HEPEVS/, a comment entry is labeled by a ISTHEP variable being greater than 10. In dependence on ISTHEP, the other elements of this line in /HEPEVS/ can be interpreted. Each comment entry in /HEPEVS/ corresponds also to a comment entry in /HEPEVE/.

In the following, both the common blocks storing general information of the generated event/processes and the comment entries are described in detail.

### 8.4.1 COMMON /PROCES/

Structure:

```
C general process information
  INTEGER IPROCE, IDNODF, IDIFR1, IDIFR2, IDDPOM, IPRON
  COMMON /POPRCS/ IPROCE, IDNODF, IDIFR1, IDIFR2, IDDPOM, IPRON(15,4)
```

In addition to the process switches IPRON(15), this common block stores the event type of the last/currently generated event.

IPROCE process number  
 1: non-diffractive inelastic process  
 2: elastic scattering  
 3: quasi-elastic vector meson production (photons only)  
 4: central diffraction (double-pomeron scattering)  
 5: single diffraction dissociation of particle 1  
 6: single diffraction dissociation of particle 2  
 7: double diffraction dissociation  
 8: direct photon-hadron or single resolved and direct photon-photon scattering

IDNODF label to characterize non-diffractive event  
 0: elastic, quasi-elastic scattering or diffraction dissociation (see IDIFR1 and IDIFR2)  
 1: scattering by reggeon exchange  
 2: scattering by pomeron exchange without hard scattering  
 3: scattering by pomeron exchange involving at least one hard scattering  
 4: scattering by hard direct pomeron-pomeron interaction (only possible if the user sets a nonvanishing direct pomeron-quark coupling)

IDIFR1 label of diffractive dissociation of particle 1  
 0: elastic scattering or quasi-elastic vector meson production  
 1: low mass diffractive dissociation (reggeon cut)  
 2: high mass diffractive dissociation (pomeron cut)  
 3: high mass diffractive dissociation by hard resolved pomeron interaction  
 4: high mass diffractive dissociation by hard direct photon/pomeron interaction

IDIFR2 label of diffractive dissociation of particle 2 (see IDIFR1)

IDDPOM label of central diffraction  
 1: pomeron-pomeron scattering by reggeon exchange  
 2: pomeron-pomeron scattering by pomeron exchange without hard scattering  
 3: pomeron-pomeron scattering by pomeron exchange involving at least one hard scattering  
 4: pomeron-pomeron scattering by hard direct pomeron-pomeron interaction (only possible if the user sets a nonvanishing direct pomeron-quark coupling)

#### 8.4.2 COMMON /DEBUG/

Structure:

```
C event debugging information
  INTEGER NMAXD
  PARAMETER (NMAXD=100)
  INTEGER IDEB, KSPOM, KHPOM, KSREG, KHDR, KACCEP, KSTRG, KHTRG, KSL00,
&        KHL00, KSDPO, KHDPO, KEVENT, KSOFT, KHRD
  COMMON /PODEBG/ IDEB(NMAXD), KSPOM, KHPOM, KSREG, KHDR, KACCEP, KSTRG,
&        KHTRG, KSL00, KHL00, KSDPO, KHDPO, KEVENT, KSOFT, KHRD
```

This common block is intended to store model specific information of the event currently under generation which can be used for event classification. In addition the flags to determine the amount of diagnostic output of the different subroutines are stored.

IDEB	output level for each subroutine (to be used for debugging)
KSPOM	number of cut pomerons (soft partons only)
KHPOM	number of cut pomerons (involving in general soft and hard partons)
KSREG	number of cut reggeons
KHDIR	(0/1/2/3) none of the particles participates directly in the hard scattering, single resolved interaction (particle 1 resolved), single resolved interaction (particle 2 resolved), direct interaction
KACCEP	number of accepted events (generated up to final state particle)
KSTRG	number of nondiffractive cuts of triple-pomeron graphs (soft partons only)
KHTRG	number of nondiffractive cuts of triple-pomeron graphs (with at least one hard parton)
KSLOO	number of nondiffractive cuts of loop-pomeron graphs (soft partons only)
KHLOO	number of nondiffractive cuts of loop-pomeron graphs (with at least one hard parton)
KSDPO	number of cuts resulting in double-pomeron scattering (soft partons only)
KHDPO	number of cuts resulting in double-pomeron scattering (with at least one hard parton)
KEVENT	number of the call to <code>EVENT</code> (without the call for initialization)
KSOFT	number of chains involving soft partons only
KHARD	number of chains involving at least one hard parton

## Chapter 9

# Amplitude construction and unitarization

### 9.1 Born graph amplitudes

#### 9.1.1 Parameters and options

- IPAMD(1) approximation used for the complex phase of the eikonal function, note that the two-channel unitarization formalism currently implemented in the program works with purely imaginary eikonal functions only (D=1):  
0: complex phase of eikonal function is calculated according to analyticity constraints and dispersion relations (different for even and odd subamplitudes in  $s$ , see for example [26,89])  
1: eikonal is assumed to be a purely imaginary function
- IPAMD(8) intercept used in the cross section calculations of enhanced graphs (i.e. diffractive cross sections). As shown in [39], effects of multi-pomeron graphs not explicitly calculated can be taken into account using an effective pomeron intercept  $\alpha_{\text{eff}}(0)$  for enhanced graphs instead of the bare pomeron intercept (D=1):  
0: bare pomeron intercept as given by ALPOM in /REGGE/ used  
1: effective pomeron intercept as given by PARMDL(48) used
- IPAMD(9) switch for the impact parameter slope of the hard scattering amplitude (D=0):  
0: energy independent constant slope as given by BOHAR in /REGGE/  
1: energy independent slope as given by BOHAR in /REGGE/, rescaled according to mass dependence as parametrized in Eq. (3.36)  
2: energy independent part  $b_A + b_B$  of slope as used for the soft amplitude  
3: energy and mass dependent slope parametrization as used for the soft amplitude
- PARMDL(48) effective pomeron intercept  $\alpha_{\text{eff}}(0)$  used for the calculation of enhanced graphs, optionally also used for the calculation of diffractive mass distributions (see ISWMDL(22), D=1.08)

#### 9.1.2 COMMON /REGGE/

Structure:

C Reggeon phenomenology parameters

DOUBLE PRECISION ALPOM,ALPOMP,GP,BOPOM,ALREG,ALREGP,GR,BOREG,

& GPPP, GPPR, BOPPP, BOPPR, VDMFAC, VDMQ2F, BOHAR, AKFAC  
 COMMON /POPREG/ ALPOM, ALPOMP, GP(2), BOPOM(2),  
 & ALREG, ALREGP, GR(2), BOREG(2),  
 & GPPP, GPPR, BOPPP, BOPPR,  
 & VDMFAC(4), VDMQ2F(4), BOHAR, AKFAC

ALPOM pomeron intercept  $\alpha_P(0)$   
 ALPOMP slope of the pomeron trajectory  $\alpha'_P(0)$  ( $\text{GeV}^{-2}$ )  
 GP(1) coupling of particle 1 to pomeron ( $\sqrt{\text{mb}}$ )  
 GP(2) coupling of particle 2 to pomeron ( $\sqrt{\text{mb}}$ )  
 BOPOM(1) exponential slope of the pomeron-particle 1 coupling ( $\text{GeV}^{-2}$ )  
 BOPOM(2) exponential slope of the pomeron-particle 2 coupling ( $\text{GeV}^{-2}$ )  
 ALREG reggeon intercept  $\alpha_R(0)$   
 ALREGP slope of the reggeon trajectory  $\alpha'_R(0)$  ( $\text{GeV}^{-2}$ )  
 GR(1) coupling of particle 1 to effective reggeon ( $\sqrt{\text{mb}}$ )  
 GR(2) coupling of particle 2 to effective reggeon ( $\sqrt{\text{mb}}$ )  
 BOREG(1) exponential slope of the reggeon-particle 1 coupling ( $\text{GeV}^{-2}$ )  
 BOREG(2) exponential slope of the reggeon-particle 2 coupling ( $\text{GeV}^{-2}$ )  
 GPPP triple-pomeron coupling ( $\sqrt{\text{mb}}/\text{GeV}^2$ )  
 GPPR pomeron-reggeon coupling ( $\sqrt{\text{mb}}/\text{GeV}^2$ )  
 BOPPP exponential slope of the triple-pomeron coupling ( $\text{GeV}^{-2}$ )  
 BOPPR exponential slope of the pomeron-reggeon coupling ( $\text{GeV}^{-2}$ )  
 VDMFAC(1) VDM factor  $4\pi\alpha_{\text{em}}/f_{q\bar{q}}^2$ , for photons effective low mass vector meson to particle 1, for hadrons one  
 VDMFAC(2) VDM factor  $4\pi\alpha_{\text{em}}/f_{q\bar{q}^*}^2$ , for photons effective high mass vector meson to particle 1, for hadrons zero  
 VDMFAC(3) VDM factor  $4\pi\alpha_{\text{em}}/f_{q\bar{q}}^2$ , for photons effective low mass vector meson to particle 2, for hadrons one  
 VDMFAC(4) VDM factor  $4\pi\alpha_{\text{em}}/f_{q\bar{q}^*}^2$ , for photons effective high mass vector meson to particle 2, for hadrons zero  
 VDMQ2F(1) VDM factor  $\text{VDMFAC}(1) * m_{q\bar{q}}^2 / (m_{q\bar{q}}^2 + P_1^2)$ , for photons effective low mass vector meson to particle 1, for hadrons one  
 VDMQ2F(2) VDM factor  $\text{VDMFAC}(2) * m_{q\bar{q}^*} / (m_{q\bar{q}^*}^2 + P_1^2)$ , for photons effective high mass vector meson to particle 1, for hadrons zero  
 VDMQ2F(3) VDM factor  $\text{VDMFAC}(3) * m_{q\bar{q}}^2 / (m_{q\bar{q}}^2 + P_2^2)$ , for photons effective low mass vector meson to particle 2, for hadrons one  
 VDMQ2F(4) VDM factor  $\text{VDMFAC}(4) * m_{q\bar{q}^*} / (m_{q\bar{q}^*}^2 + P_2^2)$ , for photons effective high mass vector meson to particle 2, for hadrons zero  
 BOHAR exponential slope assumed for the hard coupling ( $\text{GeV}^{-2}$ )  
 AKFAC  $K$  factor for cross sections calculated using the Parton Model to correct for higher order graphs  
 PHISUP suppression factor for coupling to effective high mass resonance (particle 1 and 2)

### 9.1.3 COMMON /TWOCHA/

Structure:

C parameters of 2x2 channel model

```
DOUBLE PRECISION PHISUP, RMASS, VAR, AMPFAC, ELAFAC, VFAC
COMMON /PO2CHA/ PHISUP(2), RMASS(2), VAR, AMPFAC(4), ELAFAC(4), VFAC
```

RMASS1 mass of effective high mass resonance related to particle 1 (GeV)  
RMASS2 mass of effective high mass resonance related to particle 2 (GeV)  
VAR factor for exponential suppression of large momentum transfers connected with mass excitation ( $\text{GeV}^{-2}$ )

## 9.2 Unitarization, cross section

### 9.2.1 COMMON /XSECT/

Structure:

C cross sections

```
INTEGER IPFIL, IFAFIL, IFBFIL
DOUBLE PRECISION SIGTOT, SIGELA, SIGVM, SIGINE, SIGNDF, SIGDIR,
& SIGLSD, SIGHSD, SIGLDD, SIGHDD, SIGCDF,
& SIGPOM, SIGREG, SIGHAR, SIGTR1, SIGTR2, SIGLOO,
& SIGDPO, SIG1SO, SIG1HA, SLOEL, SLOVM, SIGCOR,
& FSUP, FSUD, FSUH, ECMFIL, P2AFIL, P2BFIL
COMMON /POCSEC/ SIGTOT, SIGELA, SIGVM(0:4, 0:4), SIGINE, SIGNDF, SIGDIR,
& SIGLSD(2), SIGHSD(2), SIGLDD, SIGHDD, SIGCDF(0:4),
& SIGPOM, SIGREG, SIGHAR, SIGTR1(2), SIGTR2(2), SIGLOO,
& SIGDPO(4), SIG1SO, SIG1HA, SLOEL, SLOVM(4, 4), SIGCOR,
& FSUP(2), FSUD(2), FSUH(2), ECMFIL, P2AFIL, P2BFIL,
& IPFIL, IFAFIL, IFBFIL
```

The cross sections calculated with the model by unitarization are stored in the COMMON /XSECTP/. The cross section are always given in mb. In photoproduction, the elastic cross section is the  $\gamma h \rightarrow \gamma h$  or  $\gamma\gamma \rightarrow \gamma\gamma$  process, quasi-elastic vector meson production is treated as inelastic scattering.

SIGTOT total cross section (mb)  
SIGELA elastic cross section (mb)  
SIGELA(I,K) cross section of quasi-elastic vector meson production  
I, K are vector meson labels belonging to particle 1 and 2 as follows:  
1: cross section of quasi-elastic  $\rho^0$  production  
2: cross section of quasi-elastic  $\omega^0$  production  
3: cross section of quasi-elastic  $\phi$  production  
4: cross section of quasi-elastic  $(\pi^+\pi^-)$  production  
0: sum of cross sections 1-4  
SIGINE inelastic cross section (mb)

SIGDIR	cross section of direct photon/pomeron interaction (mb)
SIGLSD(1)	cross section of low mass single diffractive excitation of particle 1 (mb)
SIGLSD(2)	cross section of low mass single diffractive excitation of particle 2 (mb)
SIGHSD(1)	cross section of high mass single diffractive dissociation of particle 1 (mb)
SIGHSD(2)	cross section of high mass single diffractive dissociation of particle 2 (mb)
SIGLDD	cross section of low mass double diffractive excitation (mb)
SIGHDD	cross section of low-high mass and high-high mass double diffractive dissociation (mb)
SIGCDF	cross section of central diffraction (double pomeron scattering, mb)
SIGPOM	bare soft pomeron cross section (without unitarization)
SIGREG	bare reggeon cross section (mb)
SIGHAR	bare hard double resolved cross section (mb)
SIGTR1	bare triple-pomeron cross section which corresponds to diffraction dissociation of side 1 (mb)
SIGTR2	bare triple-pomeron cross section which corresponds to diffraction dissociation of side 2 (mb)
SIGLOO	bare loop-pomeron cross section which corresponds to double diffraction dissociation (mb)
SIGDPO	bare cross section of central diffraction (pomeron-pomeron scattering, mb)
SIG1SO	cross section to find one cut soft pomeron only (mb)
SIG1HA	cross section to find one cut hard pomeron only (mb)
SLOEL	forward elastic slope of elastic scattering ( $\text{GeV}^{-2}$ )
SLOVM(I,K)	forward slope of quasi-elastic vector meson production ( $\text{GeV}^{-2}$ ) where I,K stands for 1: cross section of quasi-elastic $\rho^0$ production 2: cross section of quasi-elastic $\omega^0$ production 3: cross section of quasi-elastic $\phi$ production 4: cross section of quasi-elastic $(\pi^+\pi^-)$ production
SIGGEN(1)	sampled cross section of all processes activated for MC event generation (updated after each event)
SIGGEN(2)	cross section of accepted events (can differ from SIGGEN(1) due to user rejections to pre-select specific event classes, see subroutine PRESEL)
SIGGEN(3)	cross section of all processes activated for MC event generation at last/current interaction energy
SIGGEN(4)	cross section of all processes activated for MC event generation at initialization energy
FSUP(K)	suppression factor according to the photon virtuality of side (K=1,2) calculated using GVDM (see Eq. (2.37))

# Chapter 10

## Soft interactions

The transverse momentum of the soft sea quarks is calculated to get a smooth transition to the partons of the hard scattering. Valence quarks are treated separately. The transverse momentum is sampled from the same functional form as the sea quarks, however the parameter  $\beta$  is calculated from a simple logarithmic interpolation

$$\beta = \beta_{\text{low}} + \frac{\ln(\sqrt{s}/\text{GeV})}{\ln 1000} (\beta_{\text{high}} - \beta_{\text{low}}) . \quad (10.1)$$

The values  $\beta_{\text{low}}$  and  $\beta_{\text{high}}$  are for the distributions ISWMDL(3,4) = 0

$$\beta_{\text{low}} = \text{PARMDL}(23)$$

$$\beta_{\text{high}} = \text{PARMDL}(24)$$

and for distributions ISWMDL(3,4) = 1

$$\beta_{\text{low}} = \text{PARMDL}(21)$$

$$\beta_{\text{high}} = \text{PARMDL}(22) .$$

The transverse momentum cutoff used to distinguish between soft and hard interactions is stored in PARMDL(36-39).

### 10.0.2 Parameters and options

ISWMDL(3) sampling of soft  $p_{\perp}$  distribution for quarks belonging to hadrons:  
0: Gaussian distribution

$$\frac{dN_s}{dp_{\perp}} = p_{\perp} A \exp(-\beta p_{\perp}^2) \quad (10.2)$$

1: exponential distribution

$$\frac{dN_s}{dp_{\perp}} = p_{\perp} A \exp(-\beta p_{\perp}) \quad (10.3)$$

10: no soft  $p_{\perp}$  assignment

ISWMDL(4) sampling of soft  $p_{\perp}$  distribution for quarks belonging to photons:  
0: Gaussian distribution

$$\frac{dN_s}{dp_{\perp}} = p_{\perp} A \exp(-\beta p_{\perp}^2) \quad (10.4)$$

1: exponential distribution

$$\frac{dN_s}{dp_{\perp}} = p_{\perp} A \exp(-\beta p_{\perp}) \quad (10.5)$$

2: photon wave function (lowest order pQCD), the regularization mass  $m_q$  is set by the parameter PARM DL(25)

$$\frac{dN_s}{dp_\perp} = p_\perp A(P^2) \left( x_q(1-x_q) \left( P^2 + \frac{p_\perp^2 + m_q^2}{x_q(1-x_q)} \right)^2 \right)^{-1} \quad (10.6)$$

- 10: no soft  $p_\perp$  assignment
- ISWMDL(14) treatment of enhanced graphs:  
 0: no sampling of enhanced graphs  
 1: sampling of diffractive cuts of enhanced graphs  
 2: sampling of all different possible cuts of enhanced graphs
- ISWMDL(18) method to balance soft  $p_\perp$  of partons:  
 0:  $p_\perp$  of all soft partons belonging to one pomeron (reggeon) sum up to zero  
 1:  $p_\perp$  of all soft partons sum up to zero (disregarding the creation of the partons due to different pomeron cuts)
- ISWMDL(19) flavour sampling in soft pomeron interactions (valence partons):  
 0: quark flavour sampled according to probabilities given by PARM DL(1) - PARM DL(6)  
 1: quark flavour is sampled according to constituent quark mass and available phase space (strangeness suppressed by phase space)
- ISWMDL(20) flavour sampling of sea partons (all particles):  
 0: quark flavour is sampled according to constituent quark mass and available phase space  
 1: quark flavour sampled according to probabilities given by PARM DL(1) - PARM DL(6)
- PARMDL(1) probability to have a  $d$  or  $\bar{d}$  quark at soft chain (string) ends (D=0.425)  
 PARMDL(2) probability to have a  $u$  or  $\bar{u}$  quark at soft chain (string) ends (D=0.425)  
 PARMDL(3) probability to have a  $s$  or  $\bar{s}$  quark at soft chain (string) ends (D=0.15)  
 PARMDL(4) probability to have a  $c$  or  $\bar{c}$  quark at soft chain (string) ends (D=0)  
 PARMDL(5) probability to have a  $b$  or  $\bar{b}$  quark at soft chain (string) ends (D=0)  
 PARMDL(6) probability to have a  $t$  or  $\bar{t}$  quark at soft chain (string) ends (D=0)

### 10.0.3 COMMON /ABRSOF/

Structure:

```
C light-cone x fractions and c.m. momenta of soft cut string ends
  INTEGER MAXSOF
  PARAMETER ( MAXSOF = 50 )
  INTEGER IJSI2,IJSI1
  DOUBLE PRECISION XS1,XS2,PSOFT1,PSOFT2
  COMMON /POSOF/ XS1(MAXSOF),XS2(MAXSOF),
&                PSOFT1(4,MAXSOF),PSOFT2(4,MAXSOF),
&                IJSI1(MAXSOF),IJSI2(MAXSOF)
```

The flavours are given according to the PDG conventions, but gluons with 0. The momenta stored in this common block are calculated in the overall scattering CM system of the nondiffractive scattering. This system can differ from the hadron-photon/hadron CM system (enhanced graphs).

XS1(I) : initial momentum fraction of parton I taken from incoming particle 1  
 XS2(I) : initial momentum fraction of parton I taken from incoming particle 2  
 IJSI1(I) : flavour of initial parton taken from particle 1  
 IJSI2(I) : flavour of initial parton taken from particle 2  
 PSOFT1(1,I) : momentum of parton I taken from particle 1 in the x direction after soft  $p_{\perp}$  assignment (GeV/c)  
 PSOFT1(2,I) : momentum of parton I taken from particle 1 in the y direction after soft  $p_{\perp}$  assignment (GeV/c)  
 PSOFT1(3,I) : momentum of parton I taken from particle 1 in the z direction after soft  $p_{\perp}$  assignment (GeV/c)  
 PSOFT1(4,I) : energy of parton I taken from particle 1 after soft  $p_{\perp}$  assignment (GeV)  
 PSOFT2(1,I) : momentum of parton I taken from particle 2 in the x direction after soft  $p_{\perp}$  assignment (GeV/c)  
 PSOFT2(2,I) : momentum of parton I taken from particle 2 in the y direction after soft  $p_{\perp}$  assignment (GeV/c)  
 PSOFT2(3,I) : momentum of parton I taken from particle 2 in the z direction after soft  $p_{\perp}$  assignment (GeV/c)  
 PSOFT2(4,I) : energy of parton I taken from particle 2 after soft  $p_{\perp}$  assignment (GeV)

# Chapter 11

## Hard interactions

The initialization and sampling of hard subprocesses is governed by the particle and energy specifications given in the COMMON /GLOCMS/ and /POMCMS/. The initialization of the subroutines to sample hard processes is done by

POHINI	initialization of parameters for the calculation of the different hard scales
POHMCI	calculation of weights for Monte Carlo integration of the hard cross section (using POHFAC), determination of maximum remaining weights (using POHWGX), and calculation of the total hard Parton Model cross sections in dependence on the scattering energy (using POHXT0)

The initialization is performed for four particle configurations with transverse momentum cutoffs according to the values of PARM DL(36-39). If a transverse momentum cutoff lower than 0.5 GeV/c is given, no initialization of this process is performed.

During initialization, a tables of partial hard cross sections, weight maxima and factors for MC integration are stored in /HAXSEC/ for up to 20 energies. During event generation, a double-log interpolation is used to calculate these values for the currently sampled interaction energy. The initialization of the tables in /HAXSEC/ is also needed for minimum bias event generation with fixed-energy scattering setup since inelastic diffractive events are simulated by pomeron-particle scattering taking the invariant mass of the diffractive system as scattering energy.

The kinematic variables are sampled using the method described in Ref. [10] but extended to direct processes. For cross section calculations and at the beginning of Monte Carlo event generation, the inclusive hard cross sections are calculated. The corresponding phase space integration is performed by the transformations

$$\begin{aligned}x_1, x_2, t &\longrightarrow \eta_a, \eta_b, p_\perp && \text{(resolved processes)} \\x_1, t &\longrightarrow \eta_a, p_\perp && \text{(direct/single resolved processes)} \\t &\longrightarrow p_\perp && \text{(direct processes)}\end{aligned}\tag{11.1}$$

whereas for the Monte Carlo selection the variables  $x_1, x_2, t$  are used directly.

### 11.1 Hard scattering subprocesses

In Tab. (11.1) the list of hard scattering subprocesses treated in the program is given. They are sorted according to the primary particles (hadrons and real photon, pomeron) where the partons are belonging to. The numbers given in the first column are the reference numbers used in the program. The processes listed can be switched on/off using the variable MXSECT (see COMMON /HAXSEC/). The elements with the numbers (-1) are auxiliary entries used for the MC selection.

Table 11.1: Table of hard parton scattering subprocesses sampled by PHOJET

photon-photon/hadron		pomeron-photon/hadron		pomeron-pomeron	
-1	second part of 3	-1	second part of 3	-1	second part of 3
0	total sum (9, 15)	0	total sum (9, 15)	0	total sum (9, 15)
1	$gg \rightarrow gg$	1	$gg \rightarrow gg$	1	$gg \rightarrow gg$
2	$q\bar{q} \rightarrow gg$	2	$q\bar{q} \rightarrow gg$	2	$q\bar{q} \rightarrow gg$
3	$gq \rightarrow gq$	3	$gq \rightarrow gq$	3	$gq \rightarrow gq$
4	$gg \rightarrow q\bar{q}$	4	$gg \rightarrow q\bar{q}$	4	$gg \rightarrow q\bar{q}$
5	$q\bar{q} \rightarrow q\bar{q}$	5	$q\bar{q} \rightarrow q\bar{q}$	5	$q\bar{q} \rightarrow q\bar{q}$
6	$q\bar{q} \rightarrow q'\bar{q}'$	6	$q\bar{q} \rightarrow q'\bar{q}'$	6	$q\bar{q} \rightarrow q'\bar{q}'$
7	$qq \rightarrow qq$	7	$qq \rightarrow qq$	7	$qq \rightarrow qq$
8	$qq' \rightarrow qq'$	8	$qq' \rightarrow qq'$	8	$qq' \rightarrow qq'$
9	sum of 1-8	9	sum of 1-8	9	sum of 1-8
10	$\gamma q \rightarrow gq$	10	$\mathbf{P}q \rightarrow gq$	10	$\mathbf{P}q \rightarrow gq$
11	$\gamma g \rightarrow q\bar{q}$	11	$\mathbf{P}g \rightarrow q\bar{q}$	11	$\mathbf{P}g \rightarrow q\bar{q}$
12	$q\gamma \rightarrow gq$	12	$q\mathbf{P} \rightarrow gq$	12	$q\mathbf{P} \rightarrow gq$
13	$g\gamma \rightarrow q\bar{q}$	13	$g\mathbf{P} \rightarrow q\bar{q}$	13	$g\mathbf{P} \rightarrow q\bar{q}$
14	$\gamma\gamma \rightarrow q\bar{q}$	14	$\mathbf{P}\mathbf{P} \rightarrow q\bar{q}$	14	$\mathbf{P}\mathbf{P} \rightarrow q\bar{q}$
15	sum of 10-14	15	sum of 10-14	15	sum of 10-14

In photon-photon collisions, the high- $p_{\perp}$  production of  $\tau^+\tau^-$  pairs can be simulated in lowest order QED. The current treatment simulates the  $\tau$  pair cross section with the same transverse momentum cutoff as used for the pQCD calculations.

IPAMD(64) tau pair production if the hard subprocess 14 is activated:  
0: quark-antiquark pairs only  
1: quark-antiquark and muon pair production

### 11.1.1 Scale calculations

In the program, the running hard coupling constant is approximated to one loop order

$$\alpha_s(\mu^2) = \frac{12\pi}{(11N_c - 2N_F) \ln(\mu^2/\Lambda^2)} \quad \text{with} \quad N_c = 3. \quad (11.2)$$

The scale parameter  $\Lambda$  is taken from the parton distribution functions assigned to particle 1 and 2

$$\Lambda^2 = \Lambda_1^{(4)} \Lambda_2^{(4)} \quad (11.3)$$

assuming 4 active flavours. The virtuality  $\mu$  is calculated according to the kinematics of the hard scattering in dependence of the model switches (IPAMD(65-68) and PARMDL(110-113)). In general, for example, the scale parameters in hard diffraction can be different from the scale parameters in non-diffractive hard scattering. Therefore, a table of parameters  $f_{\alpha_s}^{\text{IP}}$  is stored and can be changed by the user. We use in the following the convention

- IP = 1 interaction between particle 1 and 2
- IP = 2 interaction between pomeron/reggeon and particle 1
- IP = 3 interaction between pomeron/reggeon and particle 2
- IP = 4 interaction between pomeron/reggeon and pomeron/reggeon

For example, the scale  $\mu$  of the hard scattering could be

$$\mu^2 = f_{\alpha_s} p_{\perp}^2 . \quad (11.4)$$

Similar parameters  $f_{\text{PDF}}^{\text{IP}}$ , and  $f_{\text{ISR}}^{\text{IP}}$  are used to get the virtuality used in the PDF calculations,  $\alpha_s$  calculations for initial state state parton shower generation.

IPAMDL(64+IP) kinematic variables used for the calculation of  $\mu$  in the running coupling constant of matrix elements:

- 1:  $\mu^2 = f_{\alpha_s}^{\text{IP}} p_{\perp}^2$
- 2:  $\mu^2 = f_{\alpha_s}^{\text{IP}} Q^2$
- 3:  $\mu^2 = f_{\alpha_s}^{\text{IP}} \hat{s}$

IPAMDL(68+IP) kinematic variables used for the calculation of  $\mu$  in the running coupling constant during initial state parton shower generation:

- 1:  $\mu^2 = f_{\text{ISR}}^{\text{IP}} p_{\perp}^2$
- 2:  $\mu^2 = f_{\text{ISR}}^{\text{IP}} Q^2$

IPAMDL(76+IP) kinematic variables used for the calculation of  $\mu$  in PDF parametrizations:

- 1:  $\mu^2 = f_{\text{PDF}}^{\text{IP}} p_{\perp}^2$
- 2:  $\mu^2 = f_{\text{PDF}}^{\text{IP}} Q^2$
- 3:  $\mu^2 = f_{\text{PDF}}^{\text{IP}} \hat{s}$

PARMDL(109+IP) factor  $f_{\alpha_s}^{\text{IP}}$  to calculate renormalization scale: hard scale used in matrix element  $\alpha_s$  calculations from the kinematic expression given by IPAMDL(64+IP)

PARMDL(113+IP) factor  $f_{\text{ISR}}^{\text{IP}}$  to calculate the hard scale used in initial state parton shower generation from the kinematic expression given by IPAMDL(68+IP)

PARMDL(121+IP) factor  $f_{\text{PDF}}^{\text{IP}}$  to calculate factorization scale: hard scale used for the PDF parametrizations from the kinematic expression given by IPAMDL(76+IP)

## 11.1.2 Parameters and options

ISWMDL(11) approximation of color flow in hard scattering subprocesses (D=0):

- 0: treatment of QCD color flow according to matrix elements
- 1: large  $N_c$  approximation of color flow

ISWMDL(12) generation method for semihard processes (D=0):

- 0: conventional sampling of partons according to QCD improved parton model
- 1: reserved

ISWMDL(24) assignment of transverse momentum to spectator quarks of hard scattering (D=0):

- 0:  $p_{\perp}$  assigned according to valence quark  $p_{\perp}$  distribution
- 1:  $p_{\perp}$  assigned according to transverse momentum distribution of soft quarks
- 2:  $p_{\perp}$  assigned according to an exponential distribution with the slope given by IPAMDL(20)

IPAMDL(7) energy dependence of transverse momentum cutoff (D=1):

- 0: cutoff is independent of collision energy
- 1: cutoff increases slowly with collision energy, currently the parametrization proposed in [15] is used.

- PARMDL(36) transverse momentum cutoff for resolved direct hard processes of particle 1 and 2 according to the initial particle specification given by user
- PARMDL(37) transverse momentum cutoff for resolved and direct hard processes of particle 1 and pomeron (hard diffraction)
- PARMDL(38) transverse momentum cutoff for resolved and direct hard processes of particle 2 and pomeron (hard diffraction)
- PARMDL(39) transverse momentum cutoff for resolved and direct hard processes of pomeron-pomeron scattering

### 11.1.3 COMMON /HARSLT/

Structure:

```

C hard scattering data
  INTEGER MSCAHD
  PARAMETER ( MSCAHD = 50 )
  INTEGER LSCAHD,LSC1HD,LSIDX,
&          NINHDL,NOINHDL,NIVAL,NOIVAL,NOUTHDL,NBRAHDL,NPROHDL
  DOUBLE PRECISION PPH,PTHDL,ETAHDL,Q2SCA,PDFVA,XHDL,VHDL,XOHD
  COMMON /POHSLT/ LSCAHD,LSC1HD,LSIDX(MSCAHD),
&                PPH(8*MSCAHD,2),PTHDL(MSCAHD),ETAHDL(MSCAHD,2),
&                Q2SCA(MSCAHD,2),PDFVA(MSCAHD,2),
&                XHDL(MSCAHD,2),VHDL(MSCAHD),XOHD(MSCAHD,2),
&                NINHDL(MSCAHD,2),NOINHDL(MSCAHD,2),
&                NIVAL(MSCAHD,2),NOIVAL(MSCAHD,2),
&                NOUTHDL(MSCAHD,2),NBRAHDL(MSCAHD,2),NPROHDL(MSCAHD)

```

To get the complete information concerning the hard scatterings belonging to different pomerons the common block /HARSLT/ should be used. There is a certain overlap with the common block /ABRHRD/. In the following I labels the number of the hard interaction.

- LSCAHD number of entries (hard scatterings)
- LSC1HD total number of generated hard processes for given event (including rejected hard processes)
- ETAHD(I,K) pseudo-rapidities of hard scattered partons K=1,2
- PTHDL(I) transverse momentum of hard scattered partons
- Q2SCA(I,K)  $Q^2$  scale used for the parton density calculation for the hard scattering number I and side K = 1,2 (GeV<sup>2</sup>)
- XHDL(I,K) momentum fraction of initial parton 1 (with initial state radiation)  
If a pomeron is involved in the hard scattering XHDL(I,2) gives always the parton momentum fraction taken from the pomeron. If a photon and no pomeron are involved in the hard scattering XHDL(I,2) gives always the parton momentum fraction taken from the photon. In addition NBRAHD(I,K) contains the corresponding mother particle ID number (see below).
- VHDL(I) momentum transfer of the hard scattering scaled by the subprocess energy  $v = \hat{t}/\hat{s}$
- XOHD(I,K) momentum fraction of initial parton K as sampled according simple QCD Parton Model (without initial state radiation)

NINHDI(I,K) flavours of incoming partons K=1,2 (PDG convention but 0 for gluons) (for initial state cascade or hard scattering)  
 NOUTHDI(I,K) flavours of outgoing partons K=1,2 (PDG convention but 0 for gluons)  
 NOINHDI(I,K) flavours of incoming partons K=1,2 (PDG convention but 0 for gluons) which are closest hard scattering  
 NBRAHDI(I,K) PDG number of mother particles K=1,2 involved in hard scattering  
 NPROHDI(I) subprocess number (see Tab. (11.1))

#### 11.1.4 COMMON /HAXSEC/

Structure:

```

C hard cross sections and MC selection weights
  INTEGER Max_pro_2
  PARAMETER ( Max_pro_2 = 16 )
  INTEGER IHa_last,IHb_last,MH_pro_on,MH_tried,
& MH_acc_1,MH_acc_2
  DOUBLE PRECISION Hfac,HWgx,HSig,Hdpt,HEcm_last,HQ2a_last,HQ2b_last
  COMMON /POHRCS/ Hfac(-1:Max_pro_2),HWgx(-1:Max_pro_2),
& HSig(-1:Max_pro_2),Hdpt(-1:Max_pro_2),
& HEcm_last,HQ2a_last,HQ2b_last,IHa_last,IHb_last,
& MH_pro_on(-1:Max_pro_2,0:4),MH_tried(-1:Max_pro_2,0:4),
& MH_acc_1(-1:Max_pro_2,0:4),MH_acc_2(-1:Max_pro_2,0:4)
  
```

The common block /HAXSEC/ is used to store different kinds of MC information, rejection weights, cross sections and event statistics concerning the hard scatterings. In the following the index M labels the number of the hard scattering subprocess, IP is the index of the scattering particle combination (1..4), and IE corresponds to the entry in the energy interpolation table.

XSECTA(1,0,IP,IE) transverse momentum cutoff (GeV)  
 XSECTA(1,M,IP,IE) scaling factor used for MC integration of the hard cross section  
 XSECTA(2,M,IP,IE) maximum remaining weight for MC selection  
 XSECTA(3,M,IP,IE) total hard Parton Model cross section  $\sigma^{\text{hard}}(s,p_{\perp}^{\text{cutoff}})$  in mb  
 XSECTA(4,M,IP,IE) differential hard Parton Model cross section  $d\sigma^{\text{hard}}(s,p_{\perp})/dp_{\perp}$  in mb/GeV  
 XSECTA(4,M,IP,IE) total hard Parton Model cross section (mb)  
 XSECT(1-6,M) used to store temporarily values of XSECTA  
 MXSECT(0,M,IP) subprocess switch, 1..subprocess sampled, 0..subprocess switched off  
 MXSECT(1,M,IP) number of generated hard scattering processes  
 MXSECT(2,M,IP) number of accepted hard scattering processes without rejections due to generation of remnants and multiple interactions  
 MXSECT(3,M,IP) number of accepted hard scattering processes without rejections due to chain construction and fragmentation  
 MXSECT(4,M,IP) number of accepted hard scattering processes  
 ECMSH(IP,IE) energy values of the energy interpolation table  
 ISTTAB number of valid entries in the energy interpolation table

### 11.1.5 COMMON /HAQQAP/

Structure:

```
C scale parameters for parton model calculations
  INTEGER NQQAL,NQQALI,NQQALF,NQQPD
  DOUBLE PRECISION AQQAL,AQQALI,AQQALF,AQQPD
  COMMON /POHSCL/ AQQAL,AQQALI,AQQALF,AQQPD,
&                NQQAL,NQQALI,NQQALF,NQQPD
```

In this common block, the scale parameters used for the simulation of the last/currently calculated hard interaction are stored. These parameters are updated in POHINT each time before a hard scattering is generated.

- AQQAL: multiplication factor for the physical quantity selected by NQQAL to determine running coupling constant  $\alpha_s$  of hard scattering
- AQQALI: multiplication factor for the physical quantity selected by NQQALI to determine running coupling constant  $\alpha_s$  in initial state evolution
- AQQALF: multiplication factor for the physical quantity selected by NQQALF to determine running coupling constant  $\alpha_s$  in final state evolution
- AQQPD: multiplication factor for the physical quantity selected by NQQPD to determine scale for PDF calculation
- NQQAL: selection of scale  $\mu^2$  for  $\alpha_s(\mu^2/\Lambda^2)$  calculation in hard scattering
  - 1:  $\mu^2 = \text{AQQAL} * p_{\perp}^2$
  - 2:  $\mu^2 = \text{AQQAL} * Q^2$
  - 3:  $\mu^2 = \text{AQQAL} * \hat{s}$
- NQQALI: selection of scale  $\mu^2$  for  $\alpha_s(\mu^2/\Lambda^2)$  and PDF calculation in initial state evolution
  - 1:  $\mu^2 = \text{AQQALI} * p_{\perp}^2$
  - 2:  $\mu^2 = \text{AQQALI} * Q^2$
- NQQPD: selection of scale  $\mu^2$  for PDF calculation in hard scattering
  - 1:  $\mu^2 = \text{AQQPD} * p_{\perp}^2$
  - 2:  $\mu^2 = \text{AQQPD} * Q^2$
  - 3:  $\mu^2 = \text{AQQPD} * \hat{s}$

## 11.2 Initial and final state radiation

By default, the lower virtuality cutoff for initial state parton shower generation is identified with the transverse momentum cutoff. This provides a consistent event description in the minimum bias mode. For event generation of hard processes only (see ISWMDL(2)), the virtuality cutoff should be set to a lower value (about 1 GeV<sup>2</sup>).

- ISWMDL(8) methods of parton showering (D=3):
  - 0: no parton showers at all
  - 1: only final state parton showers by JETSET
  - 2: only initial state partons showers
  - 3: initial and final state parton showers
- IPAMD(110) simulate direct  $\gamma \rightarrow q\bar{q}$  splitting for initial state radiation of photons (D=1):
  - 0: ISR of photon is generated in the same way as for hadrons
  - 1: simulation of direct splitting

PARMDL(125+IP) lower virtuality cutoff for initial state radiation for the particle combination  
 IP=1..4 (GeV<sup>2</sup>, positive value)

### 11.3 Parton distribution functions

Within the program PHOJET the user has to connect parton distribution functions (PDF) to particles. This can be done using the input data card PDF or a call to SETPDF. The PDFs specified are handled by the subroutines SETPDF and GETPDF. For any hard process the subroutine GETPDF collects from a table the PDF parametrization connected to the particles engaged in hard scattering. For the most common particles a sensible parametrization is assigned by default. It is possible to specify PDF parametrizations even for particles not needed in the calculation. Each PDF parametrization is given by the numbers IGRP, ISET and IEXT. The variable IGRP characterizes the parametrization (i.e. group of authors MRS, GRV) and the variable ISET specifies the set taken from this parametrization. The flag IEXT is set to 0 for internal parametrizations, 1 for the call to PDLIB [90] old format, 2 for the call to PDLIB new format, 3 for the call to PHOLIB [91], and 4 for the call to photon virtuality-dependent parametrizations. All the parametrizations are assumed to be valid for "particles" (i.e. with positive numbers according to PDG convention). This means that the quark contents will be changed according to charge conjugation if a PDF parametrization is assigned to a "antiparticle" (i.e. with negative number according to PDG convention). Nevertheless the PDF parametrization has to be given for particles and antiparticles separately (and can differ from particle to antiparticle).

The two PDFs for the present/last hard interaction are stored in the COMMON /PARPDF/, but it is recommended to use the subroutine specified above for manipulations.

#### 11.3.1 COMMON /PARPDF/

Structure:

```
C currently activated parton density parametrizations
  CHARACTER*8 PDFNAM
  INTEGER IPARID, IPAVA, ITYPE, IGRP, ISET, IEXT, NPAOLD
  DOUBLE PRECISION PDLAM, PDFQ2M
  COMMON /POPPDF/ PDLAM(2), PDFQ2M(2), PDFNAM(2), IPARID(2),
&                IPAVA(2), ITYPE(2), IGRP(2), ISET(2), IEXT(2), NPAOLD
```

This common block stores the two parton distribution functions to be used for the recent calculation. It is maintained by the subroutine ACTPDF in connection with the subroutines SETPDF and GETPDF.

```
PDLAM(I):   $\Lambda_{\text{QCD}}^{(4)}$  used for PDF evolution (GeV)
PDFQ2M(I): minimum  $Q^2$  for the PDF (GeV2)
PDFNAM(I): name (abbreviation) of PDF parametrization (if available)
IPARID(I): PDG number of particle which is assigned to set of PDFs
PARVI(I):  virtuality of off-shell particles (GeV2, positive)
IPAVA(I):  valence quark flag (used for interface with DTUNUC)
           0: particle remnant without valence quarks
           1: particle with valence quarks
ITYPE(I):  particle type:
           1: nucleon
```

2: pion  
 3: photon  
 20: pomeron  
**IGRP(I)**: parametrization number (author group)  
**ISET(I)**: set of the parametrization  
**IEXT(I)**: PDF library switch:  
 0: internal PDF used (see Tab. E.1)  
 1: call to P<sub>D</sub>FLIB (old format, IGRP is used as number to identify the parametrization and the set)  
 2: call to P<sub>D</sub>FLIB (new format, ITYPE, IGRP and ISET have to be given by the user)  
 3: call to P<sub>H</sub>OLIB (only IGRP is used)  
 4: PDFs depending on photon virtuality (see Tab. E.1)

**SUBROUTINE SETPDF**(IDPDG, ITYPE, IGRP, ISET, IEXT, IPAVAL, MODE)

**purpose:** assigns PDF numbers to particles, no initialization in connection to the selected PDF is performed. The assignment of the PDF to the particles is stored in an internal table. The list of currently available PDFs is given in Table E.1. In order to link external PDF libraries, the corresponding dummy subroutines have to be removed from the end of the file **phopdf.f**. For example, in the case of P<sub>D</sub>FLIB these are PDFSET, STRUCTM and PFTOPDG.

**input:** IDPDG PDG number of particle  
 IGRP PDF parametrization (author group number)  
 ISET number of parametrization set  
 IEXT  
 0: internal parametrizations used  
 1: P<sub>D</sub>FLIB called (old interface)  
 2: P<sub>D</sub>FLIB called (new interface)  
 3: P<sub>H</sub>OLIB called  
 4: internal collection of photon PDFs depending on the photon virtuality  
 MODE  
 -1: add entry to internal table  
 1: read from table  
 2: output (printed list) of table

**output:** for MODE = 1 the following variables are set  
 IGRP PDF parametrization (author group number)  
 ISET number of parametrization set  
 ITYPE particle type  
 1: nucleon PDF  
 2: pion PDF  
 3: photon PDF  
 20: pomeron PDF  
 IPAVAL flag used for PHOJET interface to DTUNUC if IDPDG = 777 or 888  
 0: particle without valence quarks (remnant)  
 1: particle with valence quarks

SUBROUTINE GETPDF(NPAR,PDFNA,ALA,Q2MI,Q2MA,XMI,XMA)

**purpose:** get PDF information

**input:** NPAR

1: first PDF in COMMON /PARPDF/

2: second PDF in COMMON /PARPDF/

**output:** PDFNA name of the PDF parametrization (CHARACTER\*8)

ALA QCD scale parameter  $\Lambda^{(4)}$  (4 active flavours assumed)

Q2MI minimal  $Q^2$  supported

Q2MA maximal  $Q^2$  supported

XMI minimal  $x$  supported

XMA maximal  $x$  supported

SUBROUTINE ACTPDF(IDPDG,PXMASS,ISIDE)

**purpose:** set PDF for particle 1 or 2 according to IDPDG

**input:** IDPDG PDG number of particle

PXMASS squared particle mass (photon virtuality) in  $\text{GeV}^2$  (positive value)

ISIDE particle index

1: activate PDF of particle 1

2: activate PDF of particle 2

-2: output of current PDF settings

**output:** COMMON /PARPDF/ is filled with PDF data, correct  $\Lambda_{\text{QCD}}^{(4)}$  according to PDF evolution is determined

# Chapter 12

## Diffractive interactions

### 12.1 Elastic and quasi-elastic scattering

PARMDL(170) exponent  $n$  in Ross-Stodolsky parametrization of  $\rho^0$  mass distribution, see Eq. (3.31) (D=4.2)

### 12.2 Single- and double diffraction dissociation

#### 12.2.1 Parameters and options

- ISWMDL(13) method to sample momentum transfer for elastic and quasi-elastic reactions:  
0: sampling from an exponential with parameters given by the user ( $t \approx 0$ ), taken from COMMON /QEVECM/  
1: sampling from a binned distribution calculated from the complete amplitude given by the model
- ISWMDL(22) diffractive mass distribution for diffraction dissociation (with  $M$  and  $m$  denoting the diffractive mass and the mass of the incoming particle, respectively):  
1:  $d\sigma/dM^2 \approx 1/M^2$   
-1:  $d\sigma/dM^2 \approx 1/(M^2 - m^2)$   
2:  $d\sigma/dM^2 \approx 1/M^{2\alpha_{\text{eff}}(0)}$   
-2:  $d\sigma/dM^2 \approx 1/(M^2 - m^2)^{\alpha_{\text{eff}}(0)}$   
The Pomeron intercept  $\alpha_{\text{eff}}(0)$  is treated independent of the bare pomeron intercept  $\alpha_{\mathbb{P}}(0)$  which is calculated by cross section fitting. The higher order corrections to the triple-pomeron graph which are not included in the unitarization can be parametrized using an effective pomeron intercept of  $\alpha_{\text{eff}}(0) \approx 1.07 \dots 1.085$  instead of the bare pomeron intercept (see PARMDL(48)). The mass  $m$  is the mass of the incoming, diffractively dissociating particle.
- PARMDL(45) upper mass cut for diffractively produced system (coherence constraint)  $M_{D,\text{max}} = \text{PARMDL}(45) * \sqrt{s}$  (D=0.46)
- PARMDL(46) lower mass cut  $m_{\Delta}$  in diffraction, see Eq. (3.34) (GeV, D=0.3)
- PARMDL(47) regularization parameter for diffractive slope (D=4)
- PARMDL(48) renormalized pomeron intercept as used in the calculation of enhanced graphs (D=1.08)
- PARMDL(49) coherence constraint used for the eikonalization of enhanced graphs, cross sections printed during initialization refer to this constraint whereas the actually used cross section and limits for  $M_{\text{diff}}$  follow from PARMDL(45) (D= $\sqrt{0.05}$ )

### 12.2.2 COMMON /QEVECM/

Structure:

```
C parameters of the "simple" Vector Dominance Model
  DOUBLE PRECISION VMAS,GAMM,RMIN,RMAX,VMSL,VMFA
  COMMON /POSVDM/ VMAS(4),GAMM(4),RMIN(4),RMAX(4),VMSL(4),VMFA(4)
```

This common block defines the free parameters related to elastic scattering and quasi-elastic vector meson production. In the following the index I runs from 1 to 3. For pure hadronic interactions only I = 1 is used. In photoproduction I = 1,2,3 stands for quasi-elastic  $\rho^0$ ,  $\omega$  and  $\phi$  production.

VMAS(I)	average mass of particle
GAMM(I)	average decay width of particle
RMIN(I)	minimal mass sampled from Breit-Wigner distribution according to average mass and decay width
RMAX(I)	maximal mass sampled from Breit-Wigner distribution according to average mass and decay width
VMSL(I)	elastic slope in forward direction ( $\text{GeV}^{-2}$ ), this value is used only if IVMSL = 0, otherwise the model prediction calculated during initialization is used
VMFA(I)	VDM factors $4\pi\alpha_{em}/f_i^2$ determining the different contributions to the vector mesons produced by quasi-elastic scattering
TMIN(I)	minimal absolute momentum transfer (squared) sampled
TMAX(I)	maximal absolute momentum transfer (squared) sampled

## 12.3 Central diffraction

The cut on the Feynman  $x_F$  applied to the elastically scattered particles  $x_A \geq c$  and  $|x_B| \geq c$  is calculated from

$$c = \max(\text{PARMDL}(72), 1 - 1/\text{PARMDL}(70)^2) \quad (12.1)$$

to ensure that at least the minimum invariant mass of the diffractive particle system together with the elastically scattered particles (as specified by PARMDL(71)) is generated.

PARMDL(70)	lower mass cut for $\sqrt{s_1/M_{CD}^2}$ and $\sqrt{s_2/M_{CD}^2}$ in central diffraction, see Fig. 3.10. This cut is used to ensure the applicability of the double-pomeron graph approximation (D=2).
PARMDL(71)	lower mass cut for the central-diffractively produced system $M_{CD}$ , see Fig. 3.10 (GeV, D=2.0)
PARMDL(72)	lower cut $c$ on the Feynman $x_F$ of elastically scattered particles $A$ and $B$ . This cut can be used to force a rapidity gap between the central particle system and the elastically scattered particles (D=0)

## 12.4 Pomeron-particle/pomeron scattering

ISWMDL(21)	decay of diffractively produced resonances assuming transversely/longitudinally polarized photons (D=2): 0: always decay like hadroproduced resonances (see IPAMD(3))
------------	--

- 1: spin dependent decay of quasi-elastically produced low-mass vector mesons (see IPAMD(4)) ( $\rho$ ,  $\omega$  and  $\phi$ ) only
  - 2: spin dependent decay of diffractively produced low- and high-mass vector mesons (see IPAMD(4))
- ISWMDL(23) treatment of small masses in diffraction (D=1):
- 0: always fragmentation via one chain
  - 1: superposition of resonances and one-chain background according to finite mass sum rules
- IPAMD(3) decay scheme applied for resonances produced in low-mass hadron diffraction dissociation (polarizations are calculated in helicity frame, D=0):
- 0: isotropic decay according to phase space
  - 1: anisotropic decay according transverse polarization
  - 2: anisotropic decay according longitudinal polarization
  - 3: longitudinal, limited phase space model (currently not supported)
- IPAMD(4) decay scheme applied for resonances produced in low-mass photon diffraction dissociation (polarizations are calculated in helicity frame, see ISWMDL(21), D=1):
- 0: isotropic decay according to phase space
  - 1: anisotropic decay according transverse polarization
  - 2: anisotropic decay according longitudinal polarization
  - 3: longitudinal, limited phase space model (currently not supported)
- PARMDL(26) normalization of internal pomeron PDF sets (e.i. value of the momentum sum rule), does not apply to the QCD evolved CKMT set (D=0.3)
- PARMDL(74) direct pomeron-quark coupling, can be used to simulate a superhard gluonic pomeron PDF (D=0).

## Chapter 13

# Chain construction and fragmentation

### 13.0.1 Options and parameters

- ISWMDL(6) fragmentation of chain configurations, fragmentation parameters (D=2):  
0: no fragmentation at all, initial and final state radiation is generated  
1: fragmentation by JETSET without changing any Lund parameters  
2: fragmentation by JETSET without changing Lund parameters but defining stable particles according to MSTJ(22)=2 (decay length 10mm)  
3: fragmentation by JETSET with tuned parameters (currently not supported) and MSTJ(22)=2 is set (decay length 10mm)  
negative sign: fragmentation by JETSET according to the switches listed above but with strange and charm mesons/baryons are treated as stable particles
- ISWMDL(7) method to correct chain configurations with small masses. Chains with masses below the one/two-particle threshold are treated in the following way: a second chain is selected maximizing the invariant mass of the four-momentum of the two chains, then a minimum momentum transfer is exchanged to increase the mass of the first chain. Optionally, the "mass-corrected" chain can be directly converted to a single hadron/resonance (D=2):  
-1: no chain mass check at all  
0: chains with small masses (below the corresponding lowest two-particle mass threshold) are directly converted to hadrons/resonances, depending on the mass and the quantum numbers of the chain, pseudo-scalar or vector mesons are formed from  $q - \bar{q}$ , octett or decuplett baryons are formed from  $q - qq$  and  $\bar{q} - \bar{q}\bar{q}$  systems  
1: chains with masses below the one-particle threshold are corrected and directly converted to hadrons/resonances  
2: chains with masses below the one-particle threshold are corrected but not converted to hadrons/resonances  
3: rejection for configurations with very small mass, no correction for chains with small masses
- ISWMDL(17) mass fine correction for the two chains belonging to the same pomeron (D=0):  
0: no correction at all  
1: correct chains with very small masses by recombining quark-antiquark pairs to gluons (if possible)

As a cross check, energy-momentum and quantum number (charge, baryon number) conservation can be checked for each generated event (see IPAMD(15)). However, due to the single precision interface to JETSET there may be deviations of energy-momentum conservations of the order of 1%. This problem can only be solved by converting the relevant momentum variables in JETSET

to double precision. For example, if the program is used to generate diffractive events at very high energies, this may cause the output of warnings by POQCHK and finally the abort of program execution. For such configurations, the internal energy-momentum check should be switched off or the precision of the comparison should be reduced (see below).

IPAMDL(15) overall energy-momentum conservation check, check of quantum numbers (D=1):

0: no energy-momentum and quantum number check at all

1: energy-momentum check of final state particles, if some deviation is found, each step of the event generation as stored in /HEPEVS/ is checked. Events with deviations larger than the limits given by PARMDL(75,76) are printed but not accepted for event generation.

PARMDL(75) relative deviation allowed for the energy and  $x$ ,  $y$  and  $z$  momentum components (D=0.01)

PARMDL(75) absolute deviation allowed for the energy and  $x$ ,  $y$  and  $z$  momentum components (D=0.01 GeV)

### 13.0.2 COMMON /POSTRG/

Structure:

C color string configurations including collapsed strings and hadrons

INTEGER MSTR

PARAMETER (MSTR=500)

INTEGER NPOS, NCODE, IPAR1, IPAR2, IPAR3, IPAR4, NNCH, IBHAD

COMMON /POSTRG/ NPOS(4, MSTR), NCODE(MSTR),

& IPAR1(MSTR), IPAR2(MSTR), IPAR3(MSTR), IPAR4(MSTR),

& NNCH(MSTR), IBHAD(MSTR), ISTR

References of external event analysis programs to this common block should be avoided. All the data stored are also available in /HEPEVS/ and /HEPEVE/. The values of  $\Gamma$  and  $\beta_i$  giving the Lorentz transformation of the chains to the chain CMS are not calculated or used in the present version.

GAMBET(1, I):  $\Gamma\beta_x$  of Lorentz transformation into CMS of chain I

GAMBET(2, I):  $\Gamma\beta_y$  of Lorentz transformation into CMS of chain I

GAMBET(3, I):  $\Gamma\beta_z$  of Lorentz transformation into CMS of chain I

GAMBET(4, I):  $\Gamma$  of Lorentz transformation into CMS of chain I

NPOS(1, I): index of chain/hadron in COMMON /HEPEVS/

NPOS(2, I): index of first parton in COMMON /HEPEVS/ belonging to chain/hadron I, 0 for quasi-elastically scattered hadrons

NPOS(3, I): index of last parton in COMMON /HEPEVS/ belonging to chain/hadron I; can be negative, if more than 2 partons are mother particles of one or the mothers are stored sequentially; 0 for quasi-elastically scattered hadrons

NCODE(I): fragmentation label

- 3:**  $q - \bar{q}$  chain
- 4:**  $q - (qq)$  or  $\bar{q} - (\bar{q}\bar{q})$  chain
- 5:**  $(qq) - (\bar{q}\bar{q})$  chain
- 6:**  $(qq) - q$  or  $(\bar{q}\bar{q}) - \bar{q}$  chain
- 7:**  $g - g \dots g - g$  loop chain
- 99:** chain collapsed to single resonance/hadron
- 999:** deleted entry (joined with another chain)

To specify the fragmentation label, only the partons at the chain ends are considered.

**IPAR(1-4, I) :** quark numbers of the chain ends according to the compressed particle code (CPC) and fragmentation label **NCODE(I) :**

- 3:** IPAR(1, I) CPC of first quark  
IPAR(2, I) CPC of second quark
- 4:** IPAR(1, I) CPC of first quark  
IPAR(2, I) CPC of first quark belonging to diquark  
IPAR(3, I) CPC of second quark belonging to diquark
- 5:** IPAR(1, I) CPC of first quark belonging to first diquark  
IPAR(2, I) CPC of second quark belonging to first diquark  
IPAR(3, I) CPC of first quark belonging to second diquark  
IPAR(4, I) CPC of second quark belonging to second diquark
- 6:** IPAR(1, I) CPC of first quark of diquark  
IPAR(2, I) CPC of second quark of diquark  
IPAR(3, I) CPC of last quark

**NNCH(I) :** mass label of chain I

- 0:** mass of chain large enough to use string fragmentation
- 1:** cluster with quantum numbers of the hadron corresponding to the lowest mass possible
- 1:** cluster with quantum numbers of a hadron with higher mass, but below the threshold for string fragmentation

**IBHAD(I) :** not used for chains with **NNCH(I) = 0**, otherwise CPC of the hadron according to **NNCH(I)**

**ISTR:** number of valid entries in **COMMON /STRING/**

## Chapter 14

# Interactions involving weakly virtual photons

- ISWMDL(10) approximation of the cross section dependence on the photon virtuality (D=1):  
0: total and partial cross sections independent of the photon virtuality  
1: GVDM factor is used for the total cross section, the partial cross sections for hard interactions are calculated according PDF-virtuality dependence
- IPAMD(115) approximation used for virtuality dependence of the photon PDF (D=1):  
0: no dependence on photon virtuality, the photon PDFs are always calculated for real photons  
1: parametrization of PDF-virtuality dependence according Eqs. (2.38,2.39), the photon flux is calculated according to Eqs. (4.18,4.23,4.15)  
2: if available, virtuality dependence of the photon PDF parametrization is used (currently not supported)
- PARMDL(27) weight factor  $r_\rho$  used in Eq. (2.37), (D=0.65)
- PARMDL(28) weight factor  $r_\omega$ , (D=0.08)
- PARMDL(29) weight factor  $r_\phi$ , (D=0.05)
- PARMDL(29) weight factor  $r_{\text{eff}}$  to approximate effects due to higher mass vector mesons, (D=0.22)
- PARMDL(31) squared mass  $m_\rho^2$  used in Eq. (2.37), (GeV<sup>2</sup>, D=0.589824)
- PARMDL(32) squared mass  $m_\omega^2$ , (GeV<sup>2</sup>, D=0.609961)
- PARMDL(33) squared mass  $m_\phi^2$ , (GeV<sup>2</sup>, D=1.038361)
- PARMDL(34) squared mass  $m_{\text{eff}}^2$  to approximate effects due to higher mass vector mesons, (GeV<sup>2</sup>, D=1.96)
- PARMDL(35) effective mass used in Eq. (3.7) to calculate the suppression of multiple soft contributions for virtual photons (GeV<sup>2</sup>, D=0.59).

# Chapter 15

## Photon flux generation

For beamstrahlung and photon radiation due to laser backscattering, the virtuality of the colliding photons is neglected. Bremsstrahlung is simulated according to the double differential spectrum (4.15). By the MC rejection method, Eqs. (4.18,4.23) are integrated during event simulation. This means that the virtuality dependence of the photon-hadron or photon-photon cross section influences the finally observable photon spectrum (for the virtuality dependence, see Sec. 14). This method may become very inefficient if one selects high- $p_{\perp}$  events with  $ISWMDL(2)=0$ . In this case, the cross section increases very fast with the invariant mass of the photon-photon/hadron system and a large number of internal rejections is needed to integrate Eqs. (4.18,4.23).

In general, the photon emission is simulated according to the given limits in the photon virtuality  $P^2$  and the energy fraction  $y$  (see `Q2MIN`, `Q2MAX`, `YMIN`, and `YMAX` in `/LEPCUT/`). In the next step the angular constraints (`THMAX`, `THMIN`) are applied and finally the invariant mass of the photon-hadron or photon-photon system is restricted to the region given by `ECMIN` and `ECMAX`.

Note that the polar angles  $\theta$  are calculated in reference to the positive  $z$  axis, i.e. the forward scattering of electron 1 (2) corresponds to an angle of 0 ( $\pi$ ).

The code for the photon flux calculation in hadron-hadron interactions applying the semi-classical model was provided by Hencken (see [77] for details).

### 15.0.3 Parameters and options

- `IPAMD(11)` treatment of scattered electron of particle side 1 in photoproduction (`D=0`):  
0: initial and final electrons are not copied to `/HEPEVS/`  
1: initial and final electrons are stored in `/HEPEVS/`, however only the scattered electrons are copied to the JETSET common block `/HEPEVT/`.
- `IPAMD(12)` treatment of scattered electron of particle side 2 in photoproduction, see above (`D=0`).
- `ISWMD(26)` calculation of photon flux in heavy ion collisions (`D=1`):  
0: calculation allowing the ions to overlap (flux generation without  $\Theta(|\vec{B}_1 - \vec{B}_2| - R_1 + R_2)$  in Eq. (4.31)  
1: calculation according to Eq. (4.31)

### 15.0.4 COMMON /LEPCUT/

Structure:

```
C photon flux kinematics and cuts
  DOUBLE PRECISION ECMIN,ECMAX,EEMIN1,EEMIN2,
&                  YMIN1,YMAX1,YMIN2,YMAX2,
```

```

&          Q2MIN1 , Q2MAX1 , Q2MIN2 , Q2MAX2 ,
&          THMIN1 , THMAX1 , THMIN2 , THMAX2
  INTEGER  ITAG1 , ITAG2
  COMMON /POFCUT/ ECMIN , ECMAX , EEMIN1 , EEMIN2 ,
&          YMIN1 , YMAX1 , YMIN2 , YMAX2 ,
&          Q2MIN1 , Q2MAX1 , Q2MIN2 , Q2MAX2 ,
&          THMIN1 , THMAX1 , THMIN2 , THMAX2 ,
&          ITAG1 , ITAG2

```

This common block stores the kinematic limitations applied to the lepton-photon vertex. Note that the kinematics of the vertex is sampled according to the given  $y$  and  $P^2$  range. The energy cut and the polar angle cut are applied afterwards. It is assumed that electron 1 moves into positive  $z$  direction.

```

ECMIN  minimal CMS energy allowed for  $\gamma\gamma$  or  $\gamma h$  system (GeV, default 5 GeV)
ECMAX  maximal CMS energy allowed for  $\gamma\gamma$  or  $\gamma h$  system (GeV, default  $10^{30}$  GeV)
EEMIN1 minimal energy needed to detect electron 1 with the electron tagging system, all
        scattered electrons with energies below this threshold are treated as not detected
        (GeV, default 1 GeV)
EEMIN2 minimal energy needed to detect electron 2 with the electron tagging system, all
        scattered electrons with energies below this threshold are treated as not detected
        (GeV, default 1 GeV)
YMIN1  minimal energy fraction  $y_{\min,1}$  taken by the photon from the electron 1
YMIN1  maximal energy fraction  $y_{\max,1}$  taken by the photon from the electron 1
YMIN2  minimal energy fraction  $y_{\min,2}$  taken by the photon from the electron 2
YMIN2  maximal energy fraction  $y_{\max,2}$  taken by the photon from the electron 2
Q2MIN1 minimal virtuality  $P_{\min,1}^2$  of photon 1 ( $\text{GeV}^2$ , positive)
Q2MAX1 maximal virtuality  $P_{\max,1}^2$  of photon 1 ( $\text{GeV}^2$ , positive)
Q2MIN2 minimal virtuality  $P_{\min,2}^2$  of photon 2 ( $\text{GeV}^2$ , positive)
Q2MAX2 maximal virtuality  $P_{\max,2}^2$  of photon 2 ( $\text{GeV}^2$ , positive)
THMIN1 minimal polar angle  $\theta_{\min,1}$  of scattered electron 1 in LAB system (radian)
THMAX1 maximal polar angle  $\theta_{\max,1}$  of scattered electron 1 in LAB system (radian)
THMIN2 minimal polar angle  $\theta_{\min,2}$  of scattered electron 2 in LAB system (radian)
THMAX2 maximal polar angle  $\theta_{\max,2}$  of scattered electron 2 in LAB system (radian)

```

### 15.0.5 COMMON /PHOSRC/

Structure:

```

C gamma-lepton or gamma-hadron vertex information
  INTEGER IGHEL , IDPSRC , IDBSRC
  DOUBLE PRECISION PINI , PFIN , PGAM , GYY , GQ2 , GGECD , GAIMP , PFTHE , PFPHI ,
&          RADSRC , AMSRC , GMSRC
  COMMON /POFSRC/ PINI(5,2) , PFIN(5,2) , PGAM(5,2) , IGHEL(2) ,
&          GYY(2) , GQ2(2) , GGECD , GAIMP(2) , PFTHE(2) , PFPHI(2) ,
&          IDPSRC(2) , IDBSRC(2) , RADSRC(2) , AMSRC(2) , GMSRC(2)

```

This common block is filled by the routines `GGEPEM`, `GPHERA`, `GGBEAM`, `GGBLSR`, `GGHIOG`, and `GGHIOF` during the sampling of  $ee$ ,  $eh$ , or  $hh$  events. It contains the kinematic variables describing the lepton/hadron-photon vertices sampled for the current/last event. Note that in `GGEPEM` all the variables are set to physical values whereas in the other routines the common is filled partially only. In the present version of the program, the initial and final state electrons are not written to the standard common block `/HEPEVS/`.

`PINI(1-4,K)` initial four momentum of electron  $K=1,2$  (GeV/c)  
`PINI(5,K)` initial mass of electron  $K=1,2$  (GeV/c<sup>2</sup>)  
`PFNI(1-4,K)` final four momentum of electron  $K=1,2$  (GeV/c)  
`PFNI(5,K)` final mass of electron  $K=1,2$  (GeV/c<sup>2</sup>)  
`PFNI(1-4,2)` final four momentum of electron 2 (GeV/c)  
`PGAM(1-4,K)` four momentum of photon  $K=1,2$  (GeV/c)  
`PGAM(5,K)` mass/virtuality of photon  $K=1,2$  (GeV/c<sup>2</sup>)  
`GGY(K)` energy fraction taken by the photon from the electron  $K=1,2$   
`GQ2(K)` virtuality of the photons  $K=1,2$  (GeV<sup>2</sup>/c<sup>2</sup>)  
`GGECEM` CMS energy of photon-photon subsystem (GeV)  
`GAIMP(K)` impact parameter  $|\vec{B}|$  of scattering photons in the quasi-classical (geometrical) model of heavy ion collisions (GeV<sup>-1</sup>)  
`PFTHK(K)` polar angle  $\theta_k$  of scattered electrons  $K=1,2$  (radian)  
`PFPHI(K)` azimuthal angle  $\varphi_k$  of scattered electrons  $K=1,2$  (radian)  
`IDPSRC(K)` particle code of lepton/hadron according to PDG convention for side  $K=1,2$   
`IDPSRC(K)` compressed particle code of lepton/hadron on side  $K=1,2$   
`RADSRC(K)` effective radius of hadron on side  $K=1,2$  (used in heavy ion collisions, GeV<sup>-1</sup>)  
`RADSRC(K)` mass of lepton/hadron on side  $K=1,2$  (used in heavy ion collisions, GeV/c<sup>2</sup>)  
`RADSRC(K)` Lorentz factor  $\Gamma$  of hadron on side  $K=1,2$  (used in heavy ion collisions)

## Appendix A

# Kinematics of hard scattering

In the following the parton kinematics of hard scattering as used in the model is summarized. Here, we consider the general case of the scattering of two partons  $a$  and  $b$  with  $\hat{p}_1 = x_1 p_1$  and  $\hat{p}_2 = x_2 p_2$ . The scattering angle of the partons in the parton CM system follows from

$$\hat{t}^2 = (\hat{p}_1 - \hat{p}_1')^2 = -2\hat{E}_1\hat{E}_1(1 - \cos\hat{\theta}) = -\hat{s}\sin^2\frac{\hat{\theta}}{2}. \quad (\text{A.1})$$

With (A.1),  $\hat{p}_\perp^2 = \hat{p}_1^2 \sin^2\hat{\theta}$ , and  $\hat{s} = x_1 x_2 s$  one gets

$$\hat{p}_\perp^2 = \frac{\hat{t}\hat{u}}{\hat{s}}. \quad (\text{A.2})$$

In parton CMS, the longitudinal momenta of the scattered partons are given by

$$\hat{p}_{\parallel,1'} = \frac{1}{2\sqrt{\hat{s}}}(\hat{t} - \hat{u}) \quad \text{and} \quad \hat{p}_{\parallel,2'} = \frac{1}{2\sqrt{\hat{s}}}(\hat{u} - \hat{t}). \quad (\text{A.3})$$

The rapidity of the two-parton system relative to the hadron CMS is given by

$$y = \frac{1}{2} \frac{(x_1 + x_2)E^{\text{CMS}} + (x_1 - x_2)p^{\text{CMS}}}{(x_1 + x_2)E^{\text{CMS}} - (x_1 - x_2)p^{\text{CMS}}} = \frac{1}{2} \ln\left(\frac{x_1}{x_2}\right) \quad (\text{A.4})$$

To calculate the parton momenta in the hadron CMS system, the following Lorentz transformation with

$$\beta\Gamma = \frac{1}{2} \frac{x_1 - x_2}{\sqrt{x_1 x_2}} \quad \text{and} \quad \beta = \frac{x_1 - x_2}{x_1 + x_2} \quad (\text{A.5})$$

can be used. The longitudinal momenta of the scattered partons in the hadron CMS read

$$\begin{aligned} \hat{p}_{\parallel,1'} &= -\frac{1}{2}\sqrt{s} \left( \frac{\hat{t} x_1 - \hat{u} x_2}{\hat{s}} \right) \\ \hat{p}_{\parallel,2'} &= -\frac{1}{2}\sqrt{s} \left( \frac{\hat{u} x_1 - \hat{t} x_2}{\hat{s}} \right). \end{aligned} \quad (\text{A.6})$$

Since the transverse momenta are not changed by the Lorentz transformation, the rapidities of the scattered partons can be easily evaluated

$$y_1 = \frac{1}{2} \ln \frac{\hat{u} x_1}{\hat{t} x_2} \quad \text{and} \quad y_2 = \frac{1}{2} \ln \frac{\hat{t} x_1}{\hat{u} x_2}. \quad (\text{A.7})$$

Finally, we have the following set of equations for the transformation  $y_1, y_2, p_\perp \rightarrow x_1, x_2, \hat{t}$

$$\begin{aligned} x_1 &= \frac{p_\perp}{\sqrt{\hat{s}}} (e^{y_1} + e^{y_2}) \\ x_2 &= \frac{p_\perp}{\sqrt{\hat{s}}} (e^{-y_1} + e^{-y_2}) \\ \hat{t} &= -p_\perp^2 (1 + e^{y_2 - y_1}) . \end{aligned} \quad (\text{A.8})$$

For many calculations, it is convenient to transform the triple differential cross section

$$\frac{d\sigma^{\text{hard}}}{dx_1 dx_2 d\hat{t}} = \sum_{i,j,k,l} \frac{1}{1 + \delta_{k,l}} f_{A,i}(x_1, Q^2) f_{B,j}(x_2, Q^2) \frac{d\sigma_{i,j \rightarrow k,l}^{\text{QCD}}(\hat{s}, \hat{t})}{d\hat{t}} \Theta(p_\perp - p_\perp^{\text{cutoff}}), \quad (\text{A.9})$$

to the variables  $p_\perp, y_1$ , and  $y_2$  to get the final state in dependence of directly measurable quantities. Using (A.8) the differential cross section can be written in the form

$$\frac{d\sigma^{\text{hard}}}{dy_1 dy_2 dp_\perp} = 2p_\perp x_1 x_2 \frac{d\sigma^{\text{hard}}}{dx_1 dx_2 d\hat{t}} . \quad (\text{A.10})$$

For single-resolved hard scattering (for example,  $x_2 = 1$ ) one gets

$$\frac{d\sigma^{\text{hard}}}{dy_1 dp_\perp} = -2x_1 \frac{\hat{t}}{p_\perp} \frac{d\sigma^{\text{hard}}}{dx_1 d\hat{t}} . \quad (\text{A.11})$$

In the case of direct scattering, the transformation  $\hat{t} \rightarrow p_\perp$  becomes singular at  $\hat{t} = -\hat{s}/2$ . For completeness, we give the corresponding expression

$$\frac{d\sigma^{\text{hard}}}{dp_\perp^2} = \left(1 - \frac{4p_\perp^2}{\hat{s}}\right)^{-\frac{1}{2}} \frac{d\sigma^{\text{hard}}}{d\hat{t}} . \quad (\text{A.12})$$

## Appendix B

# Resonances generated in low-mass diffraction

Table B.1: Resonances used to simulate low-mass diffraction of photons

name	$\omega(1420)$	$\rho(1450)$	$\omega(1600)$	$\phi(1680)$	$\rho(1700)$
mass (MeV)	1456	1465	1623	1680	1700
decay width (MeV)	175	310	280	150	235
weight factor	1/9	1	1/9	1/10 (2/9)	1

Table B.2: Resonances used to simulate low-mass diffraction of (anti-)protons

name	$N^\pm(1440)$	$N^\pm(1710)$
mass (MeV)	1450	1710
decay width (MeV)	350	100
weight factor	1	1

# Appendix C

## Input data cards

### C.1 General structure of input cards

Each line of the input file should contain a code word at its beginning (up to 10 characters long), starting at the first column. Depending on the code word used, a number of arguments (numbers and names) has to follow in this line. There is no fixed format for the numbers necessary, but floats should be written with 'point' (i.e. 2.0 instead of 2) and integers without. All numbers must not be written before the 11th column. If an input card requires a name as argument, the name has to start exactly at the 11th column. If the same input cards is used twice, the last values will be valid in the program. The length of a input line including all parameters is limited to 80 characters. All lines beginning with a asterisk (i.e. '\*') are treated as comment entry and will be ignored.

Some examples how to run the program with input cards can be found in WWW (<http://www.physik.uni-leipzig.de/~engel/>).

### C.2 List of input cards

Below a table of valid input cards is given. Depending on the action caused, the input cards can be classified as general cards, cards for program execution, cards to modify parameters, and card for program debugging.

#### C.2.1 General cards

ENDINPUT	end of input cards assumed, following cards are ignored
STOP	termination of program execution
COMMENT	all text in this line is treated as a comment

#### C.2.2 Program execution

EVENT-CMS	generation of complete fixed energy multiparticle final states by MC, only histograms coded in the subroutines PHIST and HHIST will be filled arguments: 1 float, 1 integer: (1) CMS energy (GeV), (2) number of events to generate;
EVENT-LAB	generation of complete fixed energy multiparticle final states by MC, only histograms coded in the subroutines PHIST and HHIST will be filled arguments: 1 float, 1 integer: (1) LAB momentum of particle 1 (GeV/c), (2) number of events to generate;

GP-HERA	generation of complete multiparticle final states according to HERA kinematics (proton as particle 1, equivalent photon approximation), the lepton tagging has to be specified using the data card <b>E-TAG2</b> . arguments: 2 floats, 1 integer: (1) LAB energy of the proton, (2) LAB energy of the electron/positron, (3) number of events to generate;
GG-EPEM	generation of complete multiparticle final states according to two-photon processes at $e^+e^-$ colliders, the lepton tagging has to be specified using the data cards <b>E-TAG1</b> and <b>E-TAG2</b> . arguments: 2 floats, 1 integer: (1) LAB energy of the first electron, (2) LAB energy of the second electron, (3) number of events to generate;
GG-HION-F	generation of complete multiparticle final states according to two-photon processes at heavy-ion colliders. The photon flux is calculated using the form factor approximation. arguments: 1 floats, 3 integer: (1) LAB energy of the hadron/heavy-ion, (2) mass number, (3) charge number, (4) number of events to generate;
GG-HION-G	generation of complete multiparticle final states according to two-photon processes at heavy-ion colliders. The photon flux is calculated using the semiclassical geometrical approach. arguments: 1 floats, 3 integer: (1) LAB energy of the hadron/heavy-ion, (2) mass number, (3) charge number, (4) number of events to generate;
DSIGDT	calculation of differential elastic cross section $d\sigma/dt$ (mb/GeV <sup>2</sup> ) arguments: 3 floats, 1 integer: (1) CMS energy (GeV), (2) first $t$ value, (3) last $t$ value, (4) number of steps;
HARDTABLE1	calculation of Parton Model cross sections for the given energy range and fixed $p_\perp$ cutoff (mb) arguments: 3 floats, 1 integer: (1) first energy (GeV), (2) last energy (GeV), (3) factor to scale cross section (i.e. to change the units), (4) number of steps;
HARDTABLE2	calculation of Parton Model cross sections for the given fixed energy and the range of $p_\perp$ cuts (mb) arguments: 4 floats, 1 integer: (1) CMS energy (GeV), (2) first $p_\perp^{\text{cutoff}}$ value, (3) last $p_\perp^{\text{cutoff}}$ value, (4) factor to scale cross section (i.e. to change the units), (5) number of steps;
HARDTABLE3	calculation of Parton Model cross sections for the given energy and $p_\perp$ , the cross section break down into the cross sections of the different parton scattering processes is printed (mb) arguments: 3 floats: (1) CMS energy (GeV), (2) $p_\perp^{\text{cutoff}}$ value, (3) factor to scale cross section (i.e. to change the units);
PTTABLE	calculation of the hard differential cross sections $d\sigma/dp_\perp$ for given energy and range of $p_\perp$ (mb/GeV <sup>2</sup> ) arguments: 4 floats, 1 integer: (1) CMS energy (GeV), (2) first $p_\perp$ value, (3) last $p_\perp$ value, (4) factor to scale cross section (i.e. to change the units), (5) number of steps;
PDFTEST	generation of various tables of the PDF assigned to the selected particle ID arguments: 1 integer, 2 floats: (1) particle ID number, (2) squared $Q^2$ scale (GeV <sup>2</sup> ), (3) particle virtuality (GeV <sup>2</sup> , positive);
IMPACTAMP	calculation of impact parameter representations of the unitarized amplitudes and several partial amplitudes (low and high mass diffractive dissociation) arguments: 3 floats, 1 integer: (1) CMS energy (GeV), (2) minimal impact parameter ( $\sqrt{\text{mb}}$ ), (3) maximal impact parameter ( $\sqrt{\text{mb}}$ );

**BEGINFIT** start of PHOJET fit utility, for further information please consult the author arguments: no parameters;

### C.2.3 Changing PHOJET parameters

**PROCESS** selection of basic processes to generate  
arguments: 11 integers (0/1 allowed) to activate the different types of interactions generated: (1) non-diffractive inelastic interactions, (2) purely elastic scattering, (3) quasi-elastic  $\rho$ ,  $\omega$ ,  $\phi$  and  $\pi^+\pi^-$  production, (4) double pomeron scattering, (5) single diffractive dissociation of particle 1, (6) single diffractive dissociation of particle 2, (7) double diffractive dissociation, (8) direct photon-hadron interactions, direct and single resolved photon-photon interactions

**PARTICLE1** set scattering particle 1 (in LAB frame beam particle)  
arguments: 1 integer, 1 float: particle ID number according to the PDG convention for particle 1, virtuality of particle 1 (positive by convention,  $\text{GeV}^2$ )

**PARTICLE2** set scattering particle 2 (in LAB frame target particle)  
arguments: 1 integer, 1 float: particle ID number according to the PDG convention for particle 2, virtuality of particle 2 (positive by convention,  $\text{GeV}^2$ )

**PDF** assign a PDF set to a particle  
arguments: 4 integers: (1) particle ID number, (2) number of the PDF parametrization (author group) IGRP, (3) number of the set within this parametrization ISET, (4) library to be used IEXT:  
0: internal sets,  
1: call to PDDLIB [90] old format,  
2: call to PDDLIB new format,  
3: call to PHOLIB [91],  
4: call to built-in parametrizations with dependence on photon virtuality (for a table of the built-in PDF parametrizations, see Tab. E.1)

**SETMODEL** set model options stored in ISWMDL and IPAMD. For more information, see description of this common block.  
arguments: 2 integers: (1) index INDX of model switch according to ISWMDL(INDX) in COMMON /MODELS/, (2) new value; for negative values of INDX, the new value is assigned IPAMD(-INDX)

**SETPARAM** set model parameters PARMDL stored in the common block /MODELS/  
arguments: 1 integer, 1 float: (1) index of model parameter according to PARMDL in COMMON /MODELS/, (2) new value

**E-TAG1** limitations for photon 1 and electron 1 used for  $eh$  and  $ee$  simulation via equivalent photon approximation; the polar angle range is used for  $ee$  simulation only (for detailed description of kinematics see Sec. 4).  
arguments: 7 floats: (1) minimal electron energy needed to tag the electron, (2)  $y_{\min}$  minimal energy fraction taken by the photon from the electron, (3)  $y_{\max}$  maximal energy fraction taken by the photon from the electron, (4) minimal photon virtuality ( $\text{GeV}^2$ ), (5) maximal photon virtuality ( $\text{GeV}^2$ ), (6) minimal polar angle for scattered electron (radian), (7) maximal polar angle for scattered electron (radian);

**E-TAG2** same as E-TAG1 but for photon 2 and for electron 2  
arguments: 7 floats

**ECMS-CUT** energy cut used for  $\gamma h$  or  $\gamma\gamma$  systems. This cut is applied after the  $y_{\min}$  and  $y_{\max}$  cuts described above.

arguments: 2 floats: (1) minimal CMS energy of  $\gamma\gamma$  or  $\gamma h$  system, (2) maximal CMS energy of  $\gamma\gamma$  or  $\gamma h$  system;

**SUBPROCESS** selection of parton-parton scattering processes used for cross section calculations and event simulation. For minimum bias event simulation, all subprocesses should be switched on (default).

arguments: 3 integers: (1) subprocess number (see Tab. 11.1), (2) particle combination (IP = 1...4, see Sec. 11.1.1), (3) subprocess switch: 0: off, 1: on

#### C.2.4 Changing JETSET parameters

**LUND-MSTJ** 2 integers: (1) index of model switch according to **MSTJ** in the JETSET common block /LUDAT1/, (2) new value

**LUND-MSTU** 2 integers: (1) index of model switch according to **MSTU** in the JETSET common block /LUDAT1/, (2) new value

**LUND-PARJ** 1 integer, 1 float: (1) index of model switch according to **PARJ** in the JETSET common block /LUDAT1/, (2) new value

**LUND-PARU** 1 integer, 1 float: (1) index of model switch according to **PARU** in the JETSET common block /LUDAT1/, (2) new value

**LUND-DECAY** allow for a particle to decay or being stable.  
arguments: 2 integer: (1) particle ID number (PDG convention), (2) value to be set in **MDCY** of the JETSET common block /LUDAT3/ (0 particle is not allowed to decay, 1 particle is allowed to decay)

# Appendix D

## Table of particles

Table D.1: Particles use in the program ordered by compressed particle code (internal numbering)

internal ID	internal name	PDG name	PDG number	charge	v. quarks
1	P	$p^+$	2212	1	2 2 1
2	AP	$\bar{p}^-$	-2212	-1	-2 -2 -1
3	E-	$e^-$	11	-1	0 0 0
4	E+	$e^+$	-11	1	0 0 0
5	NUE	$\nu_e$	12	0	0 0 0
6	ANUE	$\bar{\nu}_e$	-12	0	0 0 0
7	GAM	$\gamma$	22	0	0 0 0
8	NEU	$n^0$	2112	0	2 1 1
9	ANEU	$\bar{n}^0$	-2112	0	-2 -1 -1
10	MUE+	$\mu^+$	-13	1	0 0 0
11	MUE-	$\mu^-$	13	-1	0 0 0
12	K0L	$K_L^0$	130	0	0 0 0
13	PI+	$\pi^+$	211	1	2 -1 0
14	PI-	$\pi^-$	-211	-1	1 -2 0
15	K+	$K^+$	321	1	2 -3 0
16	K-	$K^-$	-321	-1	3 -2 0
17	LAM	$\Lambda^0$	3122	0	0 0 0
18	ALAM	$\bar{\Lambda}^0$	-3122	0	0 0 0
19	K0S	$K_S^0$	310	0	0 0 0
20	SIGM-	$\Sigma^-$	3112	-1	1 1 3
21	SIGM+	$\Sigma^+$	3222	1	2 2 3
22	SIGM0	$\Sigma^0$	3212	0	2 1 3
23	PI0	$\pi^0$	111	0	2 -2 0
24	K0	$K^0$	311	0	1 -3 0
25	AK0	$\bar{K}^0$	-311	0	3 -1 0

*continued on next page*

continued from previous page

internal ID	internal name	PDG name	PDG number	charge	v. quarks
26	OM1420	$\omega(1420)$	50223	0	0 0 0 0
27	RH1450	$\rho(1450)$	40113	0	0 0 0 0
28	OM1600	$\omega(1600)$	60223	0	0 0 0 0
29	PH1680	$\phi(1680)$	10333	0	0 0 0 0
30	RH1700	$\rho(1700)$	30113	0	0 0 0 0
31	ETA550	$\eta$	221	0	3 -3 0
32	RHO+77	$\rho^+$	213	1	2 -1 0
33	RHO077	$\rho^0$	113	0	2 -2 0
34	RHO-77	$\rho^-$	-213	-1	1 -2 0
35	OM0783	$\omega$	223	0	0 0 0 0
36	K*+892	$K^{*+}$	323	1	2 -3 0
37	K*0892	$K^{*0}$	313	0	1 -3 0
38	K*-892	$K^{*-}$	-323	-1	3 -2 0
39	AK*089	$\bar{K}^{*0}$	-313	0	3 -1 0
40	KA+125	$K_1^+$	10323	1	0 0 0
41	KA0125	$K_1^0$	10313	0	0 0 0
42	KA-125	$K_1^-$	-10323	-1	0 0 0
43	AKA012	$\bar{K}_1^0$	-10313	0	0 0 0
44	K*+142		30323	1	0 0 0
45	K*0142		30313	0	0 0 0
46	K*-142		-30323	-1	0 0 0
47	AK*014		-30313	0	0 0 0
48	S+1385	$\Sigma^{*+}$	3224	1	0 0 0
49	S01385	$\Sigma^{*0}$	3214	0	0 0 0
50	S-1385	$\Sigma^{*-}$	3114	-1	0 0 0
51	L01820		3216	0	0 0 0
52	L02030		3218	0	0 0 0
53	N*++12	$\Delta^{++}$	2224	2	2 2 2
54	N*+ 12	$\Delta^+$	2214	1	2 2 1
55	N*012	$\Delta^0$	2114	0	2 1 1
56	N*-12	$\Delta^-$	1114	-1	1 1 1
57	N*++16		12224	2	0 0 0
58	N*+16		12214	1	0 0 0
59	N*016		12114	0	0 0 0
60	N*-16		11114	-1	0 0 0
61	N*+14		12212	1	0 0 0
62	N*014		12112	0	0 0 0
63	N*+15		22212	1	0 0 0

continued on next page

continued from previous page

internal ID	internal name	PDG name	PDG number	charge	v. quarks		
64	N*015		22112	0	0	0	0
65	N*+18		42212	1	0	0	0
66	N*018		42112	0	0	0	0
67	AN-12	$\bar{\Delta}^{--}$	-2224	-2	-2	-2	2
68	AN*-12	$\bar{\Delta}^{-}$	-2214	-1	-2	-2	-1
69	AN*012	$\bar{\Delta}^0$	-2114	0	-2	-1	-1
70	AN*+12	$\bar{\Delta}^{+}$	-1114	1	-1	-1	1
71	AN-16		-12224	-2	0	0	0
72	AN*-16		-12214	-1	0	0	0
73	AN*016		-12114	0	0	0	0
74	AN*+16		-11114	1	0	0	0
75	AN*-15		-2124	-1	0	0	0
76	AN*015		-1214	0	0	0	0
95	ETA*	$\eta'$	331	0	0	0	0
96	PHI	$\phi$	333	0	3	-3	0
97	TETA0	$\Xi^0$	3322	0	2	3	3
98	TETA-	$\Xi^{-}$	3312	-1	1	3	3
99	ASIG-	$\bar{\Sigma}^{-}$	-3222	-1	-2	-2	-3
100	ASIG0	$\bar{\Sigma}^0$	-3212	0	-2	-1	-3
101	ASIG+	$\bar{\Sigma}^{+}$	-3112	1	-1	-1	-3
102	ATETA0	$\bar{\Xi}^0$	-3322	0	-2	-3	3
103	ATETA+	$\bar{\Xi}^{+}$	-3312	1	-1	-3	-3
104	SIG*+	$\Sigma^{*+}$	3224	1	2	2	3
105	SIG*0	$\Sigma^{*0}$	3214	0	2	1	3
106	SIG*-	$\Sigma^{*-}$	3114	-1	1	1	3
107	TETA*0	$\Xi^{*0}$	3324	0	2	3	3
108	TETA*	$\Xi^{*-}$	3314	-1	1	3	3
109	OMEGA-	$\Omega^{-}$	3334	-1	3	3	3
110	ASIG*-	$\bar{\Sigma}^{*-}$	-3224	-1	-2	-2	-3
111	ASIG*0	$\bar{\Sigma}^{*0}$	-3214	0	-2	-1	-3
112	ASIG*+	$\bar{\Sigma}^{*+}$	-3114	1	-1	-1	-3
113	ATET*0	$\bar{\Xi}^{*0}$	-3324	0	-2	-3	3
114	ATET*+	$\bar{\Xi}^{*+}$	-3314	1	-1	-3	3
115	OMEGA+	$\bar{\Omega}^{+}$	-3334	1	-3	-3	3
116	D0	$D^0$	421	0	4	-2	0
117	D+	$D^{+}$	411	1	4	-1	0
118	D-	$D^{-}$	-411	-1	1	-4	0
119	AD0	$\bar{D}^0$	-421	0	2	-4	0

continued on next page

continued from previous page

internal ID	internal name	PDG name	PDG number	charge	v. quarks
120	F+	$D_s^+$	431	1	4 -3 0
121	F-	$D_s^-$	-431	-1	3 -4 0
122	ETAC	$\eta_c$	441	0	4 -4 0
123	D*0	$D^{*0}$	423	0	4 -2 0
124	D*+	$D^{*+}$	413	1	4 -1 0
125	D*-	$D^{*-}$	-413	-1	1 -4 0
126	AD*0	$\bar{D}^{*0}$	-423	0	2 -4 0
127	F*+	$D_s^{*+}$	433	1	4 -3 0
128	F*-	$D_s^{*-}$	-433	-1	3 -4 0
129	PSI	$\chi_1^c$	20443	0	4 -4 0
130	JPSI	$J/\psi$	443	0	0 0 0
131	TAU+	$\tau^+$	-15	1	0 0 0
132	TAU-	$\tau^-$	15	-1	0 0 0
133	NUET	$\nu_\tau$	16	0	0 0 0
134	ANUET	$\bar{\nu}_\tau$	-16	0	0 0 0
135	NUEM	$\nu_\mu$	14	0	0 0 0
136	ANUEM	$\bar{\nu}_\mu$	-14	0	0 0 0
137	C0+	$\Lambda_c^+$	4122	1	2 1 4
138	A+	$\Xi_c^+$	4232	1	2 3 4
139	A0	$\Xi_c^0$	4132	0	1 3 4
140	C1++	$\Sigma_c^{++}$	4222	2	2 2 4
141	C1+	$\Sigma_c^+$	4212	1	0 0 0
142	C10	$\Sigma_c^0$	4112	0	1 1 4
143	S+	$\Xi_c^{\prime+}$	4322	1	0 0 0
144	S0	$\Xi_c^{\prime0}$	4312	0	0 0 0
145	T0	$\Omega_c^0$	4332	0	3 3 4
146	XU++	$\Xi_{cc}^{++}$	4422	2	2 4 4
147	XD+	$\Xi_{cc}^+$	4412	1	1 4 4
148	XS+	$\Omega_{cc}^+$	4432	1	3 4 4
149	AC0-	$\bar{\Lambda}_c^-$	-4122	1	-2 -1 4
150	AA-	$\bar{\Xi}_c^-$	-4232	1	-2 -3 -4
151	A0	$\bar{\Xi}_c^0$	-4132	0	-1 -3 -4
152	AC1-	$\bar{\Sigma}_c^{--}$	-4222	-2	-2 -2 -4
153	AC1-	$\bar{\Sigma}_c^-$	-4212	1	0 0 0
154	AC10	$\bar{\Sigma}_c^0$	-4112	0	-1 -1 -4
155	AS-	$\bar{\Xi}_c^{\prime-}$	-4322	1	0 0 0
156	AS0	$\bar{\Xi}_c^{\prime0}$	-4312	0	0 0 0
157	AT0	$\bar{\Omega}_c^0$	-4332	0	-3 -3 -4

continued on next page

continued from previous page

internal ID	internal name	PDG name	PDG number	charge	v. quarks
158	AXU-	$\bar{\Xi}_{cc}^{--}$	-4422	-2	-2 -4 -4
159	AXD-	$\bar{\Xi}_{cc}^{-}$	-4412	1	-1 -4 -4
160	AXS	$\bar{\Omega}_{cc}^{-}$	-4432	-1	-3 -4 -4
161	C1*++	$\Sigma_c^{*++}$	4224	2	2 2 4
162	C1*+	$\Sigma_c^{*+}$	4214	1	2 1 4
163	C1*0	$\Sigma_c^{*0}$	4114	0	1 1 4
164	S*+	$\Xi_c^{*+}$	4324	1	2 3 4
165	S*0	$\Xi_c^{*0}$	4314	0	1 3 4
166	T*0	$\Omega_c^{*0}$	4334	0	3 3 4
167	XU*++	$\Xi_{cc}^{*++}$	4424	2	2 4 4
168	XD*+	$\Xi_{cc}^{*+}$	4414	1	1 4 4
169	XS*+	$\Omega_{cc}^{*+}$	4434	1	3 4 4
170	TETA++	$\Omega_{ccc}^{*++}$	4444	2	4 4 4
171	AC1*-	$\bar{\Sigma}_c^{*-}$	-4224	2	-2 -2 -4
172	AC1*-	$\bar{\Sigma}_c^{*-}$	-4214	-1	-2 -1 -4
173	AC1*0	$\bar{\Sigma}_c^{*0}$	-4114	0	-1 -1 -4
174	AS*-	$\bar{\Xi}_c^{*-}$	-4324	-1	-2 -3 -4
175	AS*0	$\bar{\Xi}_c^{*0}$	-4314	0	-1 -3 -4
176	AT*0	$\bar{\Omega}_c^{*0}$	-4334	0	-3 -3 -4
177	AXU*-	$\bar{\Xi}_{cc}^{*-}$	-4424	-2	-2 -4 -4
178	AXD*-	$\bar{\Xi}_{cc}^{*-}$	-4414	1	-1 -4 -4
179	AXS*-	$\bar{\Omega}_{cc}^{*-}$	-4434	-1	-3 -4 -4
180	ATET-	$\bar{\Omega}_{ccc}^{*-}$	-4444	-2	-4 -4 -4
184	pomeron		45	0	0 0 0
185	reggeon0		46	0	0 0 0
186	reggeon+		47	1	0 0 0
187	reggeon-		-47	-1	0 0 0

## Appendix E

# Parton distribution functions

Table E.1: PDF parametrizations available in PHOJET.

particle	param	IGRP	ISET	IEXT	comment
proton	GRV92 HO	5	3	0	higher order set, $\overline{MS}$ scheme, $Q_0^2 = 0.3 \text{ GeV}^2$
	GRV92 LO	5	4	0	leading order set, $Q_0 = 0.25 \text{ GeV}^2$
	GRV94 HO	5	5	0	higher order set, $\overline{MS}$ scheme, $Q_0^2 = 0.3 \text{ GeV}^2$
	GRV94 LO	5	6	0	leading order set, $Q_0^2 = 0.25 \text{ GeV}^2$
photon	GRV-G LH	5	1	0	leading part of higher order, $\overline{MS}$ scheme, $Q_0^2 = 0.3 \text{ GeV}^2$
	GRV-G HO	5	2	0	higher order set, $\overline{MS}$ scheme, $Q_0^2 = 0.3 \text{ GeV}^2$
	GRV-G LO	5	3	0	leading order set, $Q_0^2 = 0.25 \text{ GeV}^2$
	SaS 1D	1	1	4	virtual photons, $DIS$ scheme, $Q_0 = 0.6 \text{ GeV}$
	SaS 1M	1	2	4	virtual photons, $\overline{MS}$ scheme, $Q_0 = 0.6 \text{ GeV}$
	SaS 2D	1	3	4	virtual photons, $DIS$ scheme, $Q_0 = 2 \text{ GeV}$
	SaS 2M	1	4	4	virtual photons, $\overline{MS}$ scheme, $Q_0 = 2 \text{ GeV}$
pion	GRV-P HO	5	1	0	higher order set, $\overline{MS}$ scheme, $Q_0^2 = 0.3 \text{ GeV}^2$
	GRV-P LO	5	2	0	leading order set, $\overline{MS}$ scheme, $Q_0^2 = 0.3 \text{ GeV}^2$
pomeron	soft gluon	1	0	0	$xg(x) = 6N (1-x)^5$
	hard gluon 1	2	0	0	$xg(x) = 6N x(1-x)$
	hard gluon 2	3	0	0	$xg(x) = N (0.18/x + 5.46)(1-x)$
	CKMT 1	4	0	0	quark-gluon distribution, Regge factorization [92,18], DGLAP evolution $Q_0^2 = 2 \text{ GeV}^2$

# Bibliography

- [1] A. Capella, U. Sukhatme, C. I. Tan and J. Trân Thanh Vân: Phys. Rep. 236 (1994) 225
- [2] G. 't Hooft: Nucl. Phys. B72 (1974) 461
- [3] G. Veneziano: Nucl. Phys. B74 (1974) 365
- [4] H.-M. Chan, J. E. Paton and S. T. Tsou: Nucl. Phys. B86 (1975) 479
- [5] G. F. Chew and C. Rosenzweig: Nucl. Phys. B104 (1976) 290
- [6] G. F. Chew and C. Rosenzweig: Phys. Rep. 41 (1978) 263
- [7] V. N. Gribov: Sov. Phys. JETP 26 (1968) 414
- [8] V. N. Gribov and A. A. Migdal: Sov. J. Nucl. Phys. 8 (1969) 583
- [9] A. Capella, J. Trân Thanh Vân and J. Kwieciński: Phys. Rev. Lett. 58 (1987) 2015
- [10] K. Hahn and J. Ranft: Phys. Rev. D41 (1990) 1463
- [11] F. W. Bopp, A. Capella, J. Ranft and J. Trân Thanh Vân: Z. Phys. C51 (1991) 99
- [12] P. Aurenche, F. W. Bopp, A. Capella, J. Kwieciński, M. Maire, J. Ranft and J. Trân Thanh Vân: Phys. Rev. D45 (1992) 92
- [13] F. W. Bopp, D. Pertermann and J. Ranft: Z. Phys. C54 (1992) 683
- [14] R. Engel, F. W. Bopp, D. Pertermann and J. Ranft: Phys. Rev. D46 (1992) 5192
- [15] F. W. Bopp, R. Engel, D. Pertermann and J. Ranft: Phys. Rev. D49 (1994) 3236
- [16] J. Ranft: Phys. Rev. D51 (1995) 64
- [17] S. Roesler, R. Engel and J. Ranft: Z. Phys. C59 (1993) 481
- [18] R. Engel, J. Ranft and S. Roesler: Phys. Rev. D52 (1995) 1459
- [19] R. Engel: Z. Phys. C66 (1995) 203
- [20] R. Engel and J. Ranft: Phys. Rev. D54 (1996) 4244
- [21] R. Engel, J. Ranft and S. Roesler: Phys. Rev. D55 (1997) 6957
- [22] S. Roesler, R. Engel and J. Ranft: Photoproduction off nuclei and point-like photon interactions, Part II: Particle production, preprint SI 96-14, US-FT/45-96, (hep-ph/9611379), 1996

- [23] P. Aurenche, F. W. Bopp, R. Engel, D. Pertermann, J. Ranft and S. Roesler: *Comp. Phys. Commun.* 83 (1994) 107
- [24] M. M. Block and R. N. Cahn: *Rev. Mod. Phys.* 57 (1985) 563
- [25] M. Baker and K. A. Ter-Martirosyan: *Phys. Rep.* 28C (1976) 1
- [26] L. Durand and H. Pi: *Phys. Rev. Lett.* 58 (1987) 303
- [27] B. L. Ioffe, V. A. Khoze and L. N. Lipatov: *Hard Processes, Volume 1: Phenomenology Quark-Parton Model*, North-Holland Physics Publishing, Amsterdam 1984
- [28] V. M. Budnev, I. F. Ginzburg, G. V. Meledin and V. G. Serbo: *Phys. Rep.* 15C (1975) 181
- [29] I. F. Ginzburg and V. G. Serbo: *Phys. Lett.* 109B (1982) 231
- [30] PLUTO Collab.: C. Berger et al.: *Phys. Lett.* 89B (1981) 287
- [31] F. Borzumati and G. A. Schuler: *Z. Phys.* C58 (1993) 139
- [32] P. Aurenche, J. P. Guillet, M. Fontannaz, Y. Shimizu and K. Kato: *Prog. Theor. Phys.* 92 (1994) 175
- [33] M. Drees and R. M. Godbole: *Phys. Rev.* D50 (1994) 3124
- [34] M. Froissart: *Phys. Rev.* 123 (1961) 1053
- [35] A. Donnachie and P. V. Landshoff: *Phys. Lett.* B296 (1992) 227
- [36] A. B. Kaidalov: *Phys. Rep.* 50 (1979) 157
- [37] A. Capella, J. Trân Thanh Vân and J. Kaplan: *Nucl. Phys.* B97 (1975) 493
- [38] A. Capella and J. Kaplan: *Phys. Lett.* B52 (1974) 448
- [39] A. B. Kaidalov, L. A. Ponomarev and K. A. Ter-Martirosyan: *Sov. J. Nucl. Phys.* 44 (1986) 468
- [40] V. A. Abramovski, V. N. Gribov and O. V. Kancheli: *Yad. Fis.* 18 (1973) 595
- [41] R. Engel: Multiparticle Photoproduction within the two-component Dual Parton Model, in preparation, 1996
- [42] K. A. Ter-Martirosyan: *Phys. Lett.* B44 (1973) 377
- [43] A. Capella and A. Kaidalov: *Nucl. Phys.* B111 (1976) 477
- [44] G. Veneziano: *Nucl. Phys.* B117 (1976) 519
- [45] A. Capella, U. Sukhatme and J. Trân Thanh Vân: *Z. Phys.* C3 (1980) 329
- [46] A. Capella, U. Sukhatme, C. I. Tan and J. Trân Thanh Vân: *Z. Phys.* C10 (1981) 249
- [47] A. B. Kaidalov: *Phys. Lett.* B116 (1982) 459
- [48] A. B. Kaidalov and K. A. Ter-Martirosyan: *Phys. Lett.* B117 (1982) 247
- [49] S. Ritter and J. Ranft: *Acta Phys. Polon.* B11 (1980) 259
- [50] B. L. Combridge, J. Kripfganz and J. Ranft: *Phys. Lett.* B70 (1977) 234

- [51] D. W. Duke and J. F. Owens: Phys. Rev. D26 (1982) 1600
- [52] H. U. Bengtsson: Comp. Phys. Commun. 31 (1984) 323
- [53] T. Gottschalk: Nucl. Phys. B277 (1986) 700
- [54] T. Sjöstrand: Phys. Lett. B157 (1985) 321
- [55] E. Witten: Nucl. Phys. B120 (1977) 189
- [56] M. Drees: Initial state showering in resolved photon interactions, MAD/PH/797, Talk held at the 23rd International Symposium on Multiparticle Dynamics, Aspen, Colo., Sep. 1993, 1993
- [57] H. U. Bengtsson and T. Sjöstrand: Comp. Phys. Commun. 46 (1987) 43
- [58] R. Ross and V. Stodolsky: Phys. Rev. 149 (1966) 1172
- [59] D. Aston et al.: Nucl. Phys. B209 (1982) 56
- [60] T. H. Bauer, R. D. Spital and D. R. Yennie: Rev. Mod. Phys. 50 (1978) 261
- [61] K. Schilling, P. Seyboth and G. Wolf: Nucl. Phys. B15 (1970) 397
- [62] D. M. Chew and G. F. Chew: Phys. Lett. 53B (1974) 191
- [63] A. B. Kaidalov and K. A. Ter-Martirosyan: Nucl. Phys. B75 (1974) 471
- [64] K. H. Streng: Phys. Lett. 166B (1986) 443
- [65] O. Nachtmann: *Phänomene und Konzepte der Elementarteilchenphysik* Friedr. Vieweg & Sohn Braunschweig 1986
- [66] L. N. Hand: Phys. Rev. 129 (1963) 1834
- [67] C. F. von Weizsäcker: Z. Phys. 88 (1934) 612
- [68] E. J. Williams: Phys. Rev. 45 (1934) 729
- [69] M. Grabiak, B. Müller, W. Greiner, G. Soff and P. Koch: J. Phys. G15 (1989) L25
- [70] M. Drees, J. Ellis and D. Zeppenfeld: Phys. Lett. B223 (1989) 454
- [71] E. Papageorgiu: Phys. Lett. B250 (1990) 155
- [72] C. A. Bertulani and G. Baur: Phys. Rep. 163 (1988) 181
- [73] N. Baron and G. Baur: Phys. Rev. C48 (1993) 1999
- [74] E. Amaldi, S. Fubini and G. Furlan: *Pion electroproduction* Springer New York 1979
- [75] R. C. Barret and D. F. Jackson: *Nuclear size and structure* Clarendon Oxford 1977
- [76] J. D. Jackson: *Classical electrodynamics* John Wiley & Sons New York 1963
- [77] K. Hencken, D. Trautmann and G. Baur: Z. Phys. C68 (1995) 473
- [78] P. Chen: Phys. Rev. D46 (1992) 1186
- [79] P. Chen, T. L. Barklow and M. E. Peskin: Phys. Rev. D49 (1994) 3209

- [80] I. F. Ginzburg, G. L. Kotkin, V. G. Serbo and V. I. Telnov: *Prisma ZHETF* 34 (1981) 514
- [81] I. F. Ginzburg, G. L. Kotkin, V. G. Serbo and V. I. Telnov: *Nucl. Instrum. Methods* A205 (1983) 47
- [82] I. F. Ginzburg, G. L. Kotkin, V. G. Serbo and V. I. Telnov: *Nucl. Instrum. Methods* A219 (1984) 5
- [83] V. I. Telnov: *Nucl. Instrum. Methods* A294 (1990) 72
- [84] Particle Data Group: Angular-Benitez et al.: *Phys. Lett.* B170 (1986) 1
- [85] Particle Data Group: G. P. Yost et al.: *Phys. Lett.* B239 (1990) 1
- [86] S. Ritter: *Comp. Phys. Commun.* 31 (1984) 393
- [87] S. Ritter: *Comp. Phys. Commun.* 31 (1984) 401
- [88] K. Hänßgen and S. Ritter: *Comp. Phys. Commun.* 31 (1984) 411
- [89] L. Durand and H. Pi: *Phys. Rev.* D43 (1991) 2125
- [90] H. Plothow-Besch: *Comp. Phys. Commun.* 75 (1993) 396
- [91] K. Charchula: *Comp. Phys. Commun.* 69 (1992) 360
- [92] A. Capella, A. Kaidalov, C. Merino and J. Trân Thanh Vân: *Phys. Lett.* B343 (1995) 403

# Index

- ABRSOF, common block, 65  
ACTPDF, subroutine, 75
- beamstrahlung, physics, 36  
BEGINFIT, input card, 91  
bremsstrahlung, physics, 32
- central diffraction, comment entry, 57  
central diffraction, IPRON(4), 49  
chain fragmentation, /POSTRG/, 80  
comment entries in /HEPEVS/, 54  
comment entries, hard interactions, 54  
comment entry, central diffraction, 57  
comment entry, diffractive dissociation, 55  
comment entry, elastic/quasi-elastic scattering, 56  
COMMENT, input card, 89  
coupling constant  $\alpha_s$ , 68  
cross sections, unitarized, 62
- DEBUG, common block, 58  
diffractive dissociation, comment entry, 55  
diffractive dissociation, IPRON(5-7), 49  
direct, single-resolved interactions, IPRON(9), 49  
DSIGDT, input card, 90
- E-TAG1, input card, 91  
E-TAG2, input card, 91  
ECMS-CUT, input card, 91  
elastic scattering, IPRON(2), 49  
elastic/quasi-elastic scattering, comment entry, 56  
ENDINPUT, input card, 89  
EVENT, subroutine, 46  
EVENT-CMS, input card, 89  
EVENT-LAB, input card, 89
- flavour, selection in low  $p_{\perp}$  interactions, 24
- GETPDF, subroutine, 75  
GG-EPEM, input card, 90  
GG-HION-F, input card, 90  
GG-HION-G, input card, 90
- GP-HERA, input card, 90
- HAQQAP, common block, 72  
hard diffraction, IPRON(9-11), 49  
hard interactions, comment entries, 54  
hard processes, matrix elements, 24  
hard processes, table, 68  
hard scattering, kinematics, 86  
HARDTABLE1, input card, 90  
HARDTABLE2, input card, 90  
HARDTABLE3, input card, 90  
HARSLT, common block, 70  
HAXSEC, common block, 71  
HEPEVS, common block, 51  
histograming, 45  
histograming, POLUHI, POHIST, 44, 45
- IMPACTAMP, input card, 90  
initial state radiation, 26  
input cards, list of, 89  
IPAMDL(1), complex phase of the eikonal function, 60  
IPAMDL(11,12), electrons in photoproduction, 83  
IPAMDL(110), direct photon-quark coupling in ISR, 72  
IPAMDL(115), PDFs of virtual photons, 82  
IPAMDL(15), energy-momentum check, 80  
IPAMDL(3), decay of hadroproduced resonances, 78  
IPAMDL(4), decay of photoproduced resonances, 78  
IPAMDL(64),  $\tau^+\tau^-$  pair production, 68  
IPAMDL(65-80), scales in hard scattering, 69  
IPAMDL(7), energy dependence of  $p_{\perp}^{\text{cutoff}}$ , 69  
IPAMDL(8), intercept used for enhanced graphs, 60  
IPAMDL(9), slope of hard scattering amplitude, 60  
IPAMDL, input card SETMODEL, 91  
IPOBA3, function, 54  
IPOCH3, function, 54  
IPRON, common /PROCESS/, 48

ISWMDL(10), cross section of virtual photons, 82  
 ISWMDL(11), hard color flow, 69  
 ISWMDL(12), semihard processes, 69  
 ISWMDL(13), diffractive momentum transfer, 76  
 ISWMDL(14), treatment of enhanced graphs, 65  
 ISWMDL(15), multiple non-diffractive interactions, 49  
 ISWMDL(16), multiple diffractive interactions, 50  
 ISWMDL(17), chain fusion, 79  
 ISWMDL(18), soft  $p_{\perp}$  assignment, 65  
 ISWMDL(19), flavour sampling, pomeron, 65  
 ISWMDL(2), minimum bias events, 49  
 ISWMDL(20), flavour sampling, sea, 65  
 ISWMDL(21), resonance decay in diffraction, 77  
 ISWMDL(22), diffractive mass distribution, 76  
 ISWMDL(23), fragmentation in diffraction, 78  
 ISWMDL(24), spectator quark  $p_{\perp}$ , 69  
 ISWMDL(25), multiple interactions in double-pomeron scattering, 50  
 ISWMDL(26), photon flux in heavy ions, 83  
 ISWMDL(3), soft  $p_{\perp}$  distribution in hadrons, 64  
 ISWMDL(4), soft  $p_{\perp}$  distribution in photons, 64  
 ISWMDL(6), fragmentation, 79  
 ISWMDL(7), chain mass correction, 79  
 ISWMDL(8), parton showering, 72  
 ISWMDL, how to set, 91  
 ISWMDL, in /MODELS/, 49  
 ISWMDL, input card SETMODEL, 91  
  
 JETSET, 42  
  
 kinematics, hard scattering, 86  
  
 laser backscattering, physics, 36  
 LEPCUT, common block, 83  
 lepton-photon vertex, kinematics, 32  
 lepton/hadron-photon vertex, /LEPCUT/, 83  
 lepton/hadron-photon vertex, /PHOSRC/, 84  
 lepton/hadron-photon vertex, program overview, 44  
 low-mass diffraction, table of resonances, 88  
 Lund Monte Carlo programs, 42  
  
 LUND-DECAY, declare stable particles, 92  
 LUND-MSTJ, input card, 92  
 LUND-MSTU, input card, 92  
 LUND-PARJ, input card, 92  
 LUND-PARU, input card, 92  
  
 MCIHAD, function, 53  
 MODELS, common block, 49  
 MPDGHA, function, 53  
  
 non-diffractive scattering, IPRON(1), 49  
  
 PANAME, function, 53  
 PARMDL(1-6), soft quark flavours, 65  
 PARMDL(110-125), scales in hard scattering, 69  
 PARMDL(126-129), virtuality cutoff for ISR, 73  
 PARMDL(21-24), valence quark  $p_{\perp}$ , 64  
 PARMDL(26), normalization of pomeron PDF, 78  
 PARMDL(27-34), GVDM suppression factor, 82  
 PARMDL(35), suppression of multiple soft interactions, 82  
 PARMDL(36), transverse momentum cutoff, 70  
 PARMDL(36-39), transverse momentum cutoff, 67  
 PARMDL(45), coherence constraint in diffraction, 76  
 PARMDL(46), lower mass cut in diffraction, 76  
 PARMDL(47), regularization parameter for diffractive slope, 76  
 PARMDL(48), effective pomeron intercept, enhanced graphs, 60  
 PARMDL(48), renormalized pomeron intercept, 76  
 PARMDL(49), coherence constraint for diffraction, 76  
 PARMDL(70), cut in central diffraction, 77  
 PARMDL(71), mass cut in central diffraction, 77  
 PARMDL(72),  $x_F$  cut in central diffraction, 77  
 PARMDL(74), direct pomeron-quark coupling, 78  
 PARMDL(75,76), energy-momentum check, 80  
 PARMDL, input card SETPARAM, 91

PARPDF, common block, 73  
particle codes, table, 93  
particle numbering, 93  
PARTICLE1, input card, 91  
PARTICLE2, input card, 91  
parton distribution functions, table, 98  
PDF assignment, /PARPDF/, 73  
PDF assignment, GETPDF, 75  
PDF assignment, SETPDF, 74  
PDF assignment, table, 98  
PDF, input card, 91  
PDFTEST, input card, 90  
PHOINP, subroutine, 46  
PHOSRC, common block, 84  
photon flux calculation, 31  
POHIST, subroutine, 48  
POLUHI, subroutine, 47  
pomeron, pointlike coupling, 25  
POPAMA, function, 54  
POSTRG, common block, 80  
PROCES, common block, 48, 57  
PROCESS, input card, 91  
PTTABLE, input card, 90  
PYTHIA, 42

QEVECM, common block, 77

REGGE, common block, 60

scale, in hard interactions, 68  
SETMODEL, input card, 91  
SETPAR, subroutine, 47  
SETPARAM, input card, 91  
SETPDF, subroutine, 74  
SIGGEN, in /XSECTP/, 63  
STOP, input card, 89  
SUBPROCESS, input card, 92

tau pair production, 68  
transverse momentum, valence quarks, 64  
TWOCHA, common block, 62

updates and bugfixes, 41

vector meson production, IPRON(3), 49

WWW home page of the program, 40, 41

XSECTP, common block, 62